

Brachiopod origins - Supplementary material -
Phylogenetic analysis

Sun, Hai-Jing; Smith, Martin Ross; Zhu, Mao-Yan; Zeng, Han; Zhao, Fang-Chen

2018-03-12

Contents

Brachiopod origins	5
1 The dataset	7
2 Parsimony analysis	9
2.1 Search parameters	9
2.2 Analysis	9
2.3 Results	10
3 Character reconstructions	15
4 Fitch parsimony	111
4.1 Implied weights	111
4.2 Equal weights	111
5 Bayesian analysis	117

Brachiopod origins

This document provides a detailed discussion of analyses of the morphological dataset constructed to accompany Sun *et al.* [2018], and their results.

We first discuss the results presented in the main paper, which employ the algorithm described by Brazeau, Guillaume and Smith [2017a] for correct handling of inapplicable data in a parsimony setting, and explore how each character is reconstructed on an optimal tree.

For completeness, we also document the results of standard Fitch parsimony analysis, and the results of Bayesian analysis, neither of which treat inapplicable data in a logically consistent fashion.

Chapter 1

The dataset

Analysis was performed on a new matrix of 35 early brachiozoan taxa, including hyoliths, tommotiids and mickwitiids, which were coded for 95 morphological characters (42 neomorphic, 53 transformational).

The dataset can be viewed and downloaded at Morphobank (project 2800), where each character is defined and its coding for each taxon discussed.

Characters are coded following the recommendations of Brazeau, Guillerme and Smith [Brazeau et al., 2017a]. In brief, we have employed reductive coding, using a distinct state to mark character inapplicability. Character specifications follow the model of Sereno [2007].

We have distinguished between neomorphic and transformational characters [sensu Sereno, 2007] by reserving the token 0 to refer to the absence of a neomorphic character. The states of transformational characters are represented by the tokens 1, 2, 3, ...

Following the recommendations of Brazeau, Guillerme and Smith [Brazeau et al., 2017a, supplementary discussion], we code the absence of neomorphic ontologically dependent characters [sensu Vogt, 2017] as absence, rather than inapplicability.

Chapter 2

Parsimony analysis

The phylogenetic dataset contains a high proportion of inapplicable codings ($404 / 3325 = 12\%$ of tokens), which are known to introduce error and bias to phylogenetic reconstruction ([Maddison, 1993, Brazeau et al., 2017a]). As such, phylogenetic search employed a new algorithm that correctly handles inapplicable data [Brazeau et al., 2017a]. This algorithm is implemented in the *MorphyLib* C library [Brazeau et al., 2017b], and phylogenetic search was conducted using the *R* package *TreeSearch* v0.0.8 [Smith, 2018].

Namacalathus is included in the matrix but has been excluded from analysis due to its potentially long branch, which is likely to mislead analysis.

2.1 Search parameters

Heuristic searches were conducted using the parsimony ratchet [Nixon, 1999] under equal and implied weights [Goloboff, 1997] with a variety of concavity constants. The consensus tree presented in the main manuscript represents a strict consensus of all trees that are most parsimonious under one or more of the concavity constants (k) 2, 3, 4.5, 7, 10.5, 16 and 24, an approach that is known to produce higher accuracy than equal weights at any fixed level of precision [Smith, 2017].

2.2 Analysis

2.2.1 Load data

2.2.2 Generate starting tree

Dailyatia is used as an outgroup.

```
nj.tree <- NJTree(my_data)
rooted.tree <- EnforceOutgroup(nj.tree, 'Dailyatia')
start.tree <- TreeSearch(tree=rooted.tree, dataset=my_data, maxIter=3000,
                        EdgeSwapper=RootedNNISwap, verbosity=0)
```

2.2.3 Implied weights analysis

```

for (k in kValues) {
  iw.tree <- IWRatchet(start.tree, iw_data, concavity=k,
    ratchHits = 60, searchHits=55,
    swappers=list(RootedTBRSwap, RootedSPRSwap, RootedNNISwap),
    verbosity=0)
  score <- IWScore(iw.tree, iw_data, concavity=k)
  # Write single best tree
  write.nexus(iw.tree, file=paste0("TreeSearch/hy_iw_k", k, "_", signif(score, 5), ".nex", collapse=''))

  suboptFraction = 0.02
  iw.consensus <- IWRatchetConsensus(iw.tree, iw_data, concavity=k,
    swappers=list(RootedTBRSwap, RootedNNISwap),
    searchHits=4,
    suboptimal=score * suboptFraction,
    nSearch=150, verbosity=0L)
  write.nexus(iw.consensus, file=paste0("TreeSearch/hy_iw_k", k, "_", signif(IWScore(iw.tree, iw_data,
}

```

2.2.4 Equal weights analysis

```

ew.tree <- Ratchet(start.tree, my_data, verbosity=0L,
  ratchHits = 10, searchHits=55,
  swappers=list(RootedTBRSwap, RootedSPRSwap, RootedNNISwap))
write.nexus(best.tree, file=paste0("TreeSearch/hy_ew_", Fitch(ew.tree, my_data), ".nex", collapse=''))

ew.consensus <- RatchetConsensus(ew.tree, my_data, nSearch=150,
  swappers=list(RootedTBRSwap, RootedNNISwap),
  verbosity=0L)
write.nexus(ew.consensus, file=paste0("TreeSearch/hy_ew_", Fitch(ew.tree, my_data), ".nex", collapse=''))

```

2.3 Results

2.3.1 Implied weights results

```

# Read results from files
iw.trees <- lapply(kValues, function (k) {
  iw.best <- list.files('TreeSearch',
    pattern=paste0('hy_iw_k',
      gsub('\\.', '\\\\\\\\.', k),
      '_\\d+\\.?.\\d*\\.all\\.nex'),
    full.names=TRUE)

  # Return:
  if (length(iw.best) == 0) {
    list()
  } else {
    read.nexus(iw.best[which.max(file.mtime(iw.best))])
  }
})

```

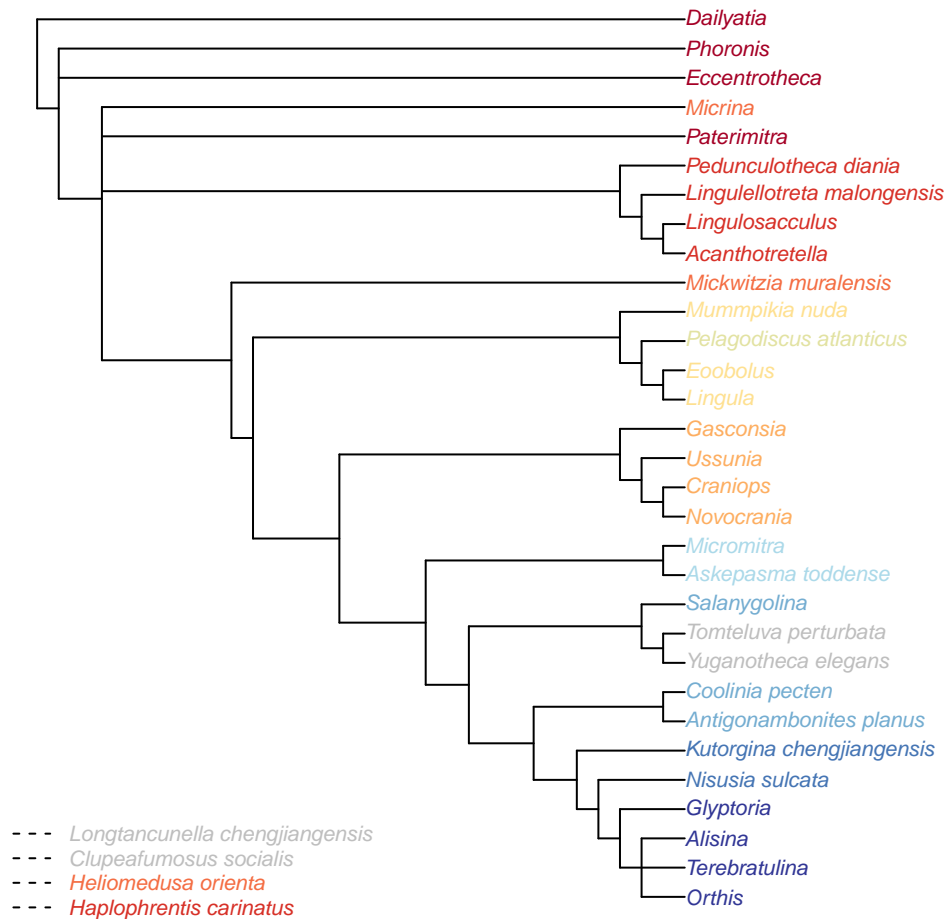


Figure 2.1: Consensus of implied weights analyses at all values of k

```
omit=c(lon, 'Clupeafumosus_socialis',
        'Heliomedusa_orienta', 'Haplophrentis_carinatus')
ColPlot(ConsensusWithout(lapply(iw.trees, consensus), omit))
ColMissing(omit)

# Plot consensus results
par(mfrow=c(4, 2), mar=rep(0.2, 4))

ColPlot(consensus(lapply(iw.trees, consensus)))
text(-0.5, 1, pos=4, "Consensus of all k values", cex=0.8)

# Plot results for each value of k
for (i in seq_along(iw.trees)) {
  ColPlot(consensus(iw.trees[[i]]))
  text(1, 1, paste0('k = ', kValues[i]), pos=4)
}
```

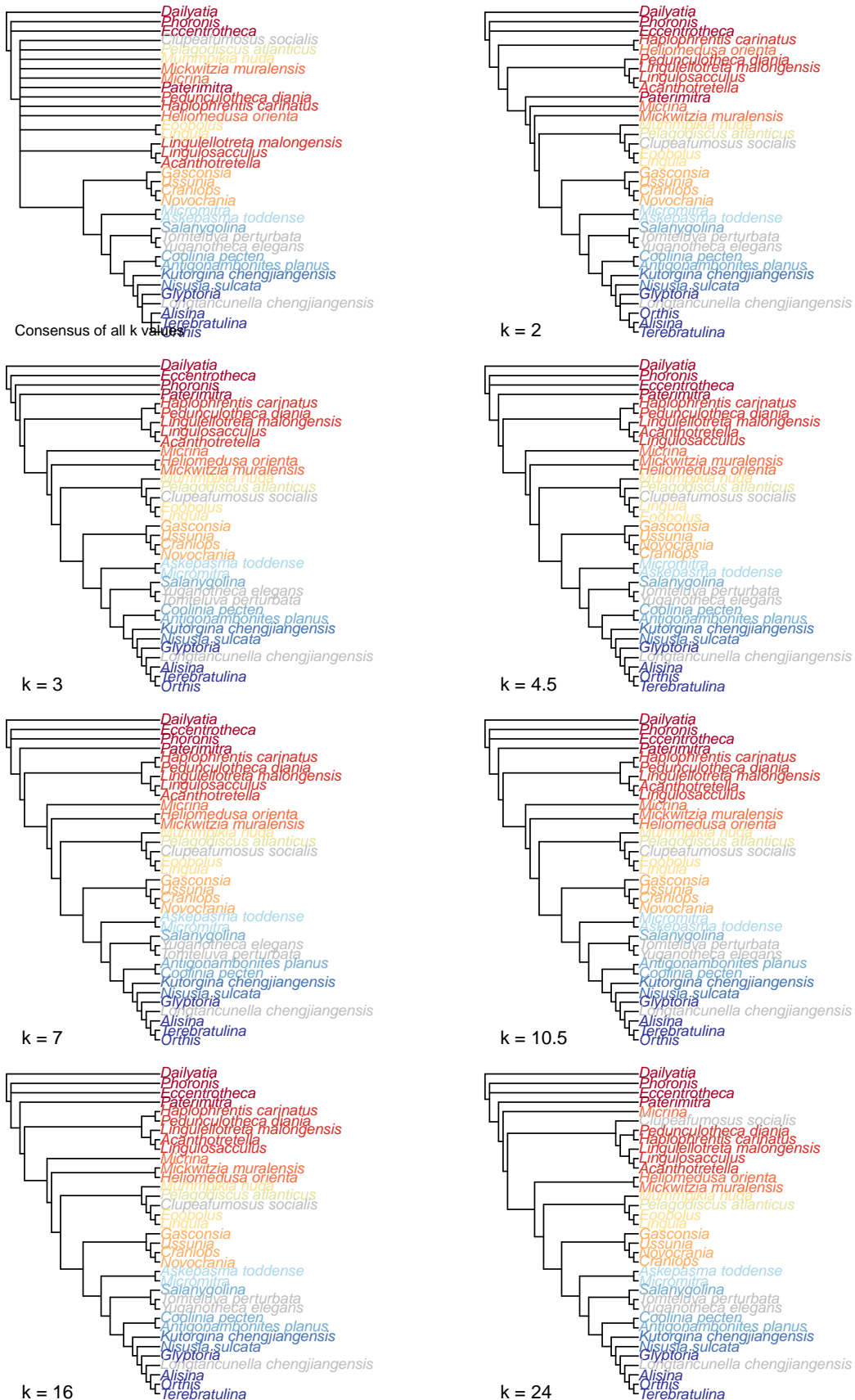


Figure 2.2: Implied weights results

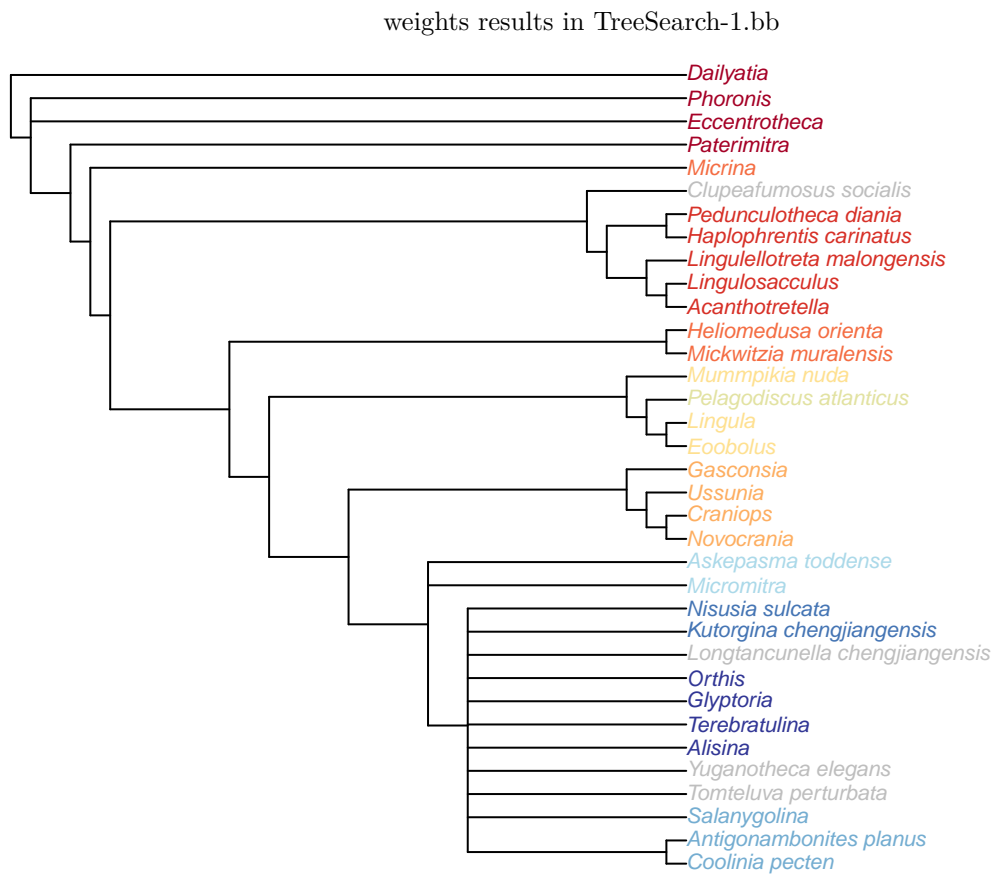


Figure 2.3: (#fig:equal weights results in TreeSearch)Strict consensus of equal weights results

2.3.2 Equal weights results

```
ew.best <- list.files('TreeSearch', pattern='hy_ew_\\d*\\.nex', full.names=TRUE)
ew.tree <- read.nexus(file=ew.best[which.max(file.mtime(ew.best))])
ColPlot(consensus(ew.tree))

omit <- c(lon)
ColPlot(ConsensusWithout(ew.tree, omit))
ColMissing(omit)
```

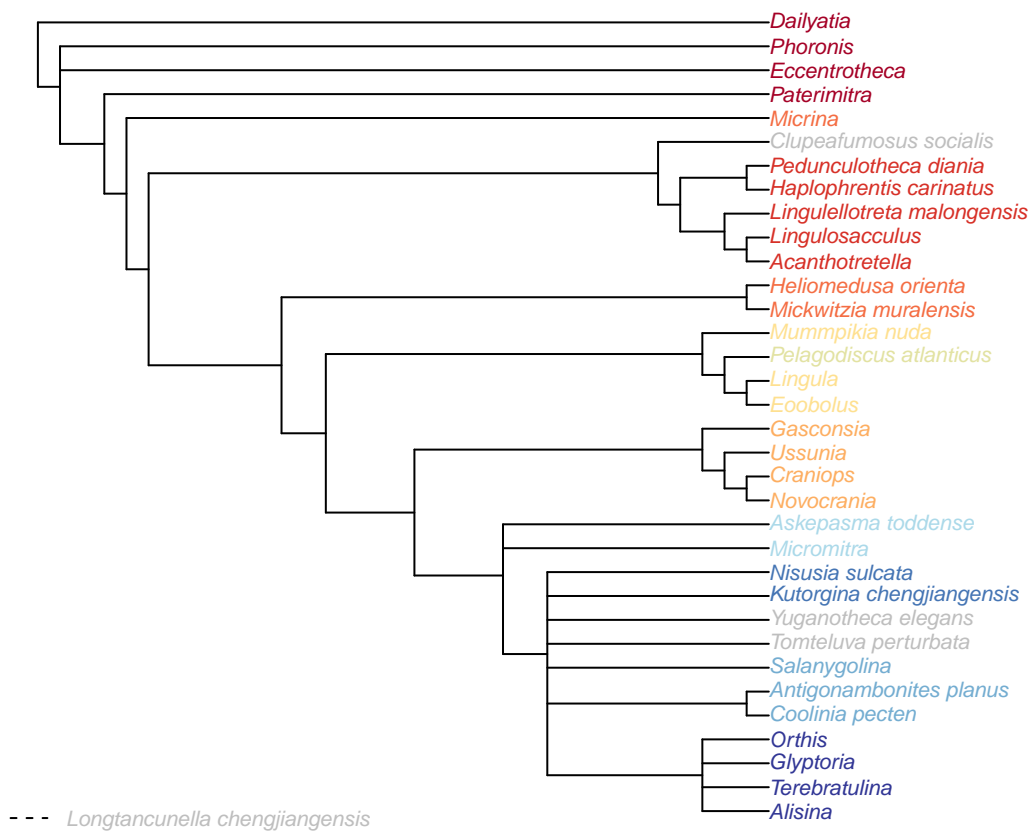
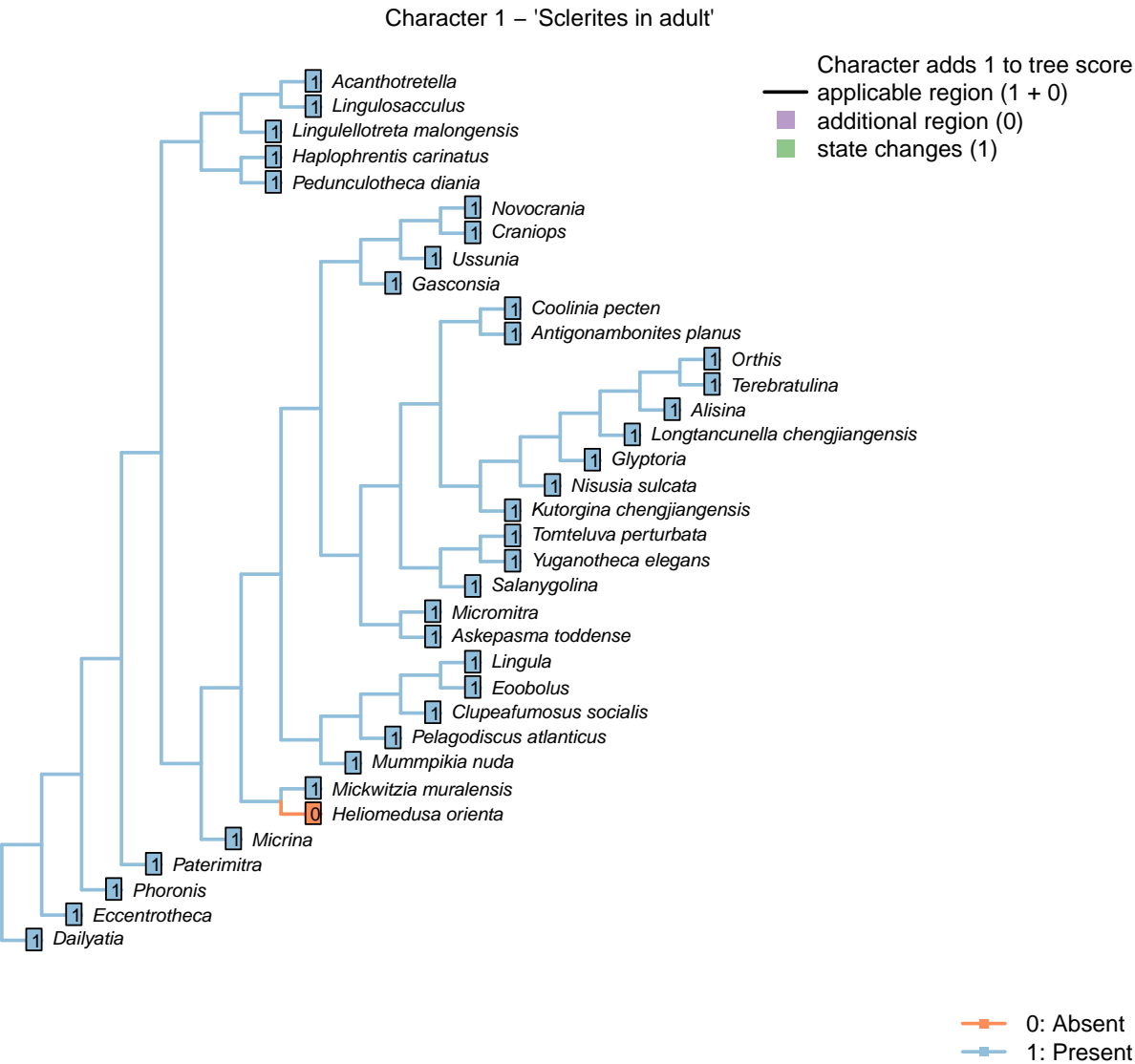


Figure 2.4: Strict consensus of equal weights results, taxa excluded

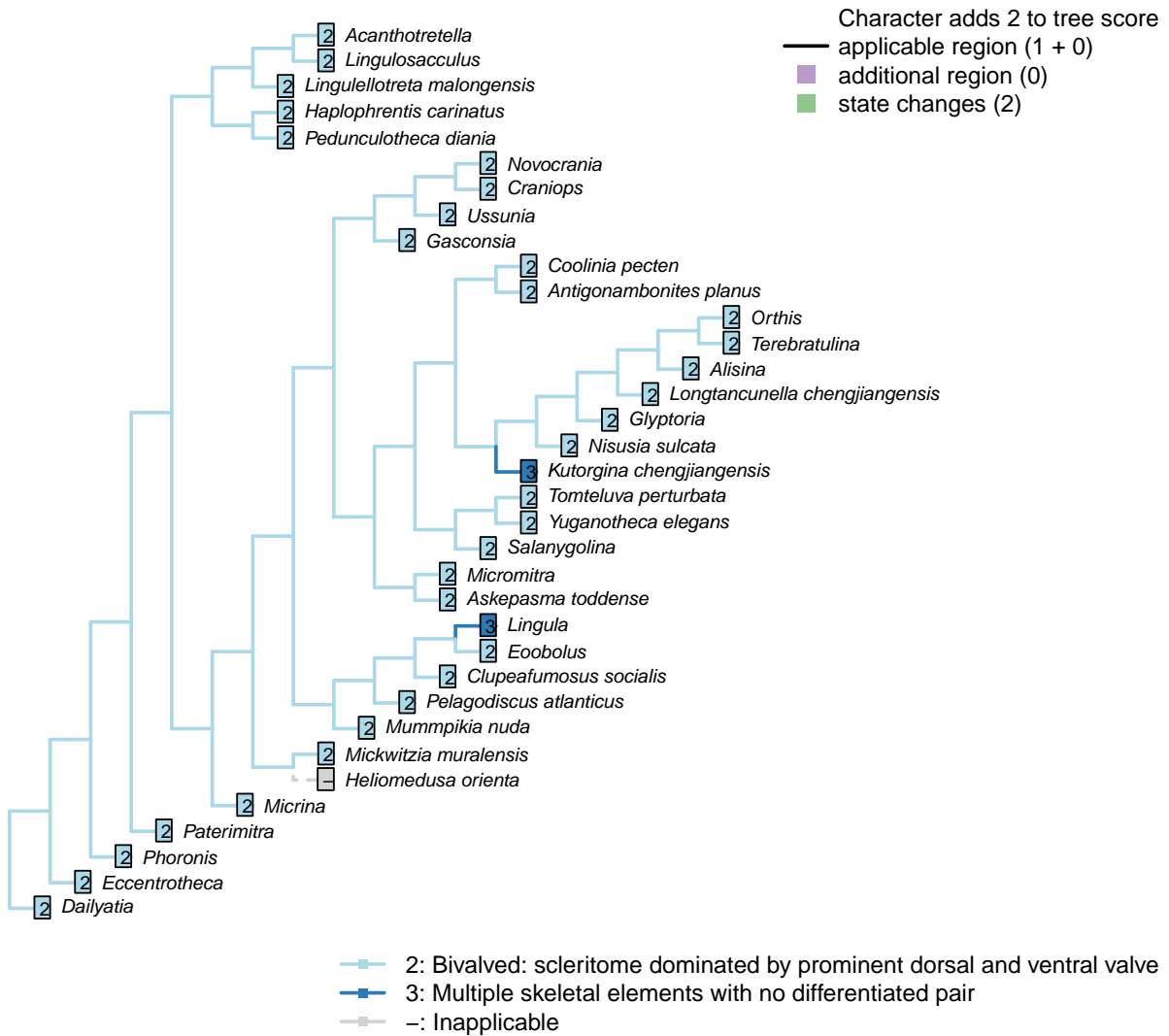
Chapter 3

Character reconstructions

Here's how each character maps onto one of the most parsimonious trees (obtained under implied weighting, $k = 4.5$):

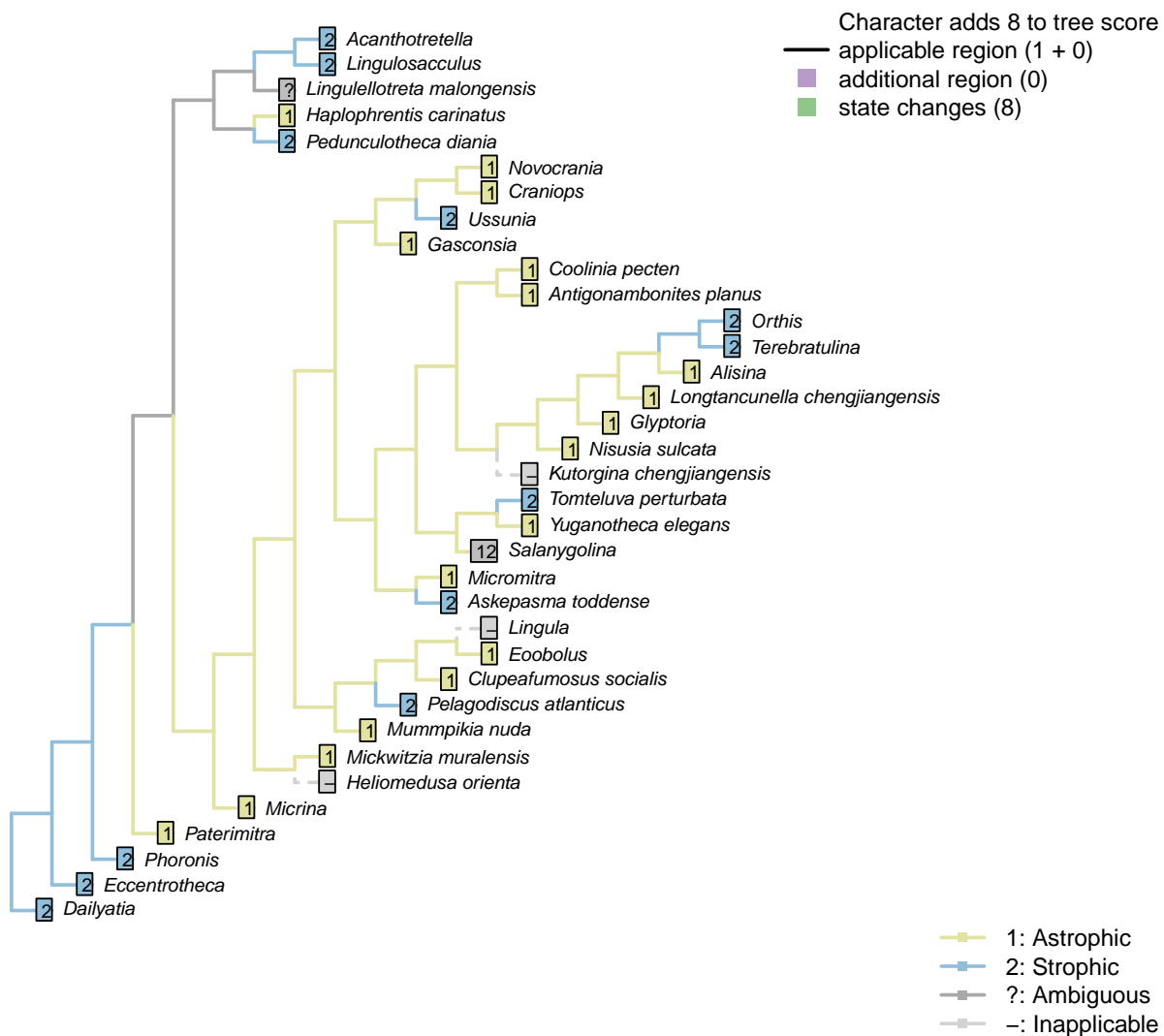


Character 2 – 'Sclerites: disposition'



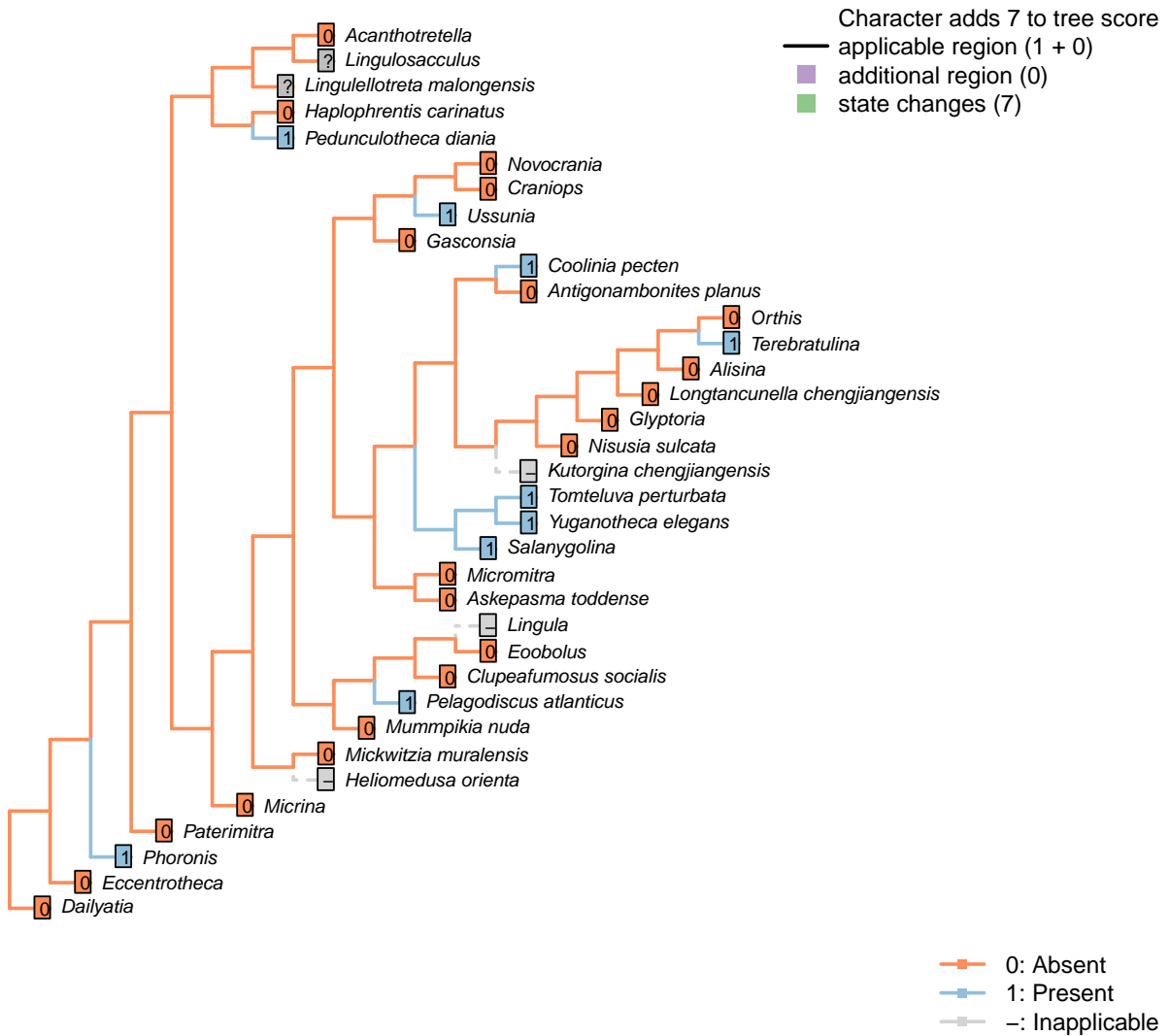
Character 2 – 'Sclerites: disposition'

Character 3 – 'Sclerites: Bivalved: Hinge line shape'



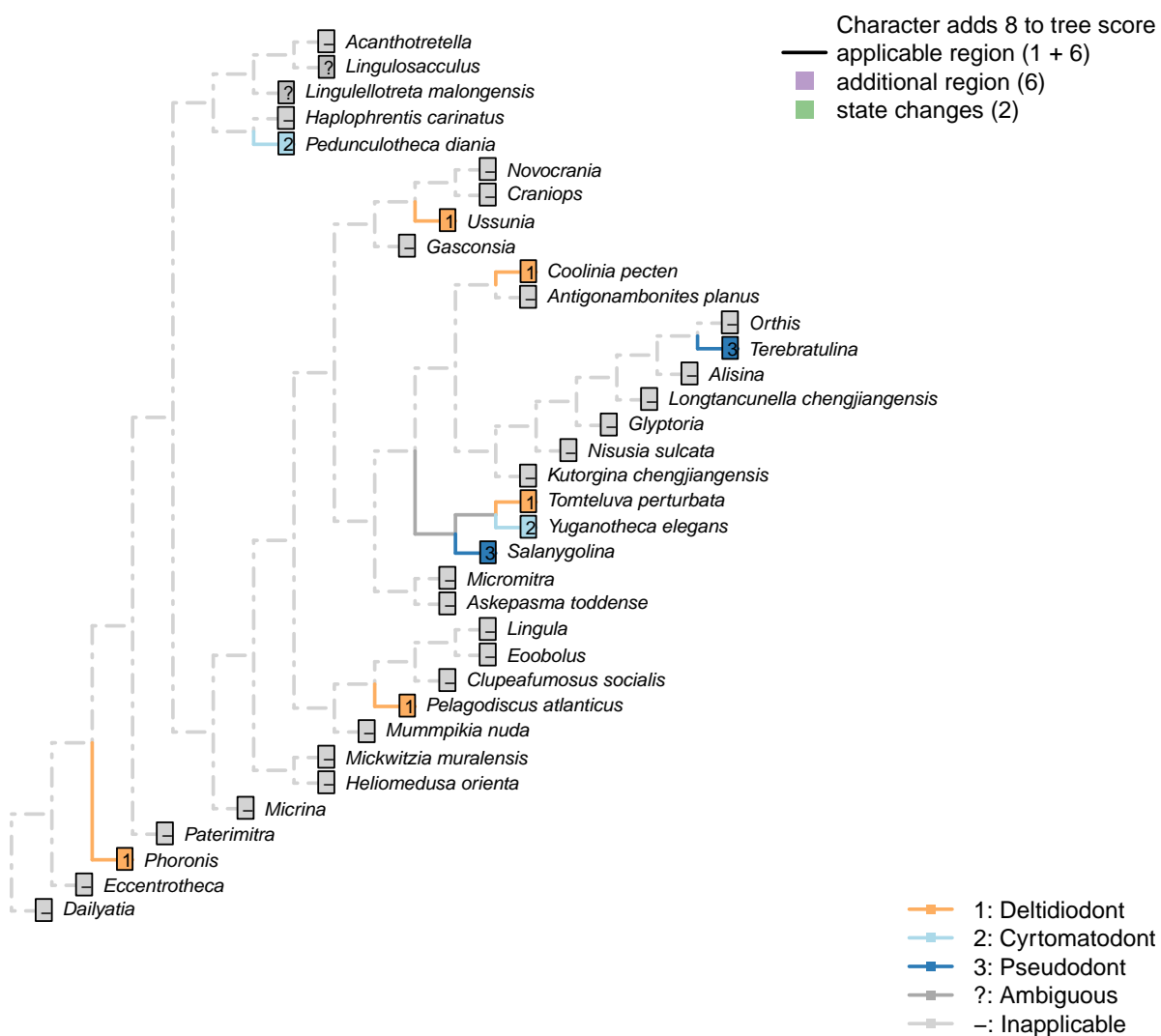
Character 3 – 'Sclerites: Bivalved: Hinge line shape'

Character 4 – 'Sclerites: Bivalved: Apophyses'



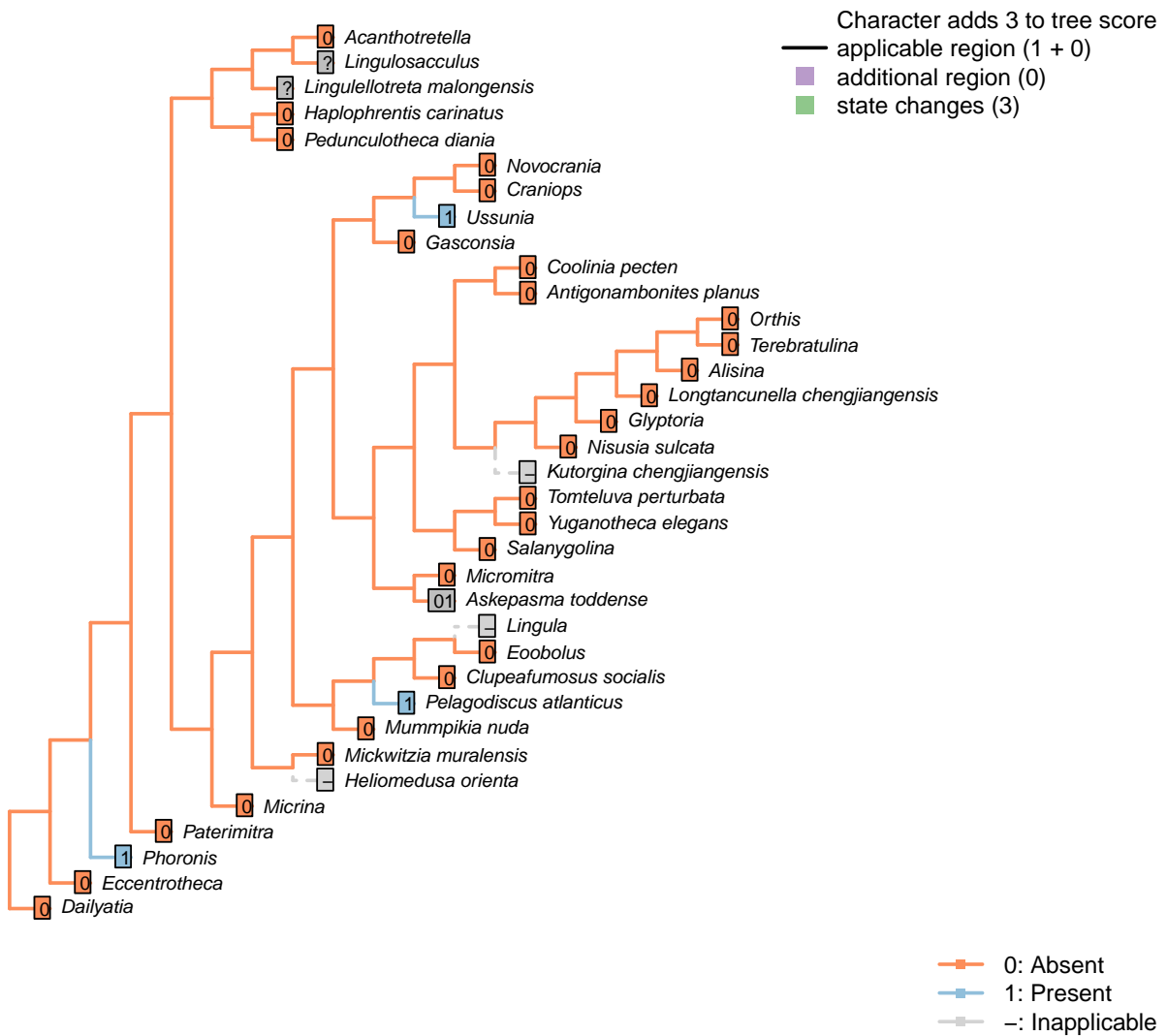
Character 4 – 'Sclerites: Bivalved: Apophyses'

Character 5 – 'Sclerites: Bivalved: Apophyses: Morphology'



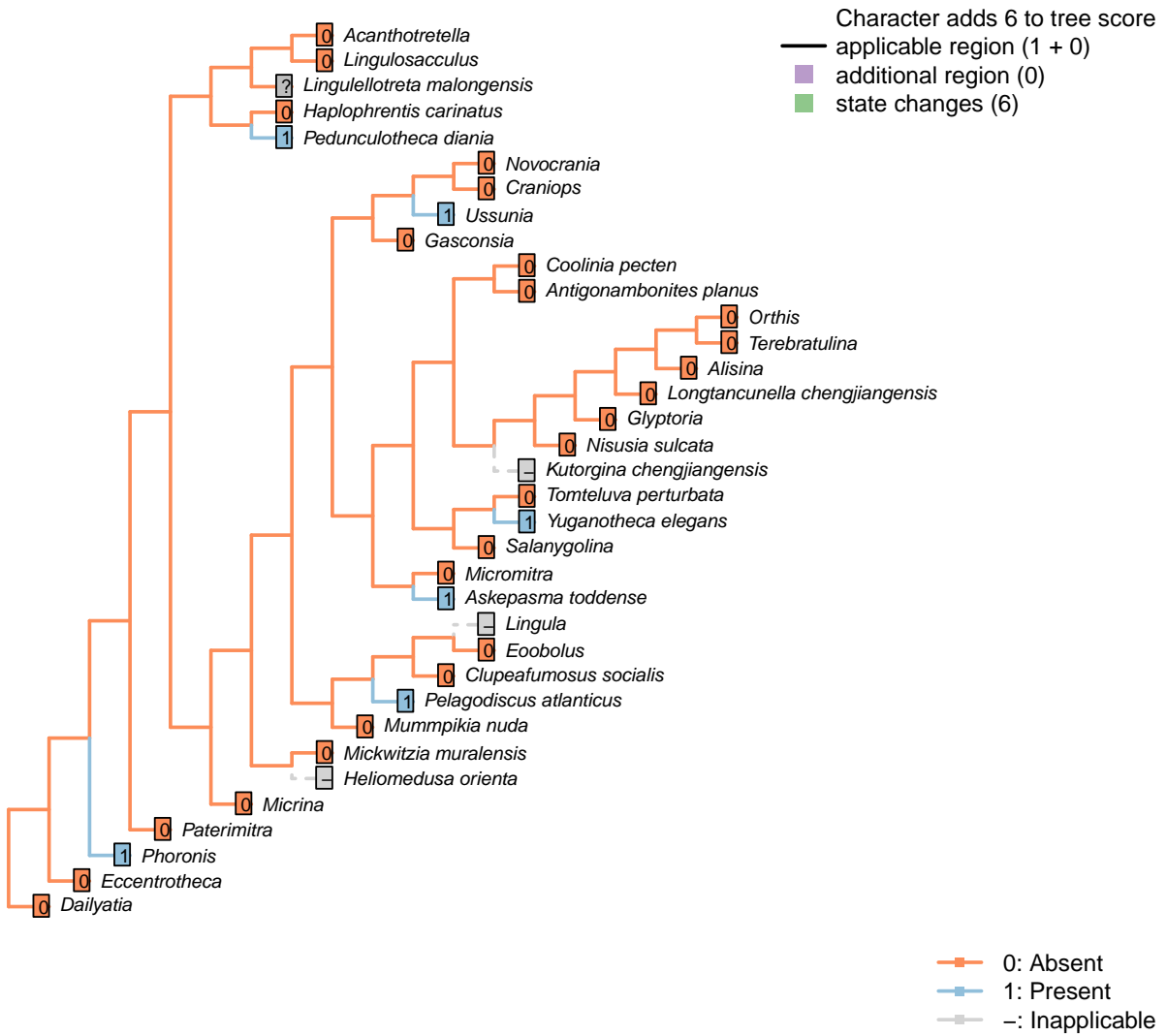
Character 5 – 'Sclerites: Bivalved: Apophyses: Morphology'

Character 6 – 'Sclerites: Bivalved: Apophyses: Dental plates'

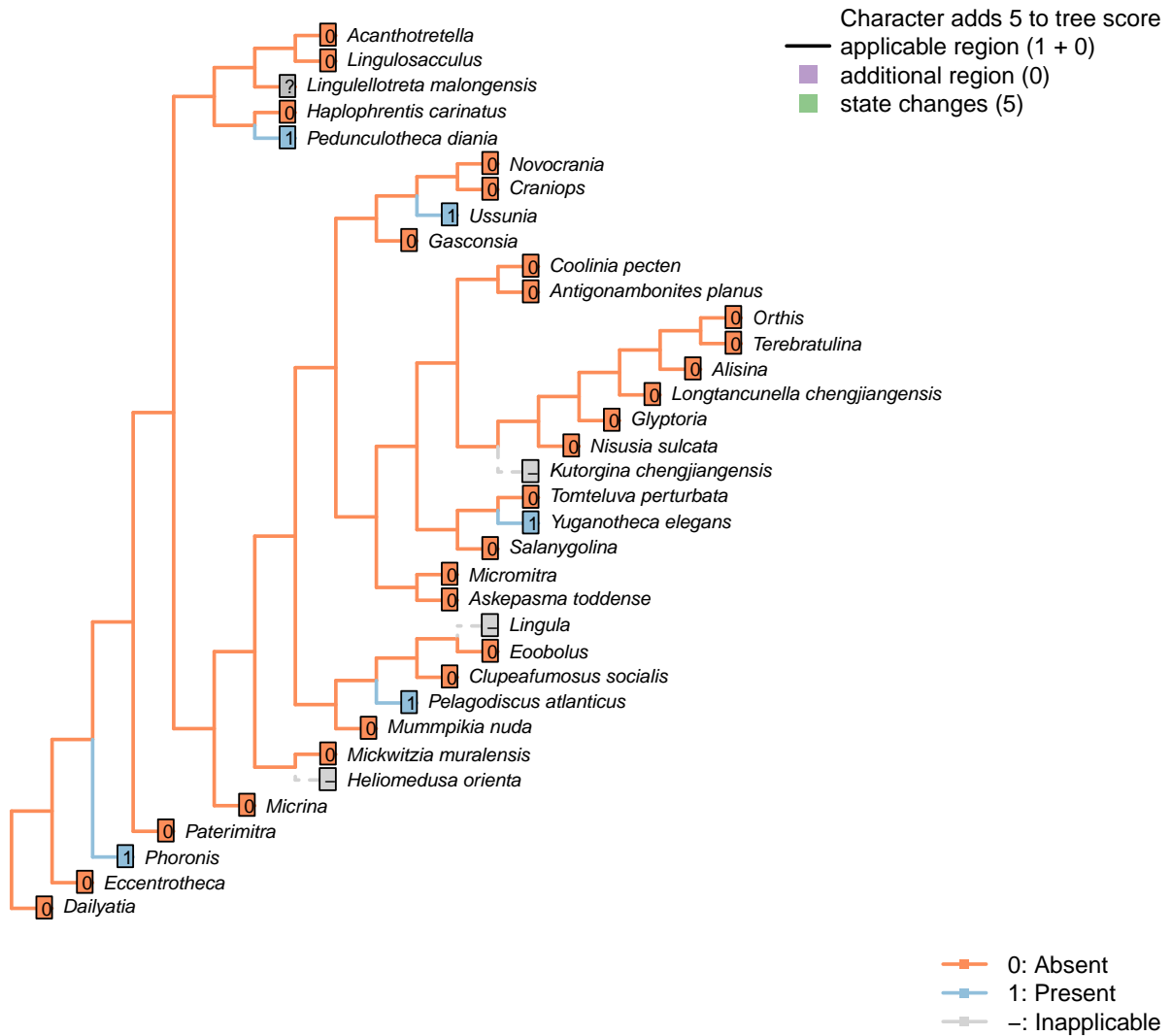


Character 6 – 'Sclerites: Bivalved: Apophyses: Dental plates'

Character 7 – 'Sclerites: Bivalved: Sockets'

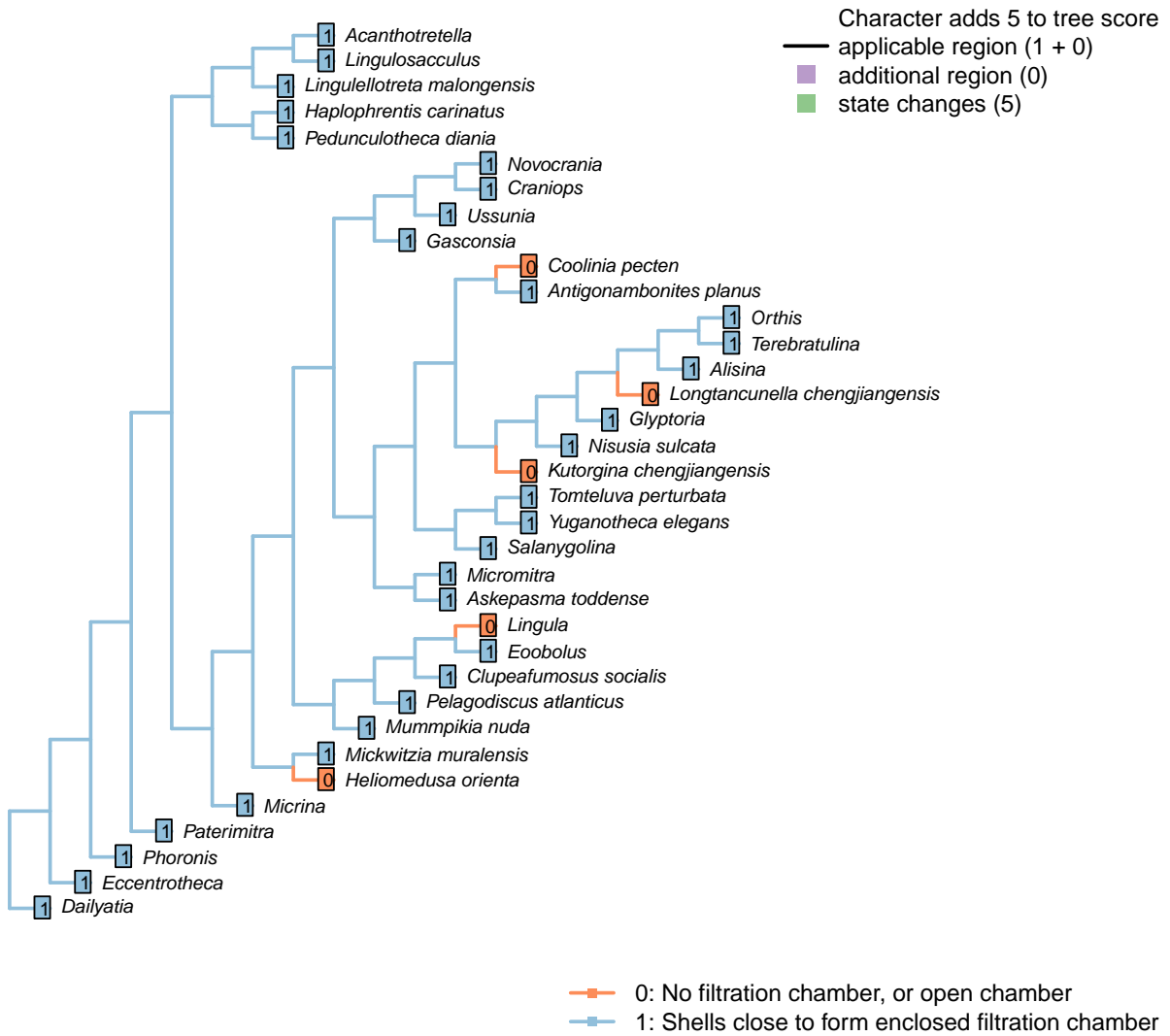


Character 8 – 'Sclerites: Bivalved: Socket ridges'



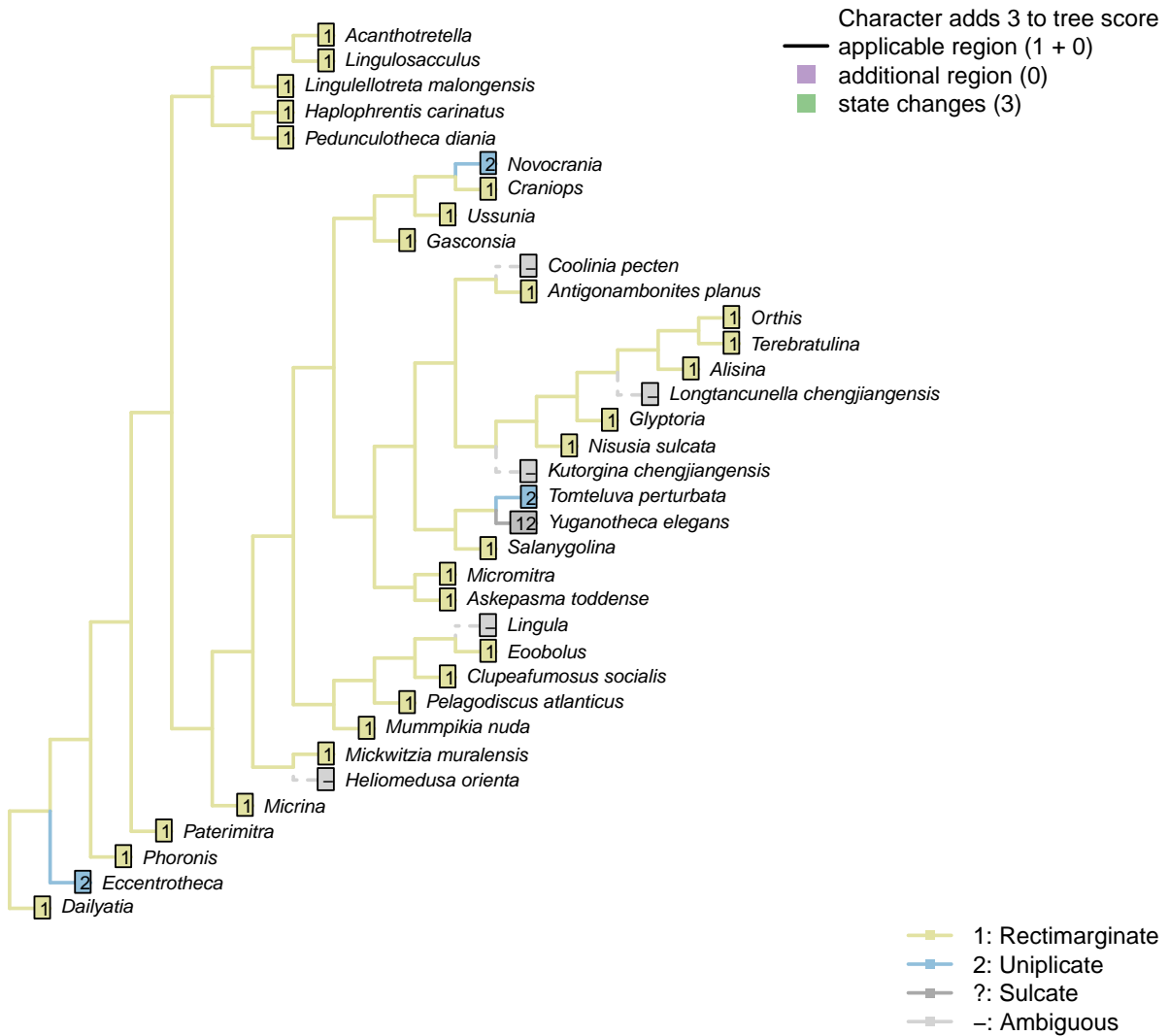
Character 8 – 'Sclerites: Bivalved: Socket ridges'

Character 9 – 'Sclerites: Bivalved: Enclosing filtration chamber'

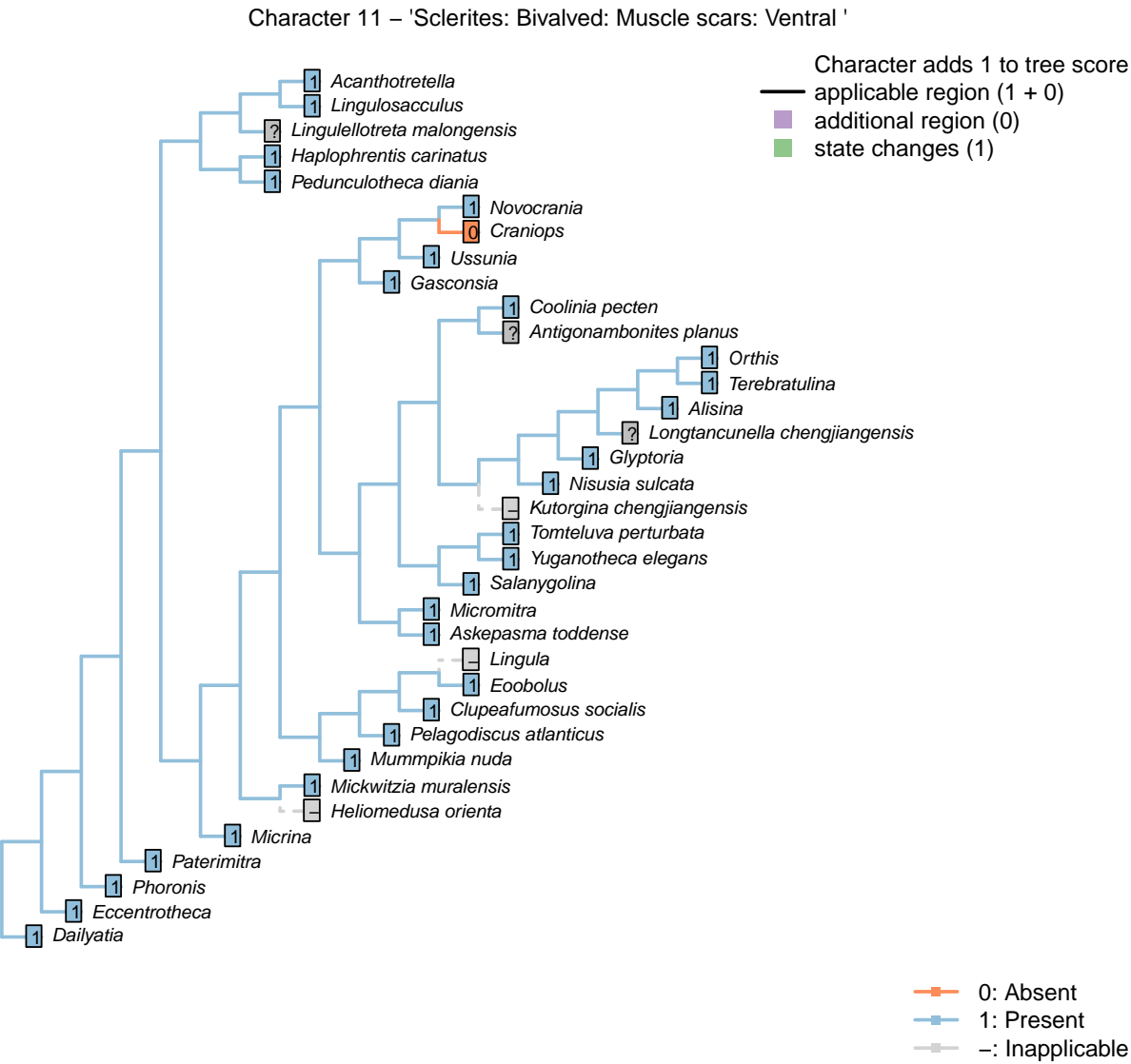


Character 9 – 'Sclerites: Bivalved: Enclosing filtration chamber'

Character 10 – 'Sclerites: Bivalved: Commissure'

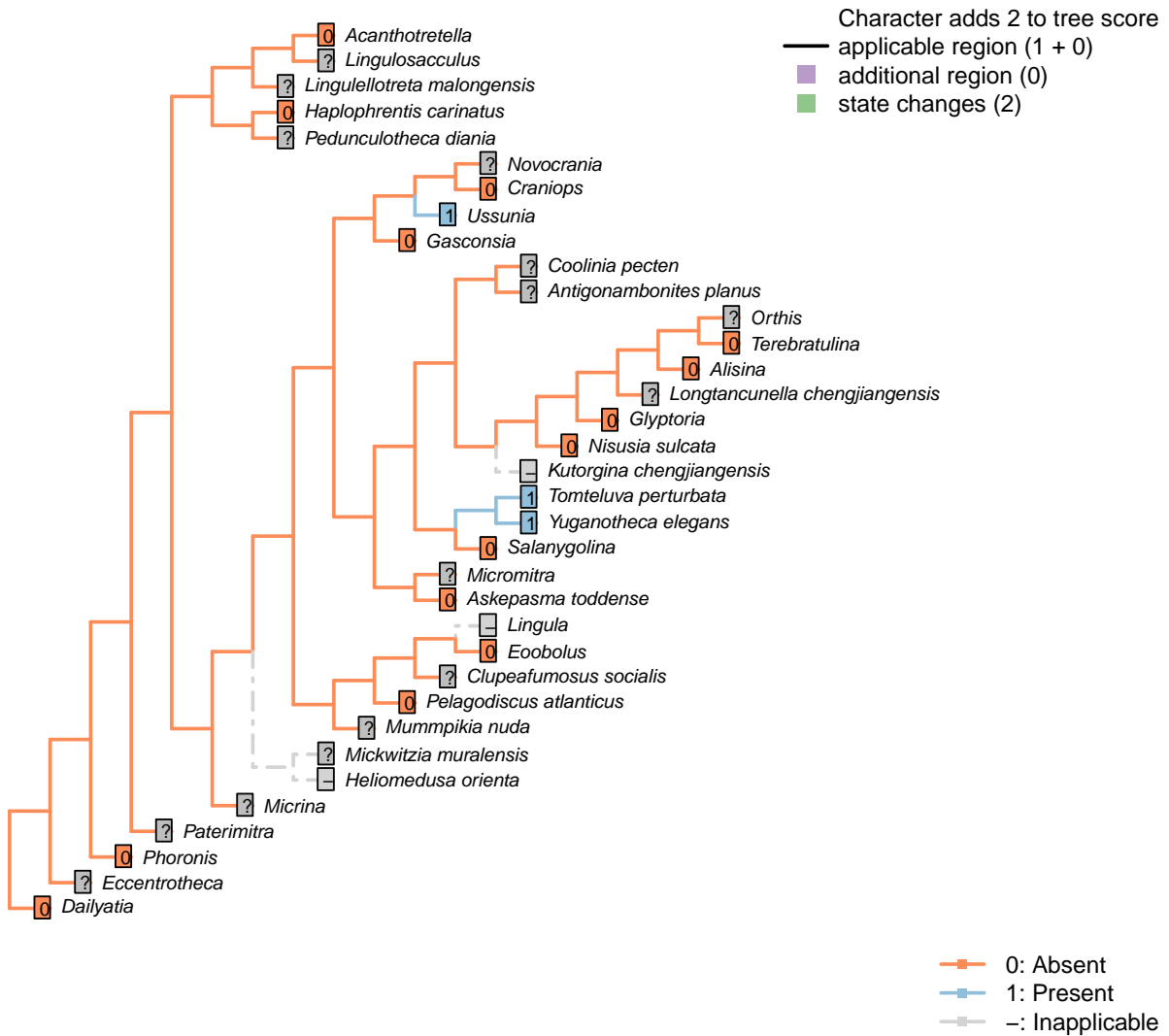


Character 10 – 'Sclerites: Bivalved: Commissure'



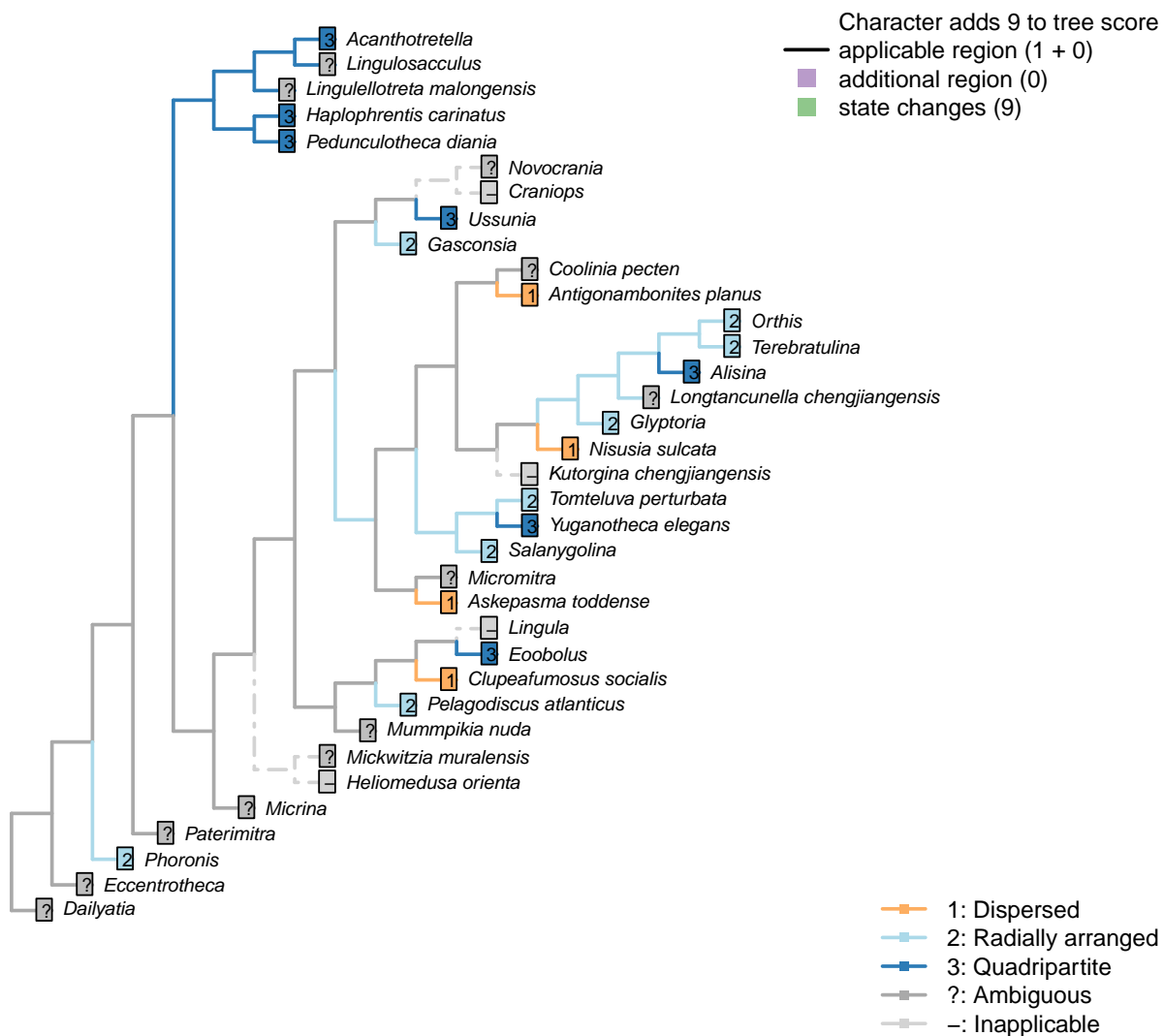
Character 11 – 'Sclerites: Bivalved: Muscle scars: Ventral '

Character 12 – 'Sclerites: Bivalved: Muscle scars: Adjustor'



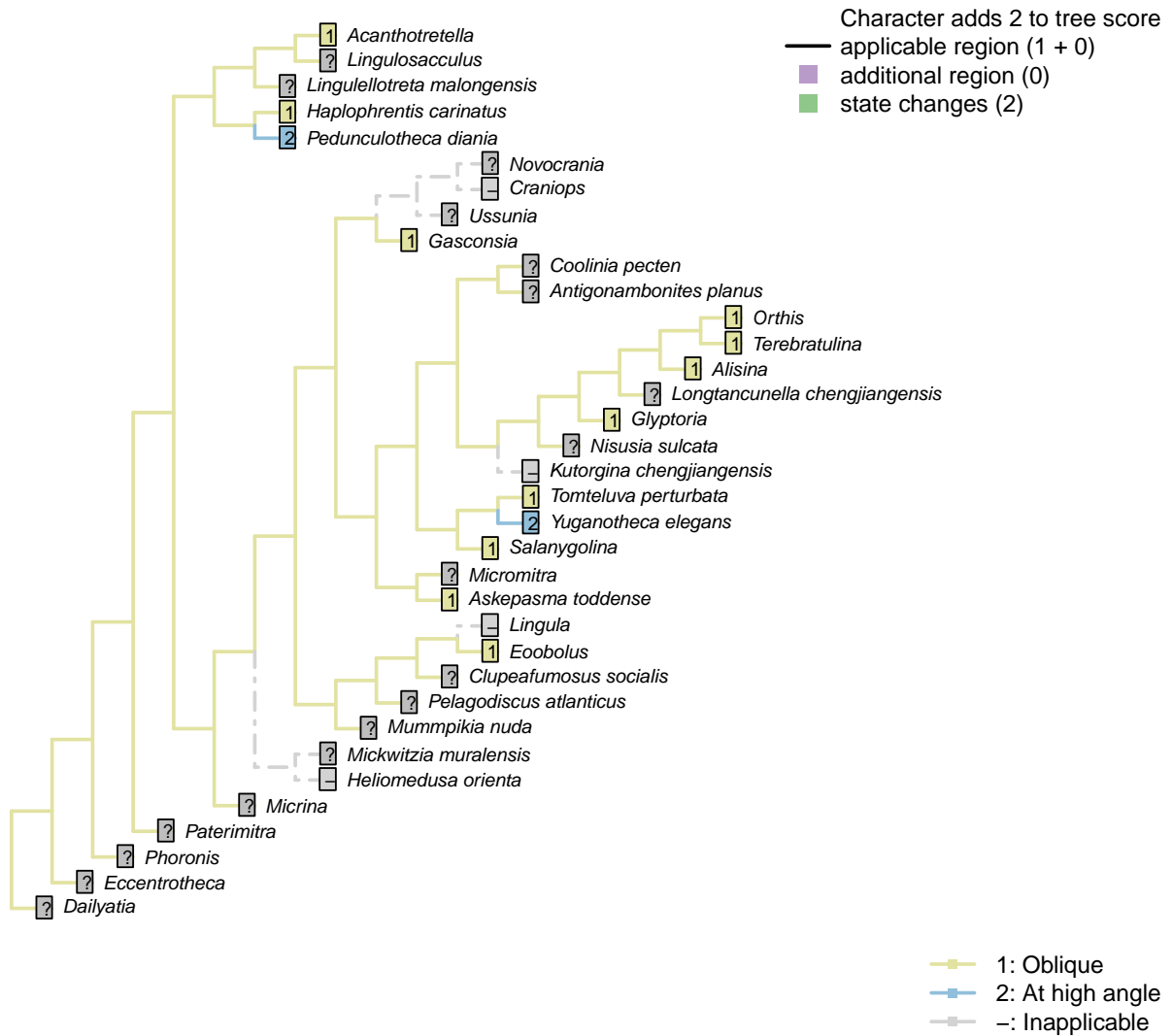
Character 12 – 'Sclerites: Bivalved: Muscle scars: Adjustor'

Character 13 – 'Sclerites: Bivalved: Muscle scars: Dorsal adductor'



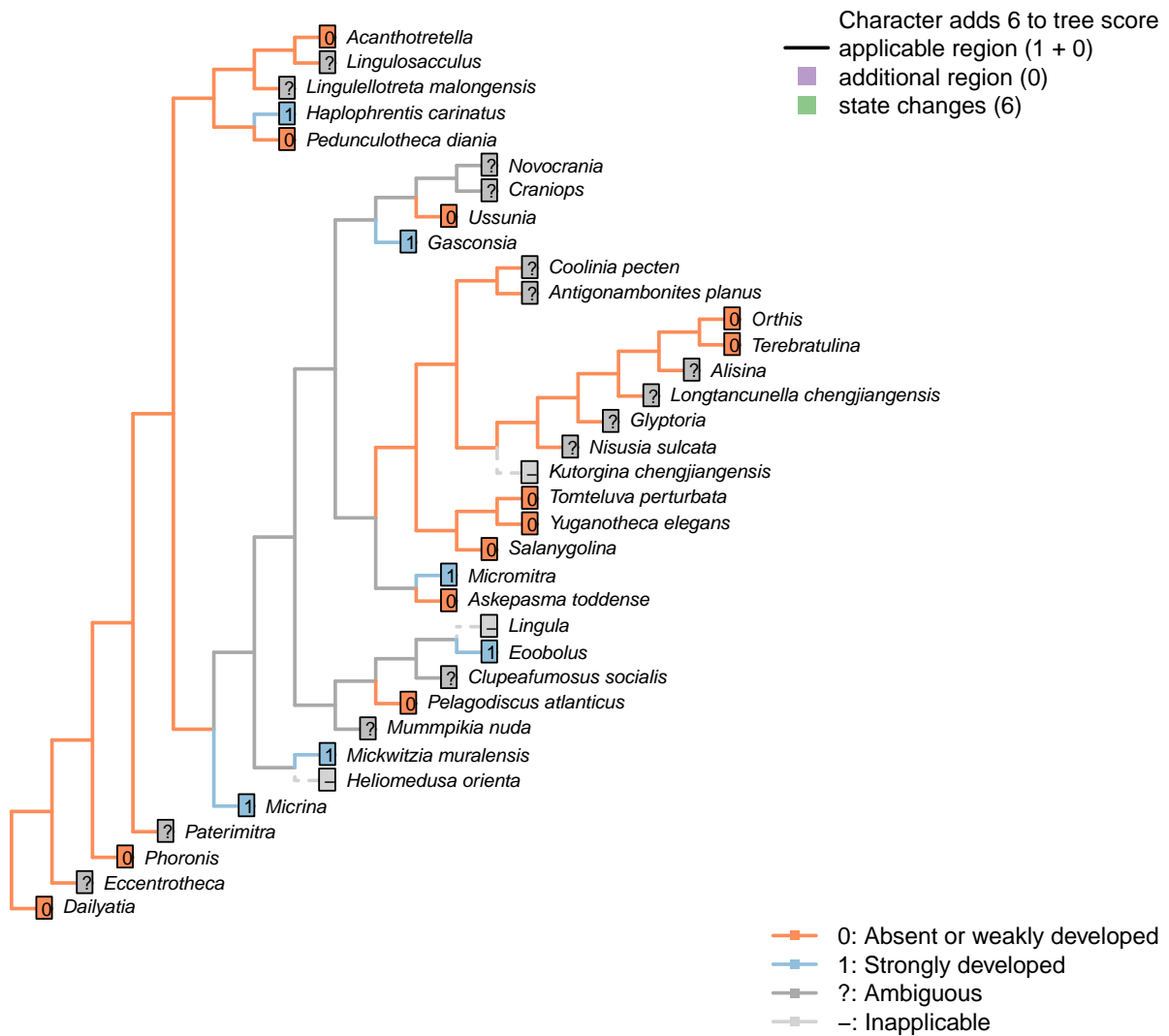
Character 13 – 'Sclerites: Bivalved: Muscle scars: Dorsal adductor'

Character 14 – 'Sclerites: Bivalved: Muscle scars: Adductors: Position'



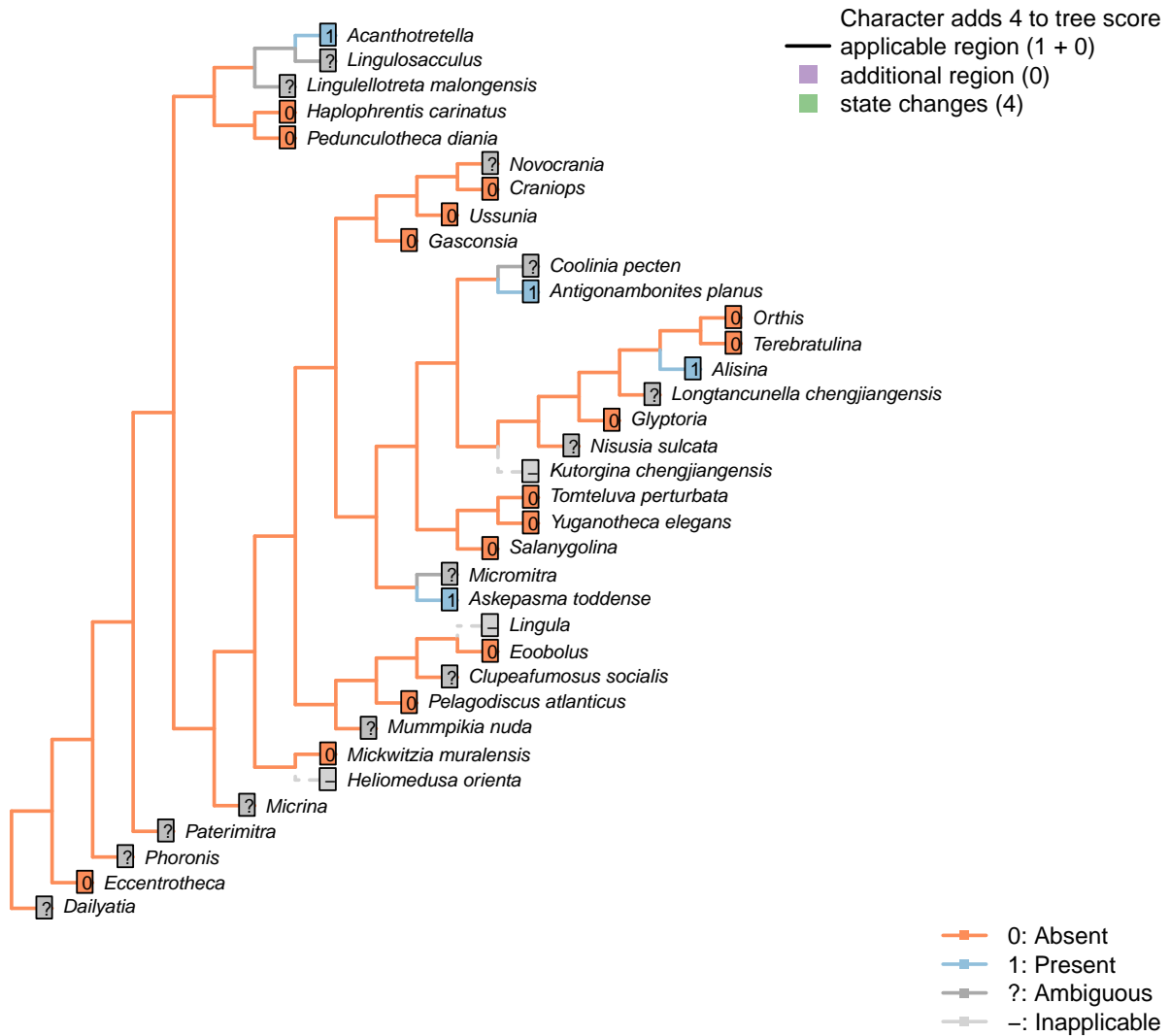
Character 14 – 'Sclerites: Bivalved: Muscle scars: Adductors: Position'

Character 15 – 'Sclerites: Bivalved: Muscle scars: Dermal muscles'



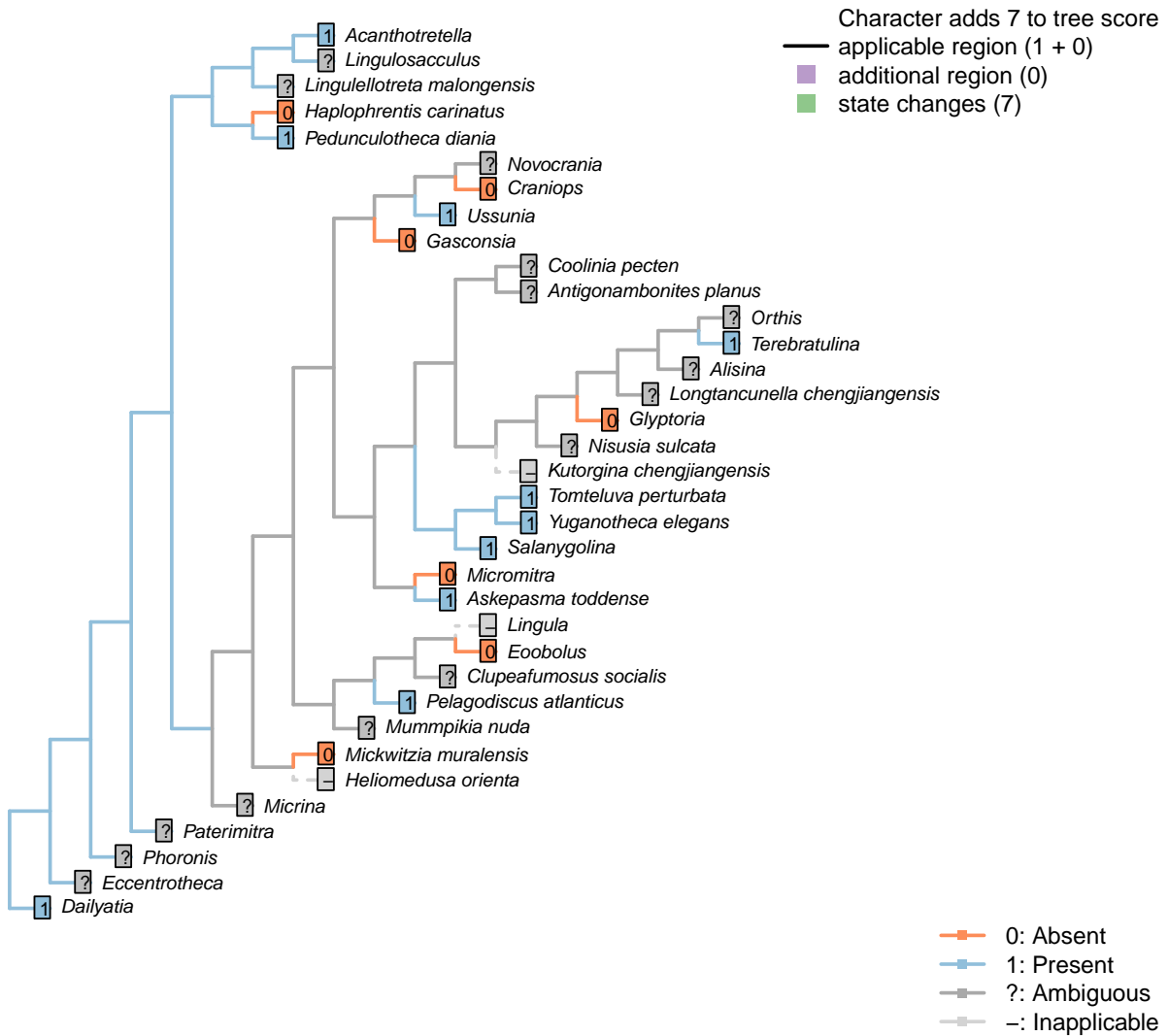
Character 15 – 'Sclerites: Bivalved: Muscle scars: Dermal muscles'

Character 16 – 'Sclerites: Bivalved: Muscle scars: Unpaired median (levator ani)'



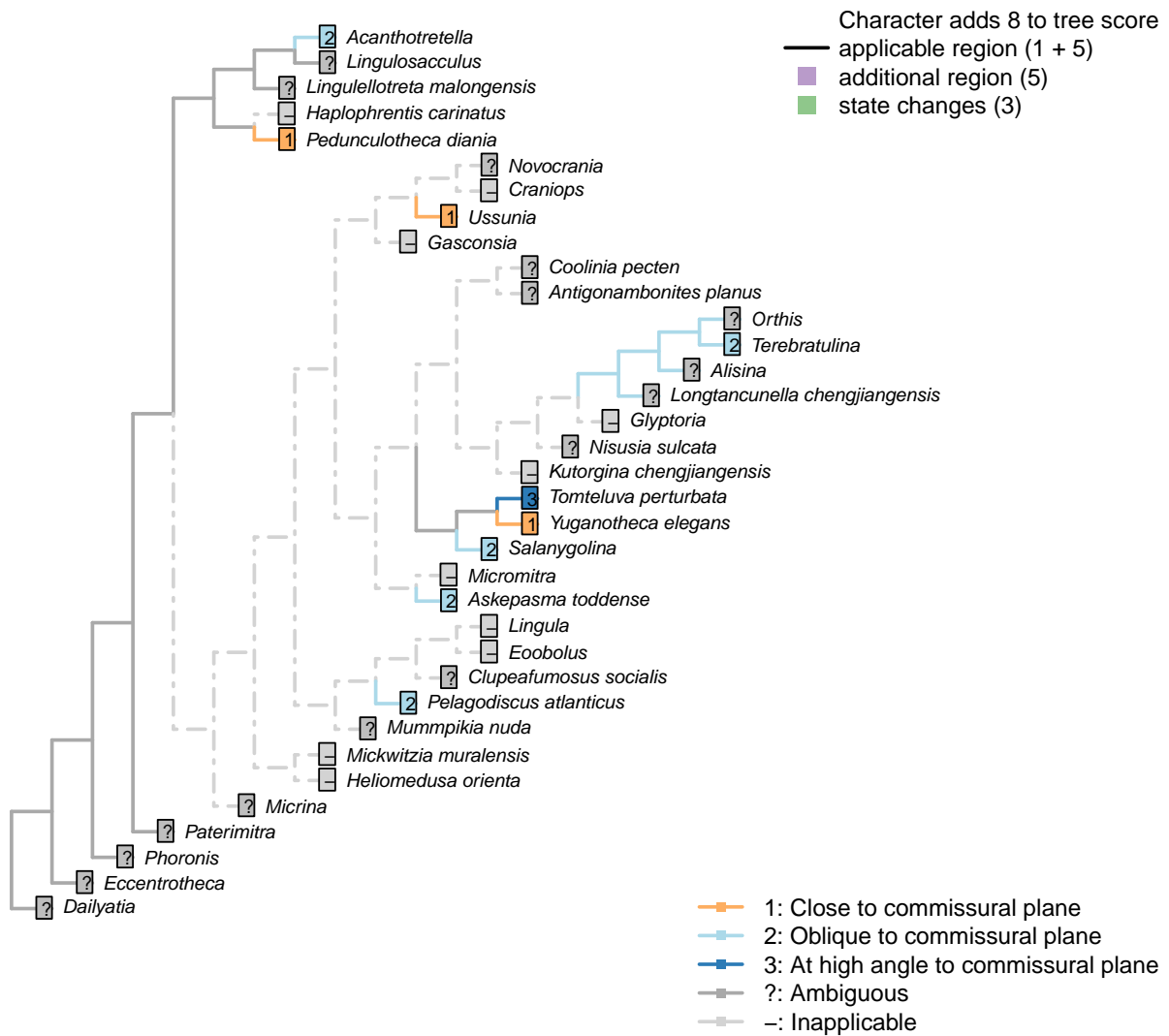
Character 16 – 'Sclerites: Bivalved: Muscle scars: Unpaired median (levator ani)'

Character 17 – 'Sclerites: Bivalved: Muscle scars: Dorsal diductor'



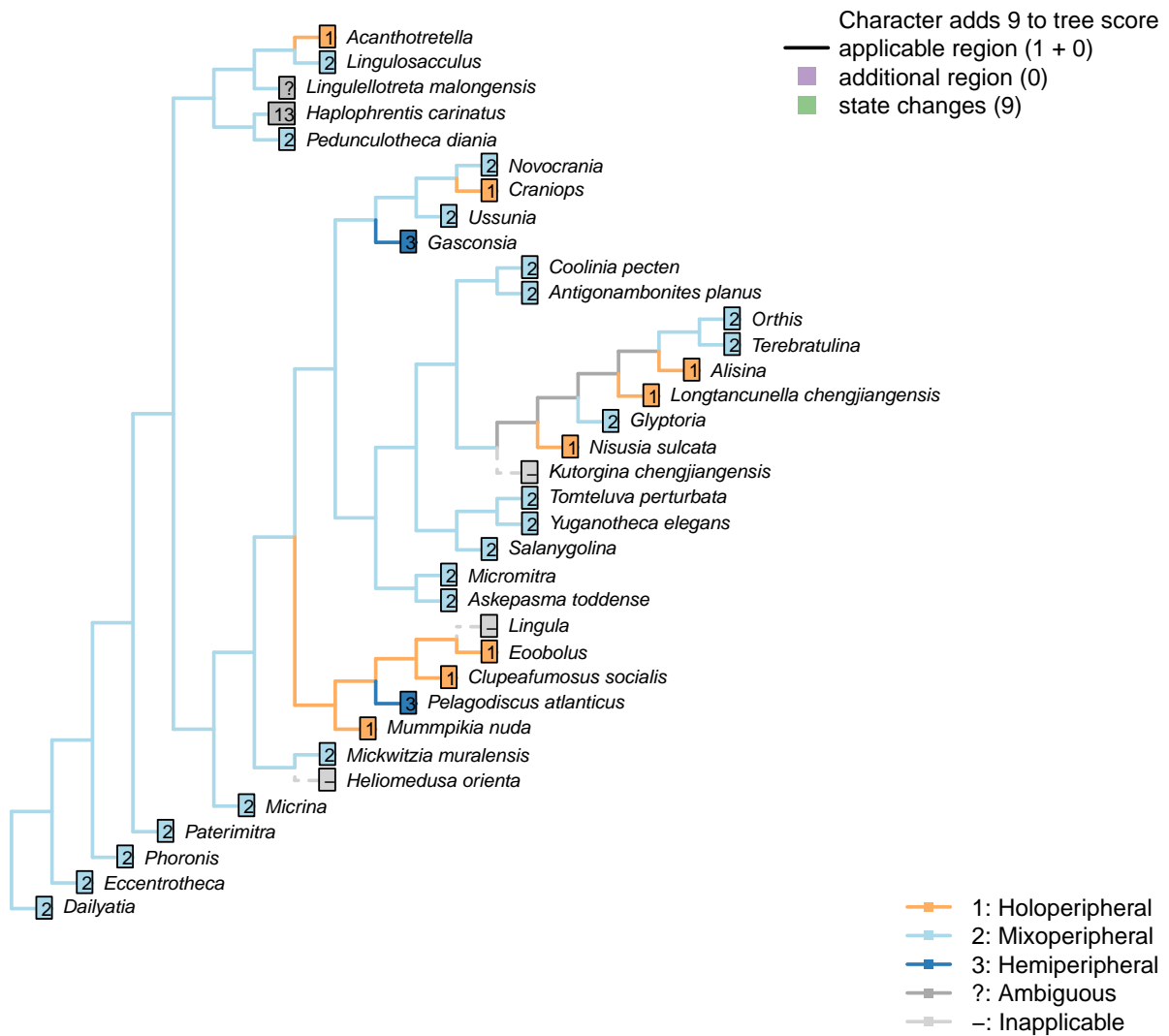
Character 17 – 'Sclerites: Bivalved: Muscle scars: Dorsal diductor'

Character 18 – 'Sclerites: Bivalved: Muscle scars: Dorsal diductor: position'



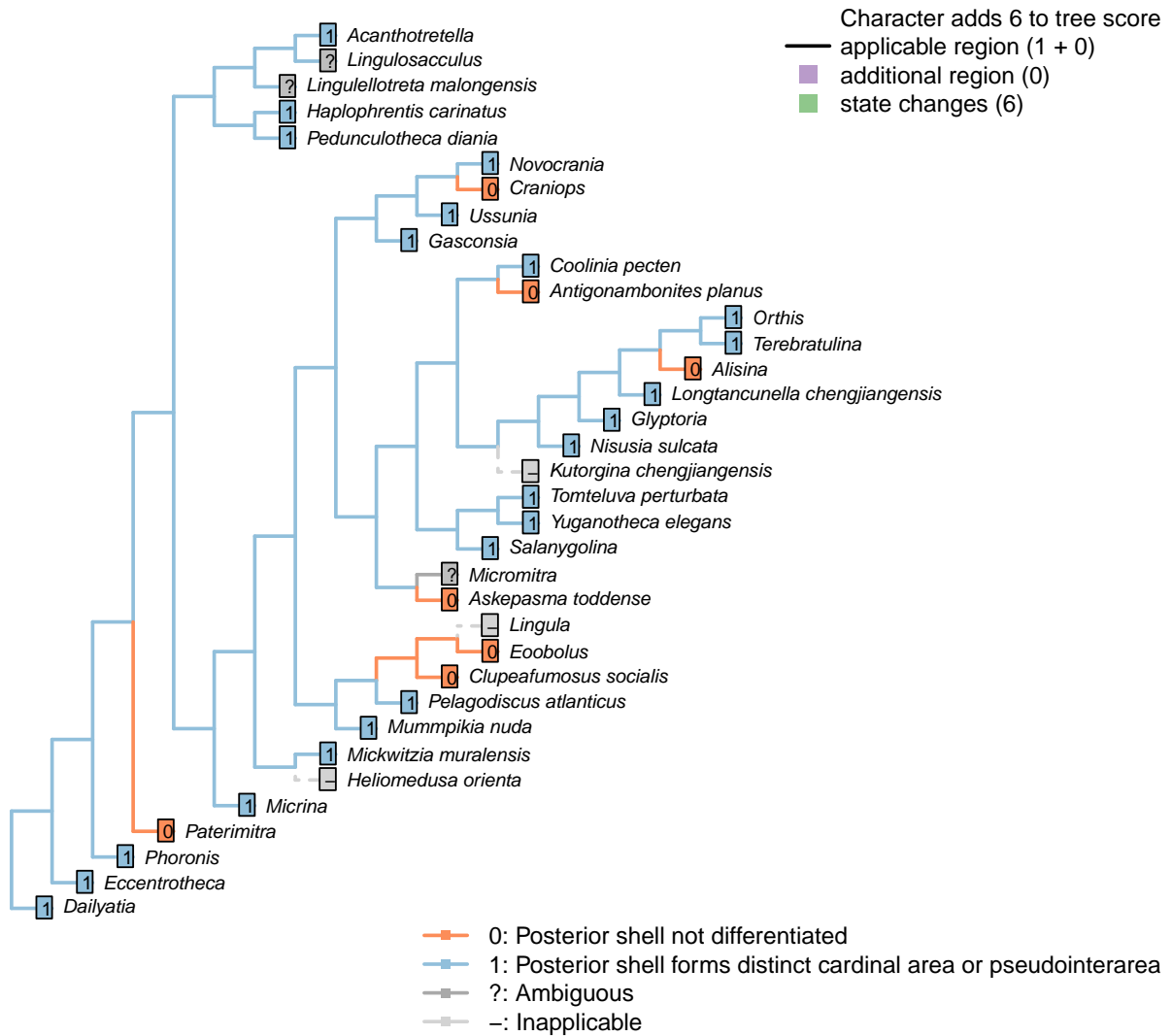
Character 18 – 'Sclerites: Bivalved: Muscle scars: Dorsal diductor: position'

Character 19 – 'Sclerites: Dorsal valve: Growth direction'



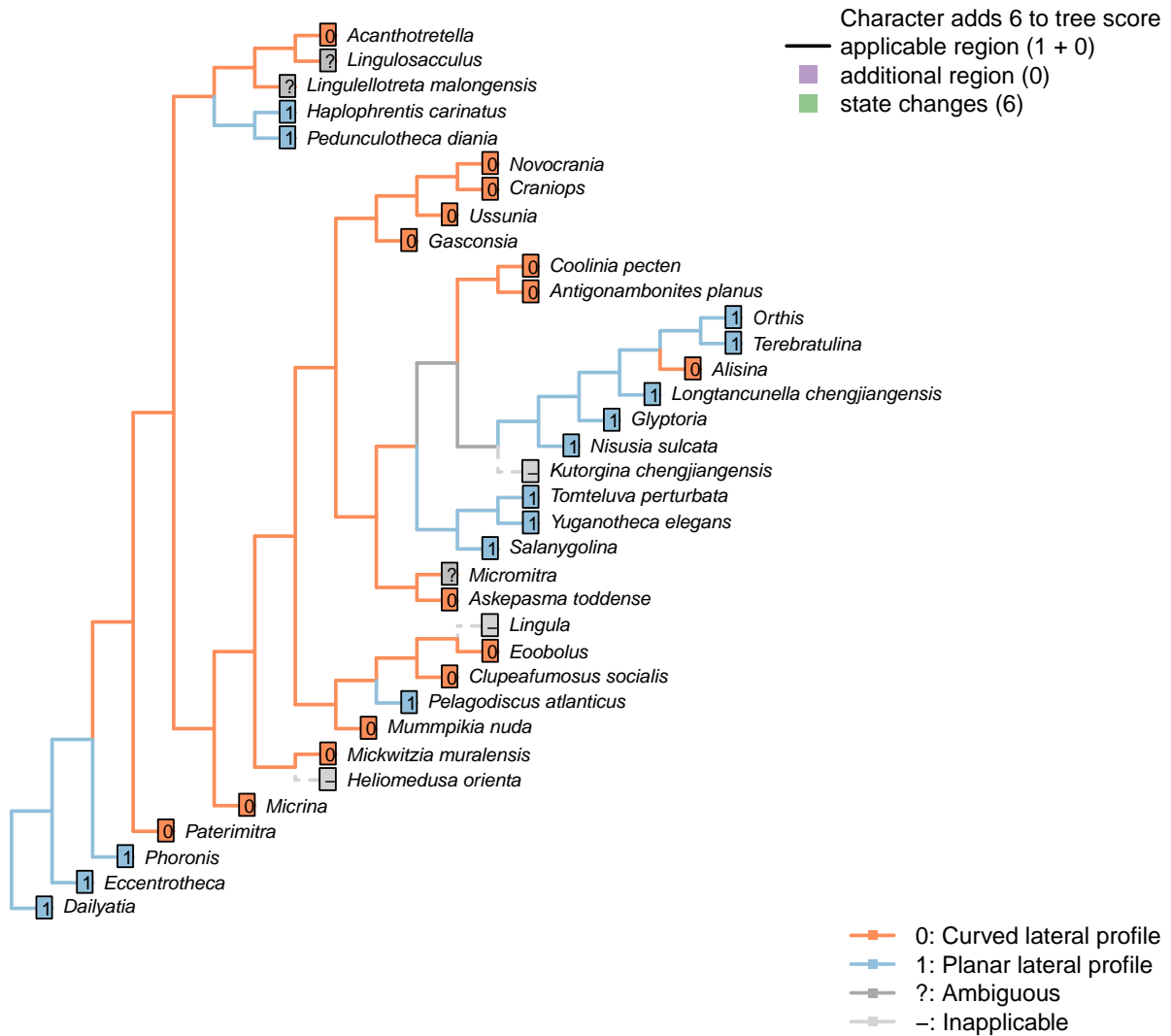
Character 19 – 'Sclerites: Dorsal valve: Growth direction'

Character 20 – 'Sclerites: Dorsal valve: Posterior surface: Differentiated'

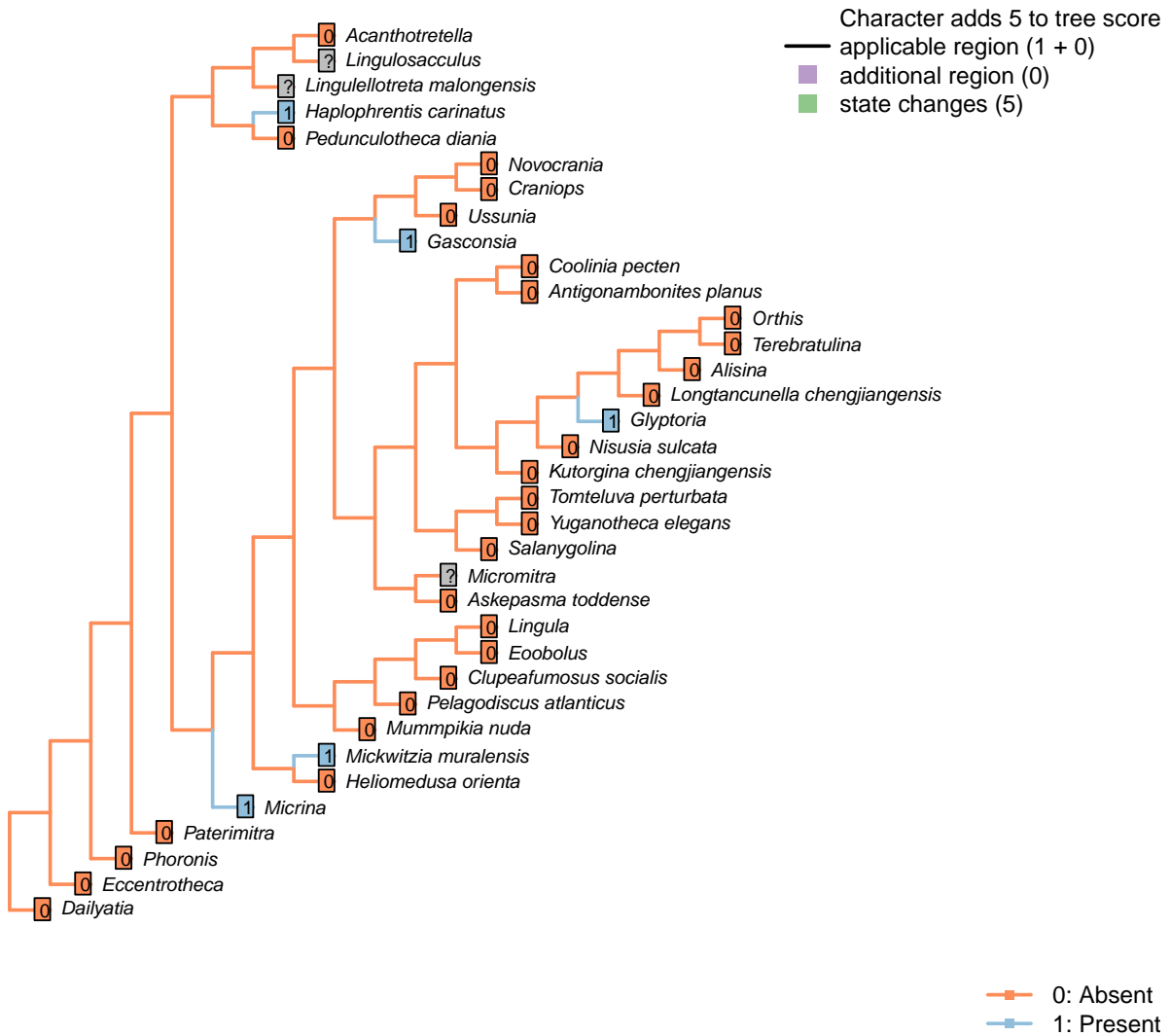


Character 20 – 'Sclerites: Dorsal valve: Posterior surface: Differentiated'

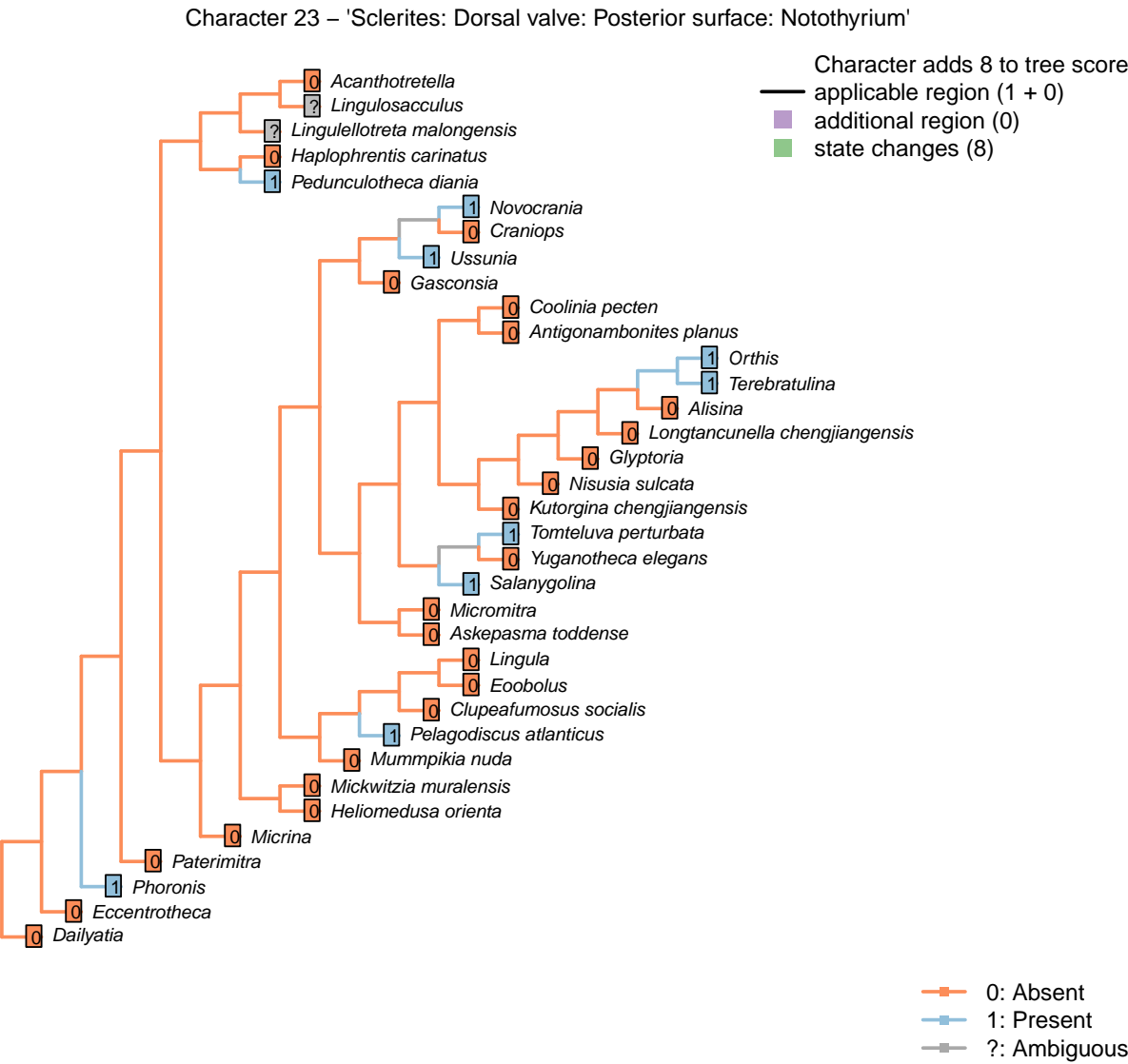
Character 21 – 'Sclerites: Dorsal valve: Differentiated posterior surface: Morphology'



Character 22 – 'Sclerites: Dorsal valve: Posterior surface: Medial groove'

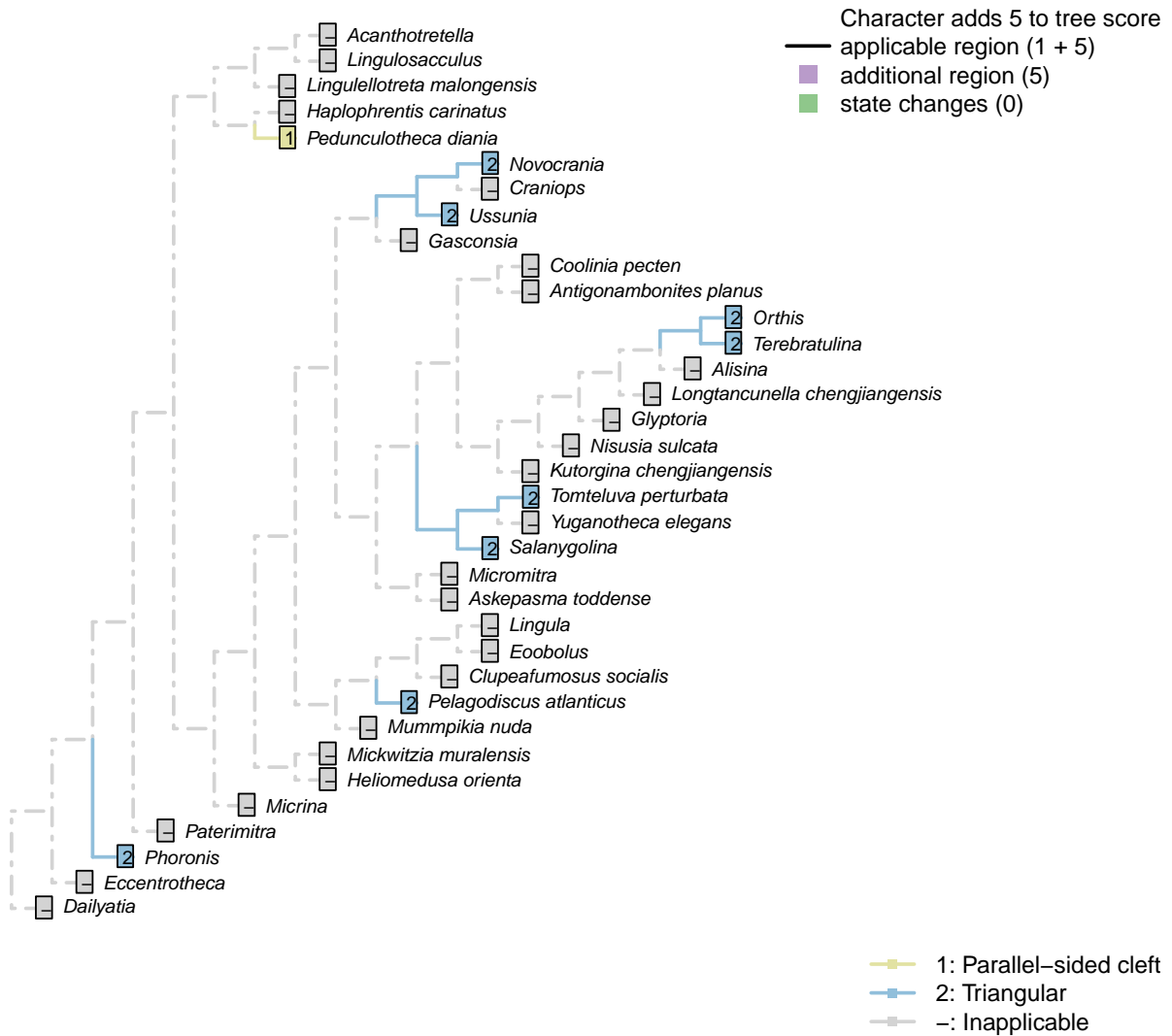


Character 22 – 'Sclerites: Dorsal valve: Posterior surface: Medial groove'



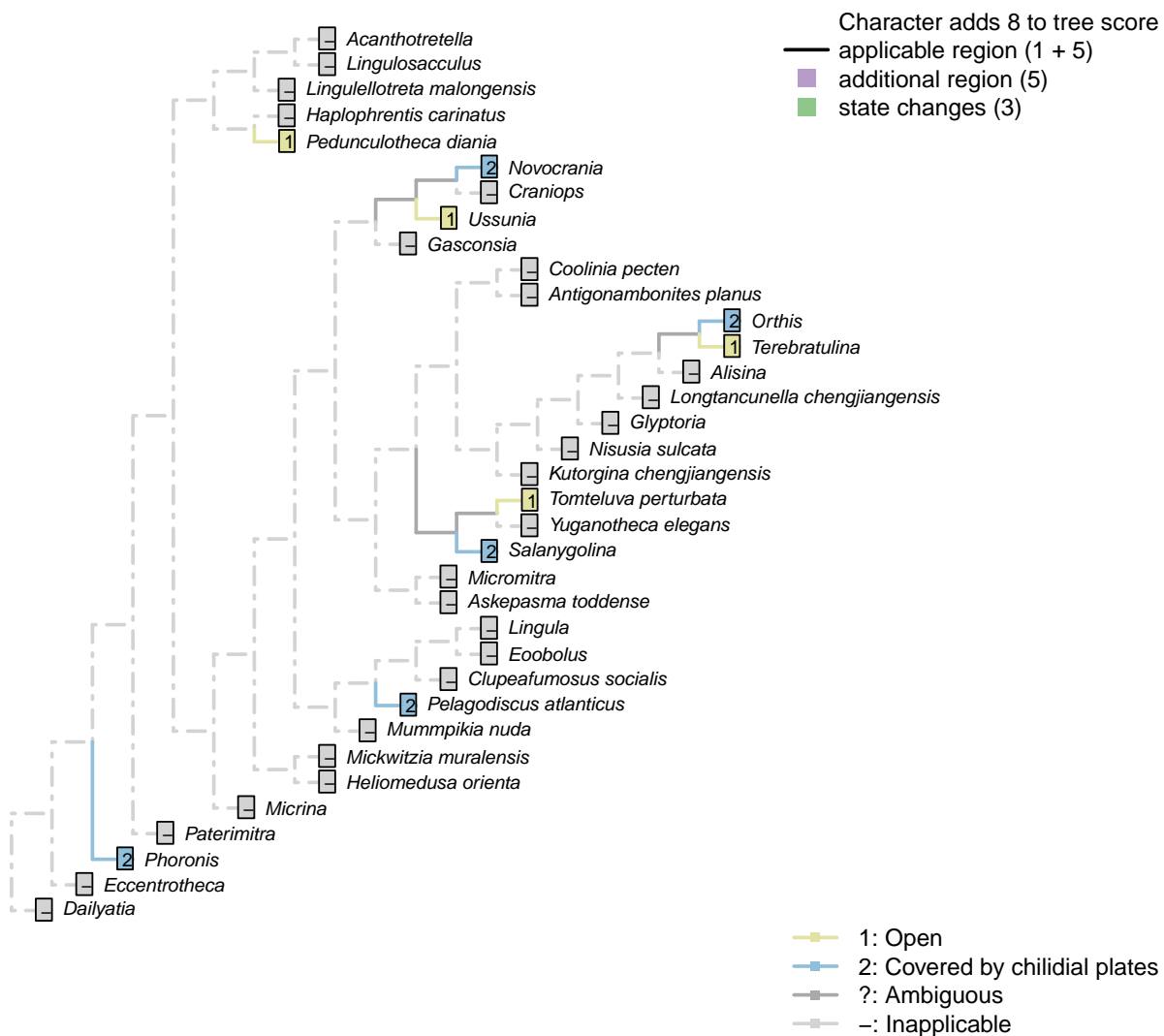
Character 23 – 'Sclerites: Dorsal valve: Posterior surface: Notothyrium'

Character 24 – 'Sclerites: Dorsal valve: Posterior surface: Notothyrium: Shape'



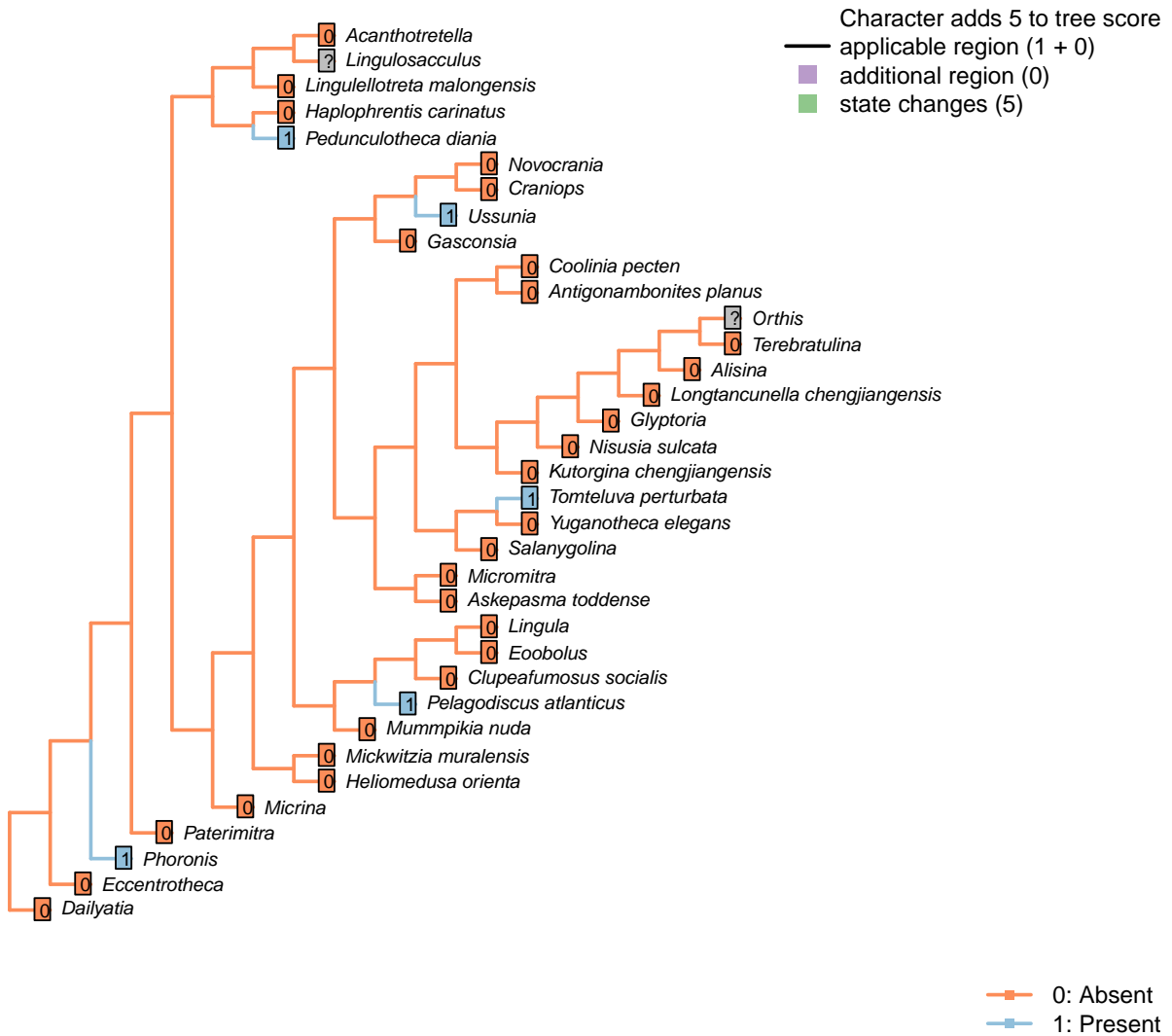
Character 24 – 'Sclerites: Dorsal valve: Posterior surface: Notothyrium: Shape'

Character 25 – 'Sclerites: Dorsal valve: Posterior surface: Notothyrium: Chilidial plates'



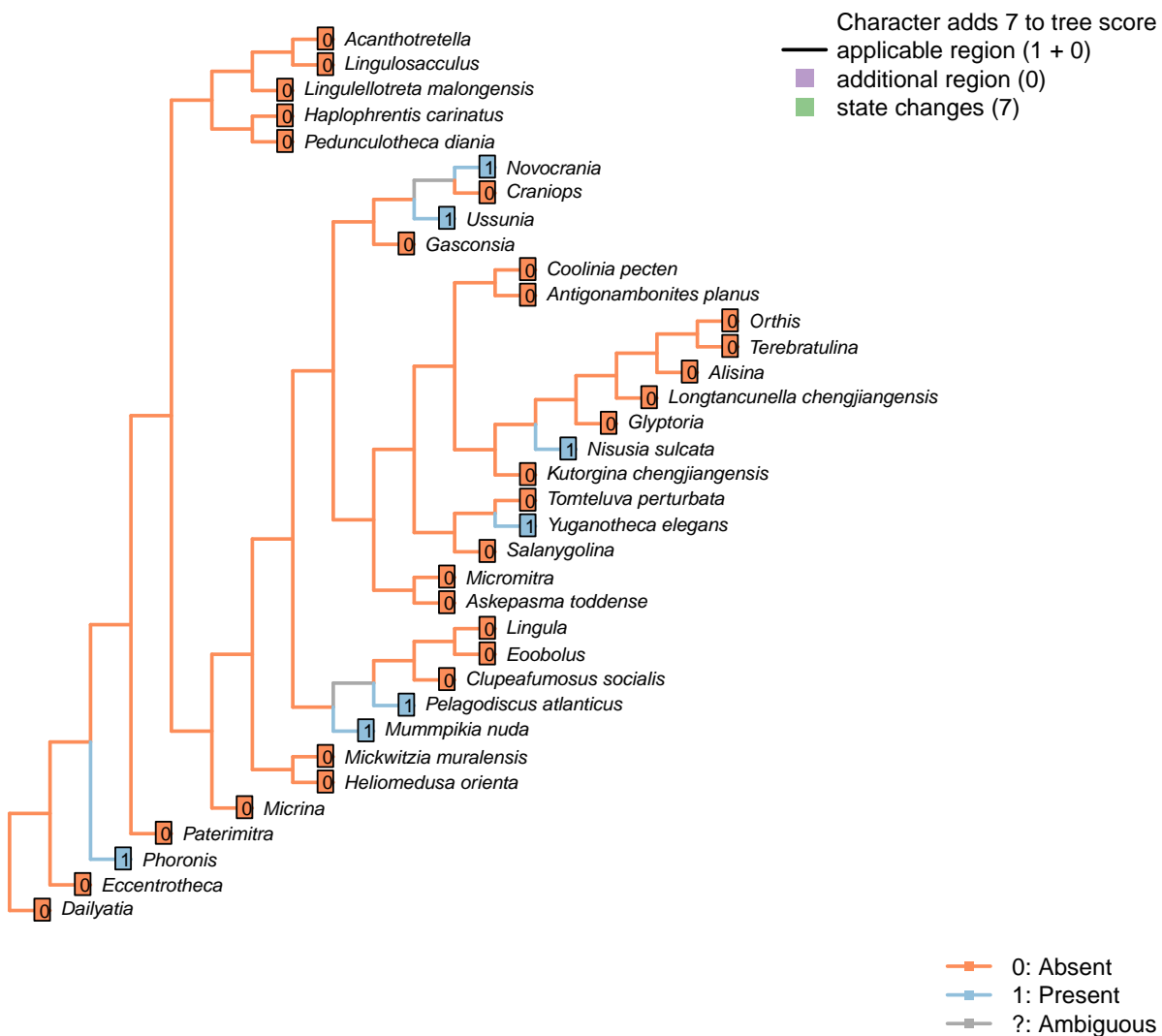
Character 25 – 'Sclerites: Dorsal valve: Posterior surface: Notothyrium: Chilidial plates'

Character 26 – 'Sclerites: Dorsal valve: Notothyrial platform'



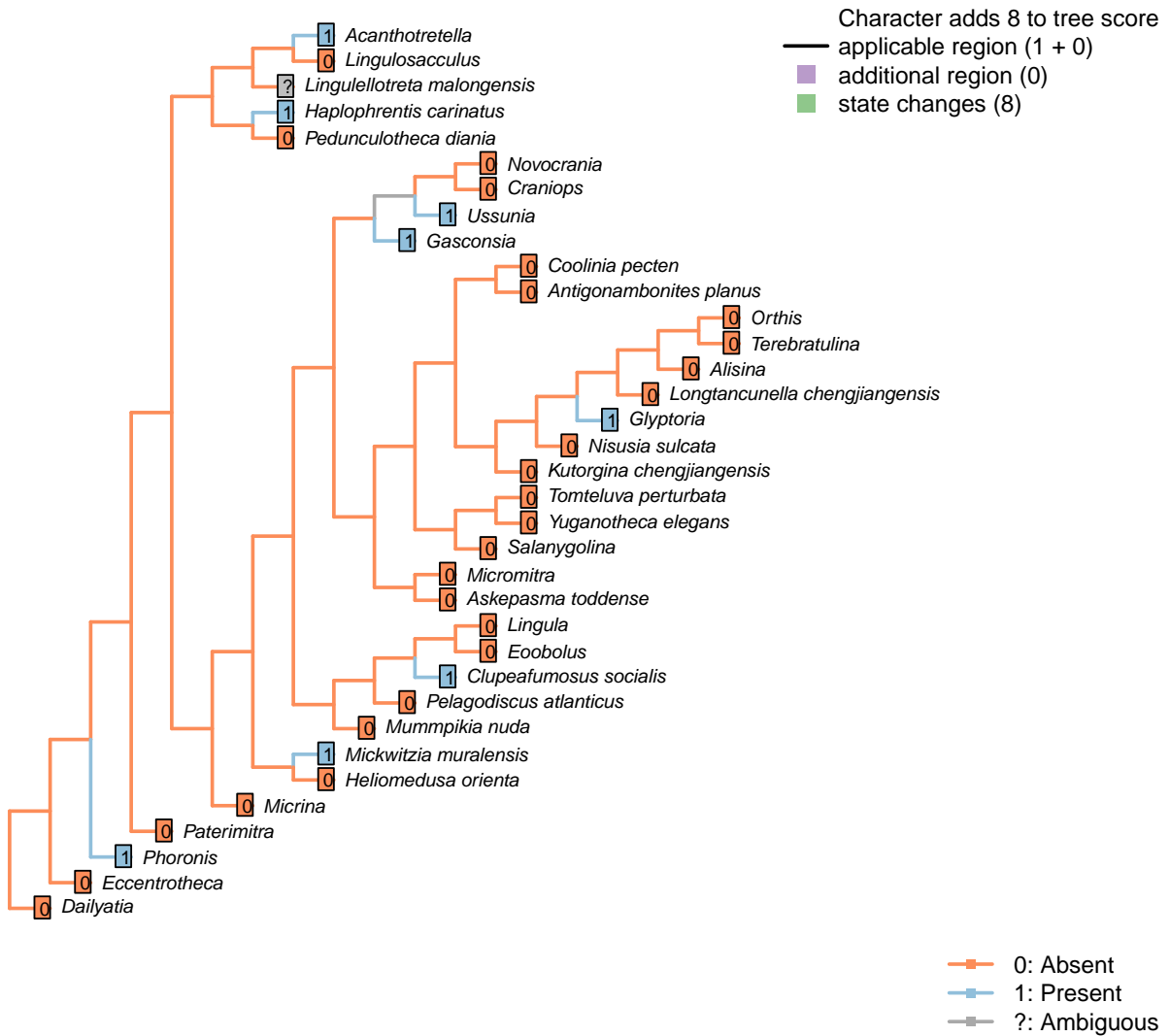
Character 26 – 'Sclerites: Dorsal valve: Notothyrial platform'

Character 27 – 'Sclerites: Dorsal valve: Cardinal processes'



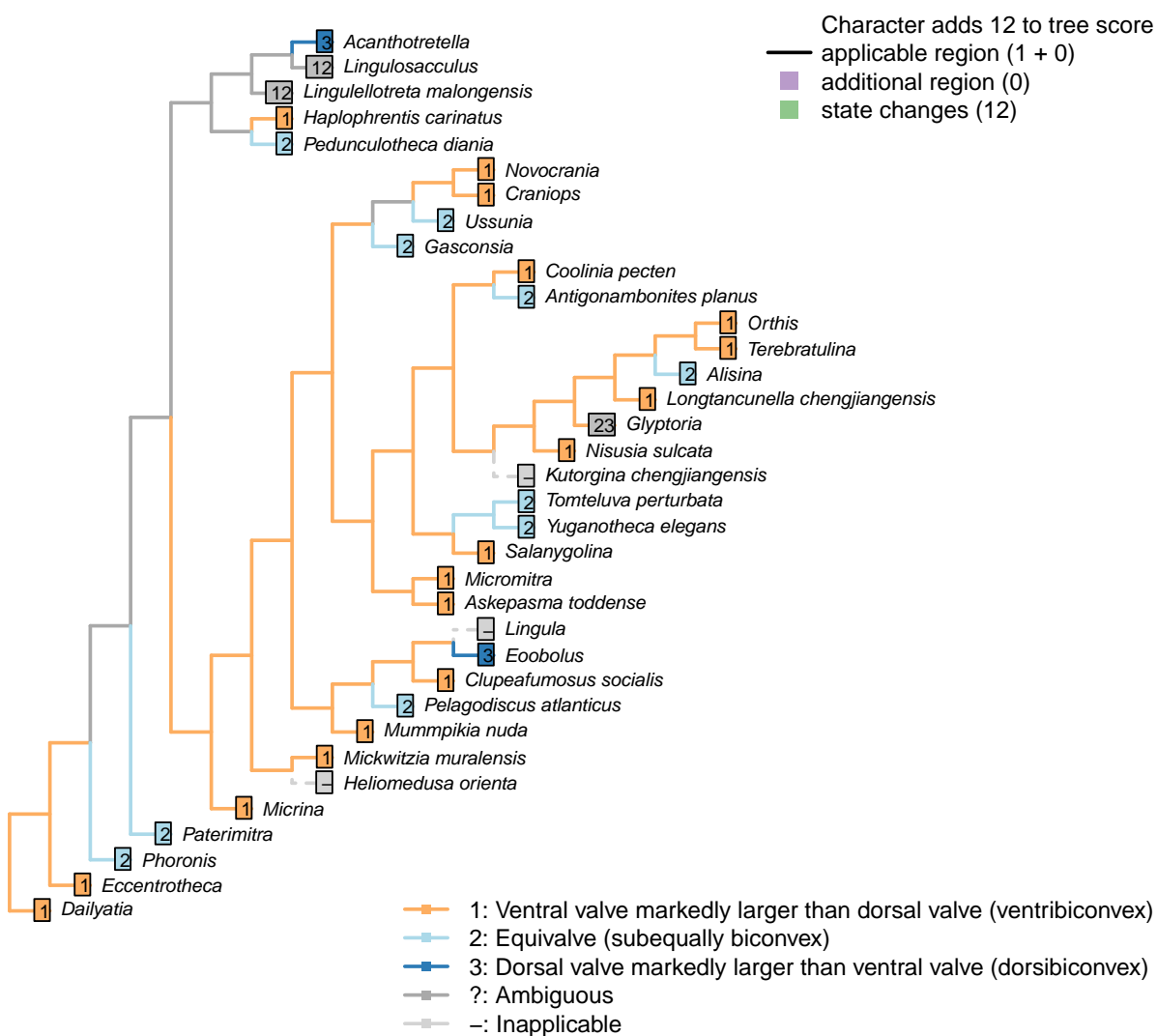
Character 27 – 'Sclerites: Dorsal valve: Cardinal processes'

Character 28 – 'Sclerites: Dorsal valve: Medial septum'



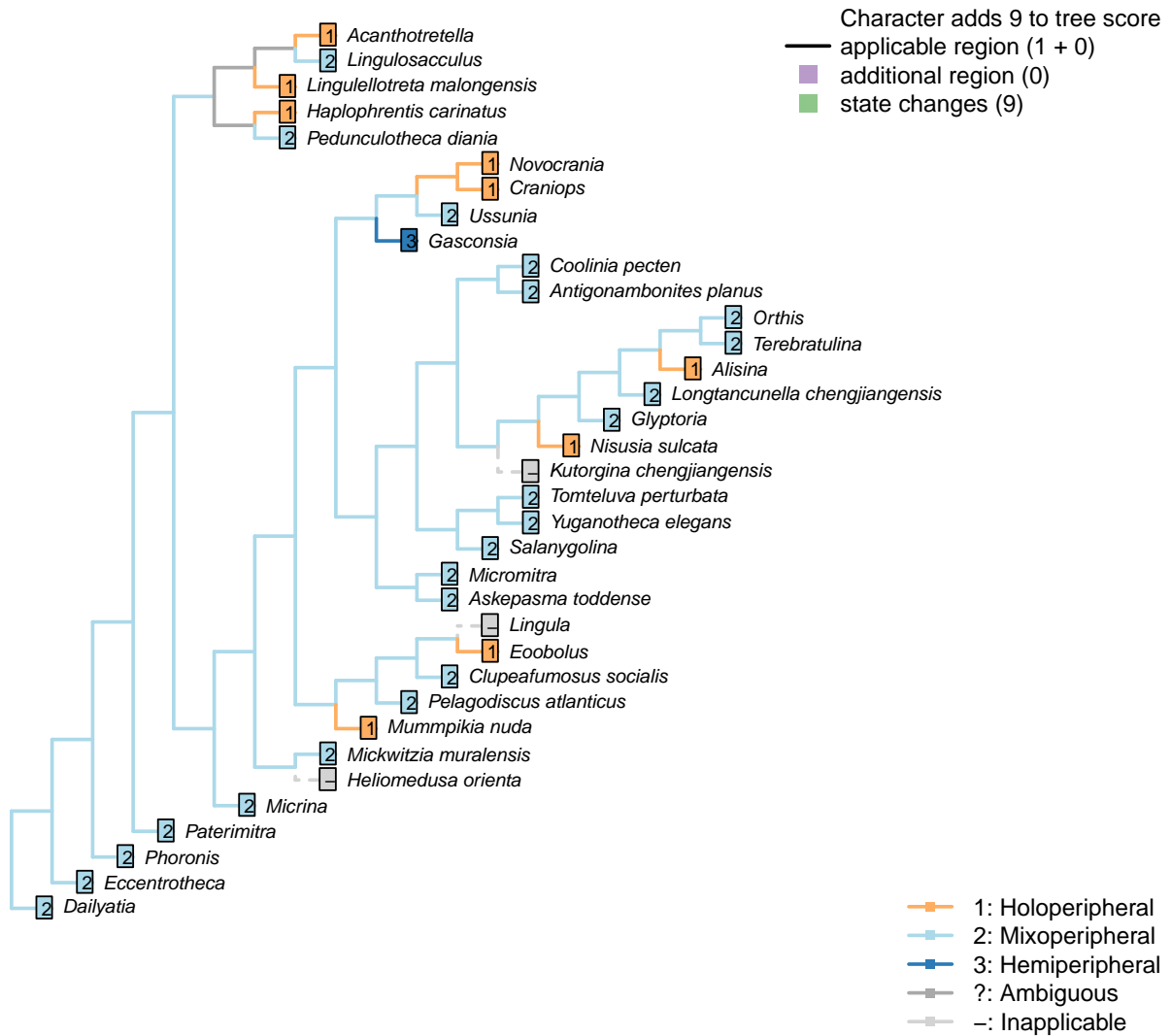
Character 28 – 'Sclerites: Dorsal valve: Medial septum'

Character 29 – 'Sclerites: Ventral valve: Relative size'



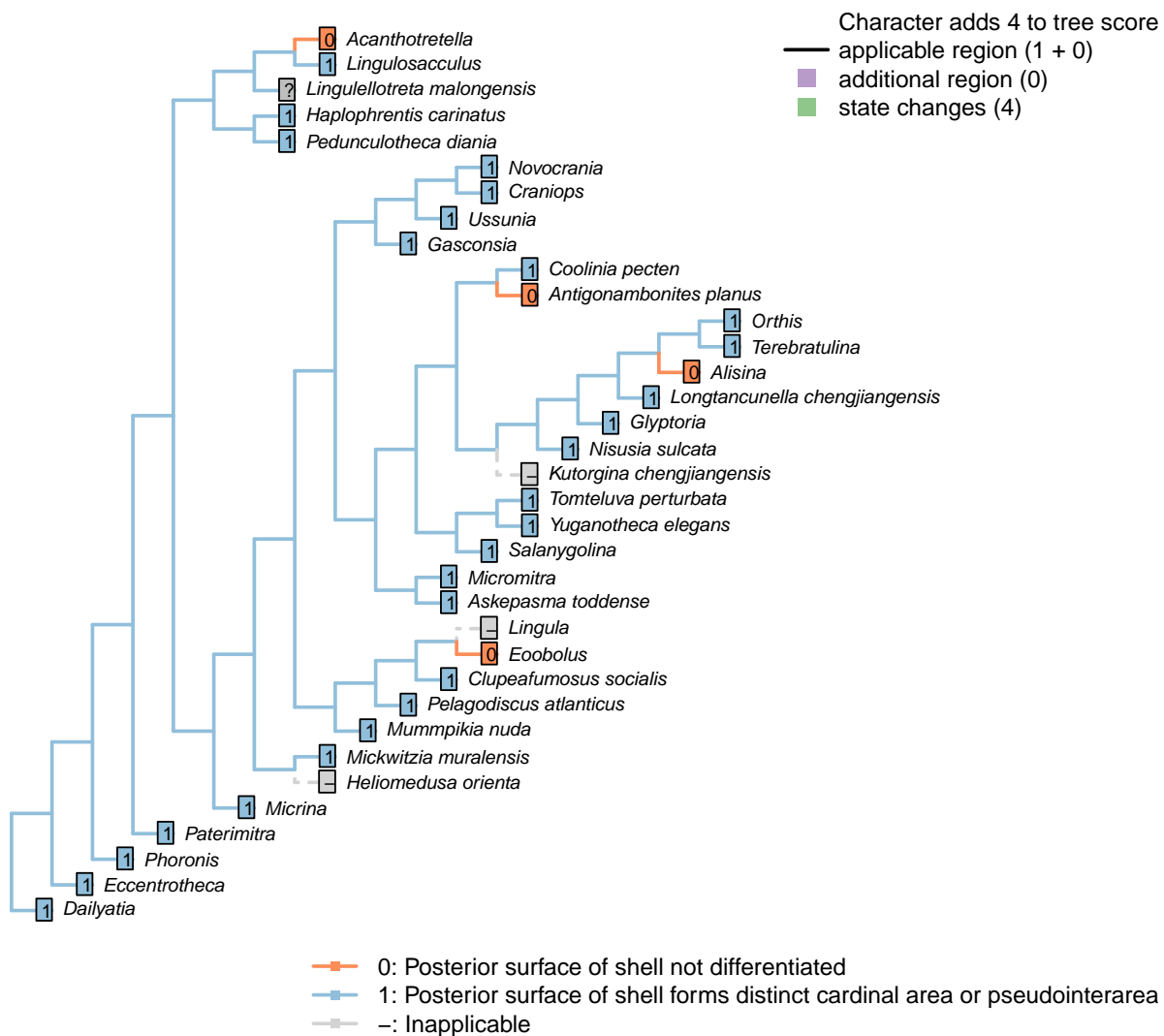
Character 29 – 'Sclerites: Ventral valve: Relative size'

Character 30 – 'Sclerites: Ventral valve: Growth direction'

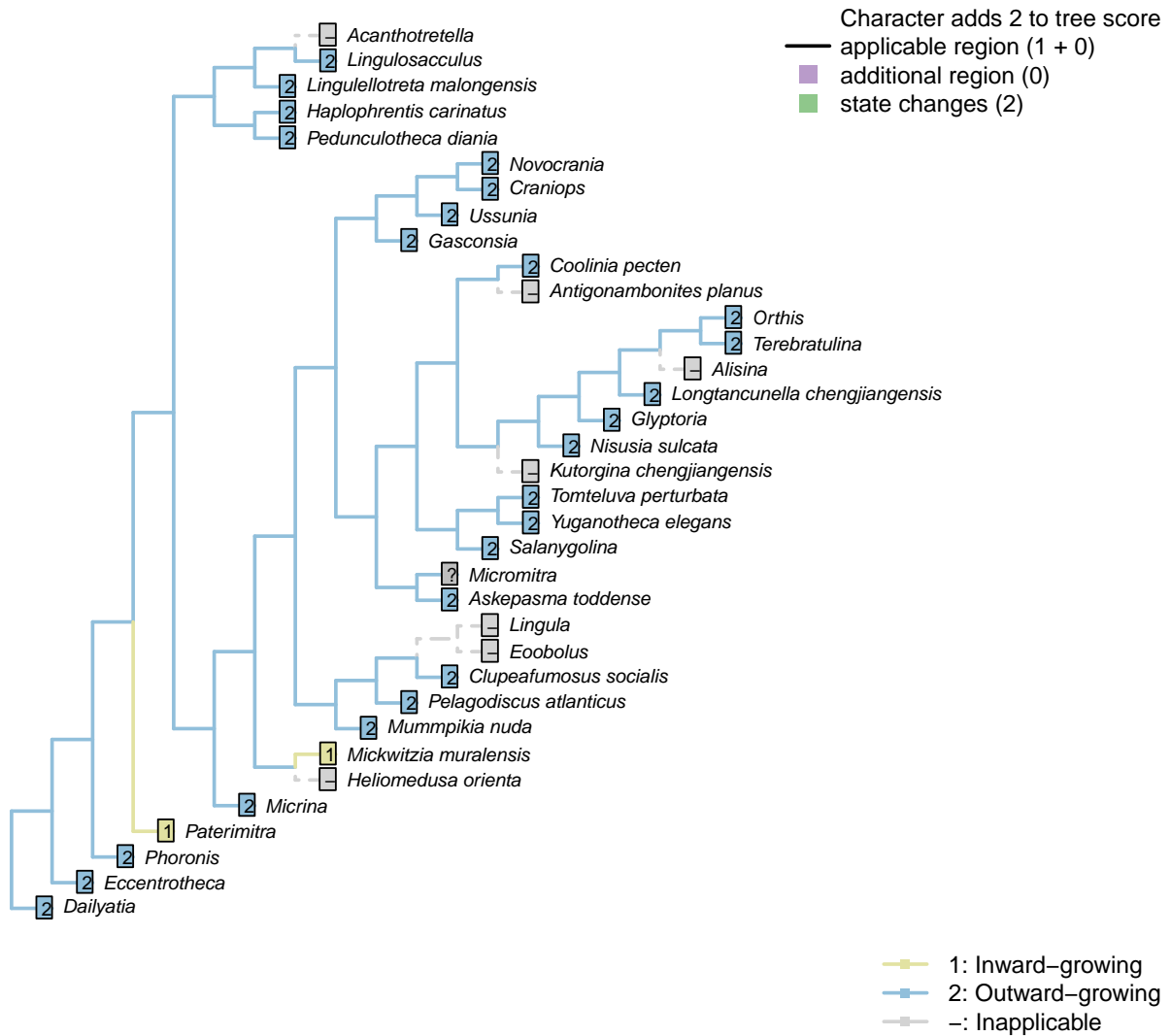


Character 30 – 'Sclerites: Ventral valve: Growth direction'

Character 31 – 'Sclerites: Ventral valve: Posterior surface: Differentiated'

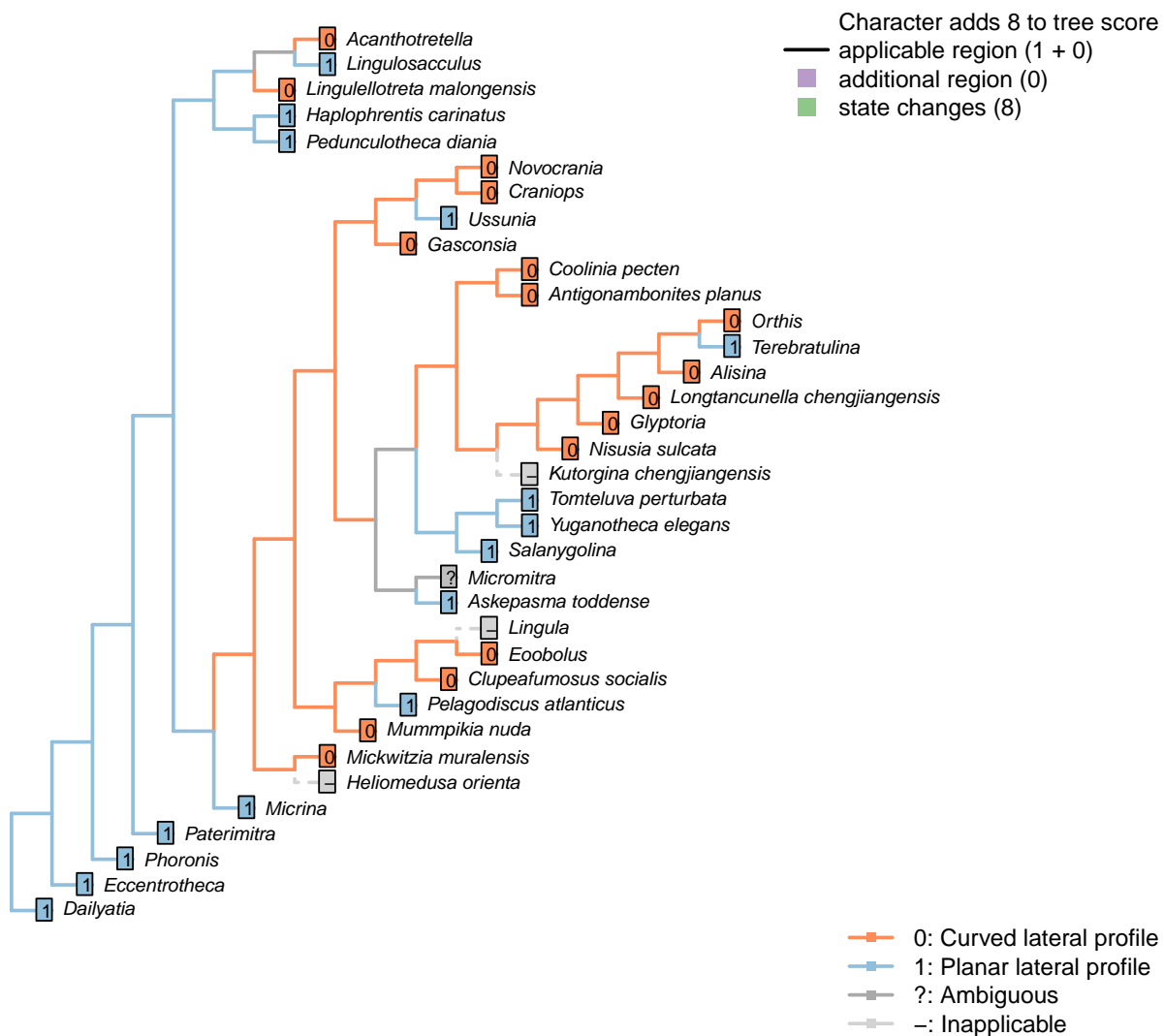


Character 32 – 'Sclerites: Ventral valve: Posterior margin growth direction'



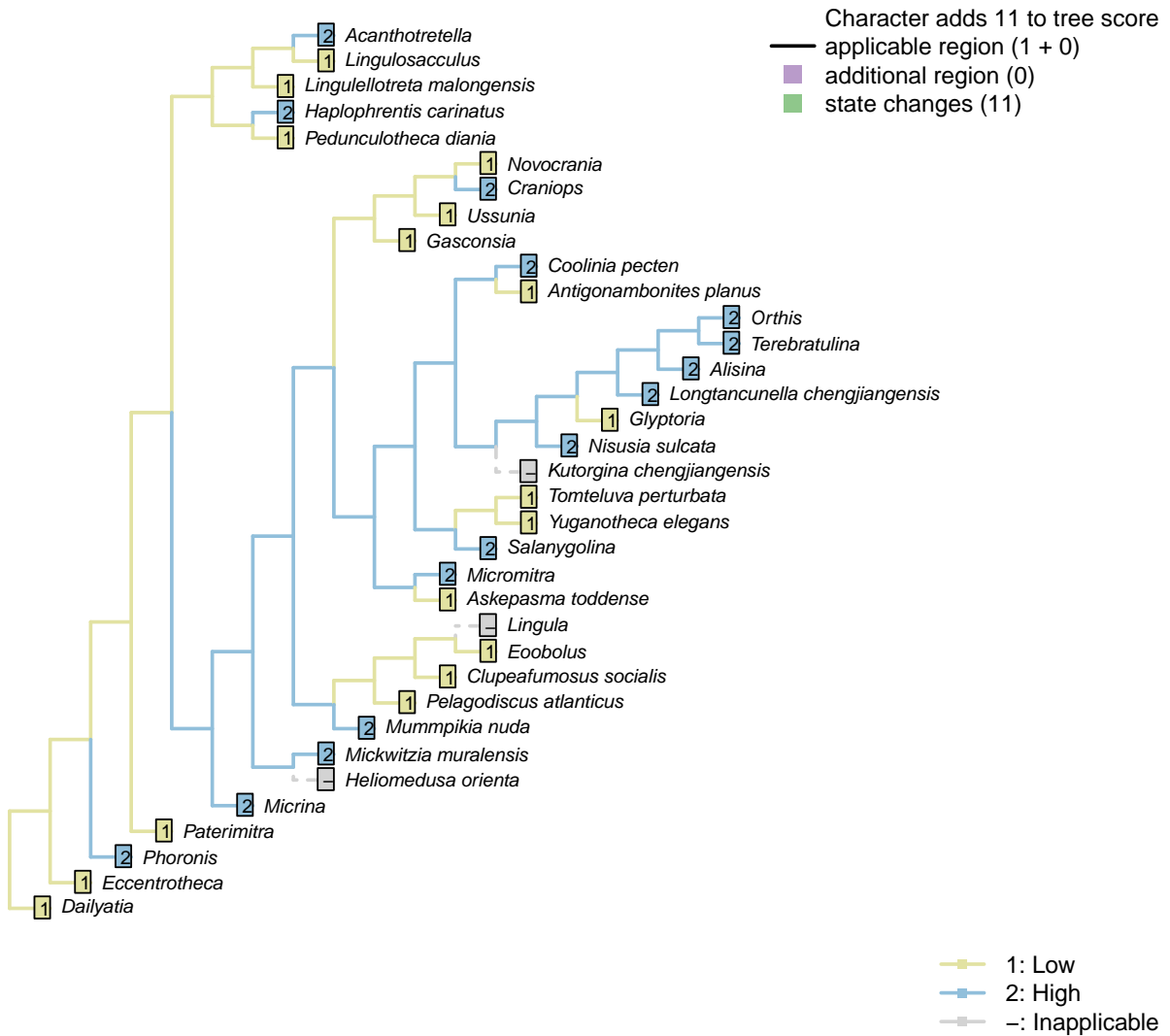
Character 32 – 'Sclerites: Ventral valve: Posterior margin growth direction'

Character 33 – 'Sclerites: Ventral valve: Posterior surface: Planar'



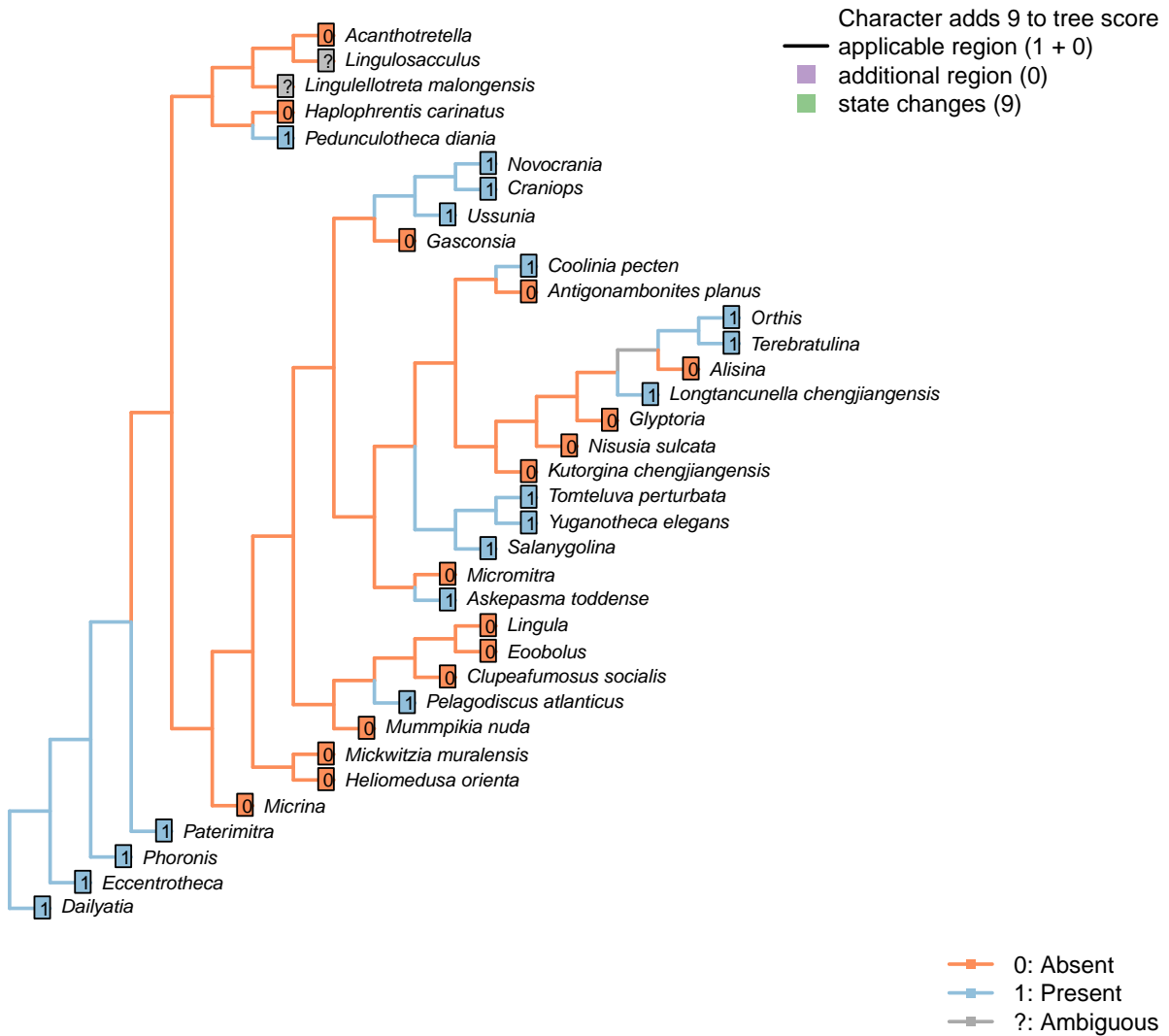
Character 33 – 'Sclerites: Ventral valve: Posterior surface: Planar'

Character 34 – 'Sclerites: Ventral valve: Posterior surface: Extent'



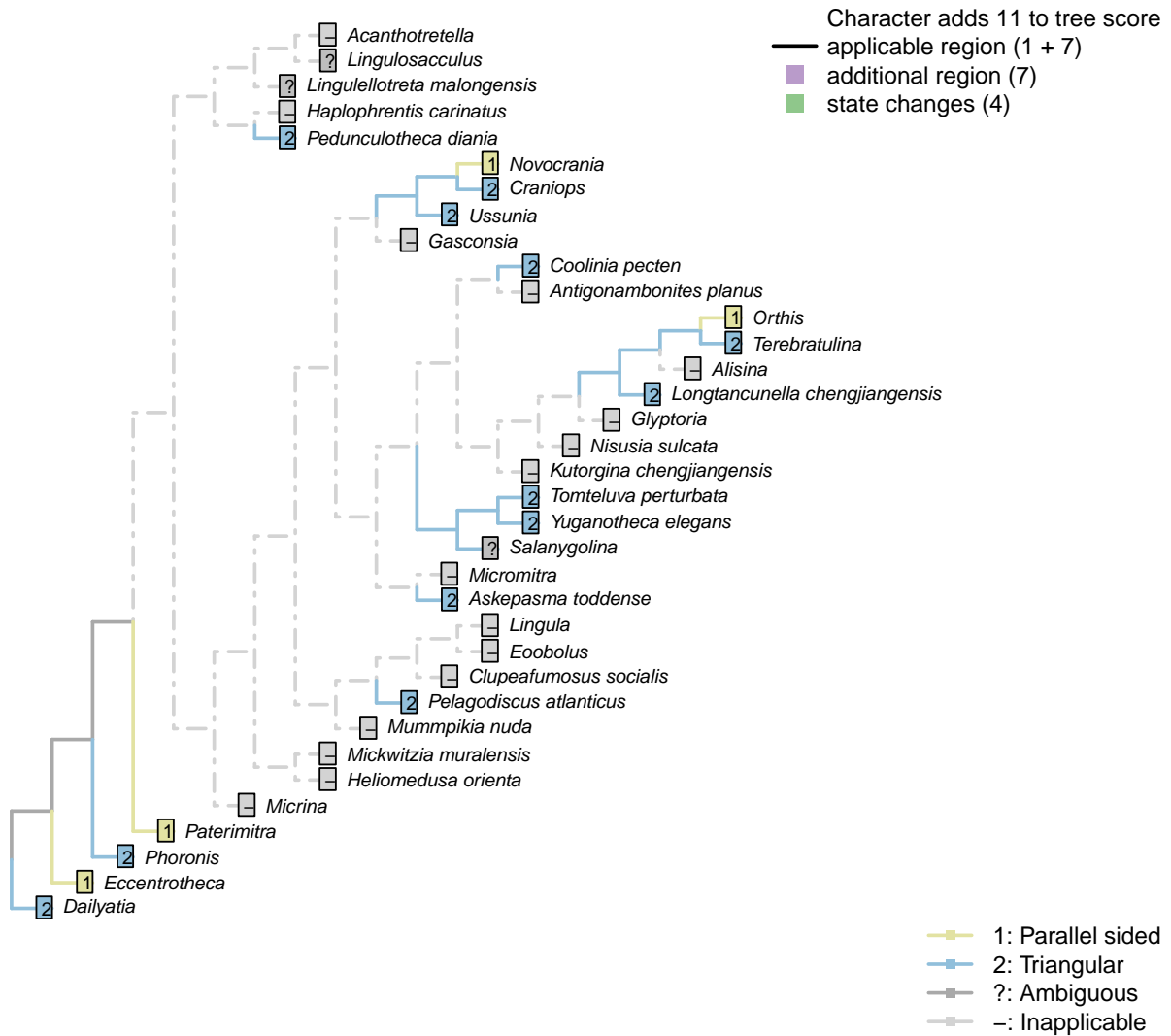
Character 34 – 'Sclerites: Ventral valve: Posterior surface: Extent'

Character 35 – 'Sclerites: Ventral valve: Posterior surface: Delthyrium'



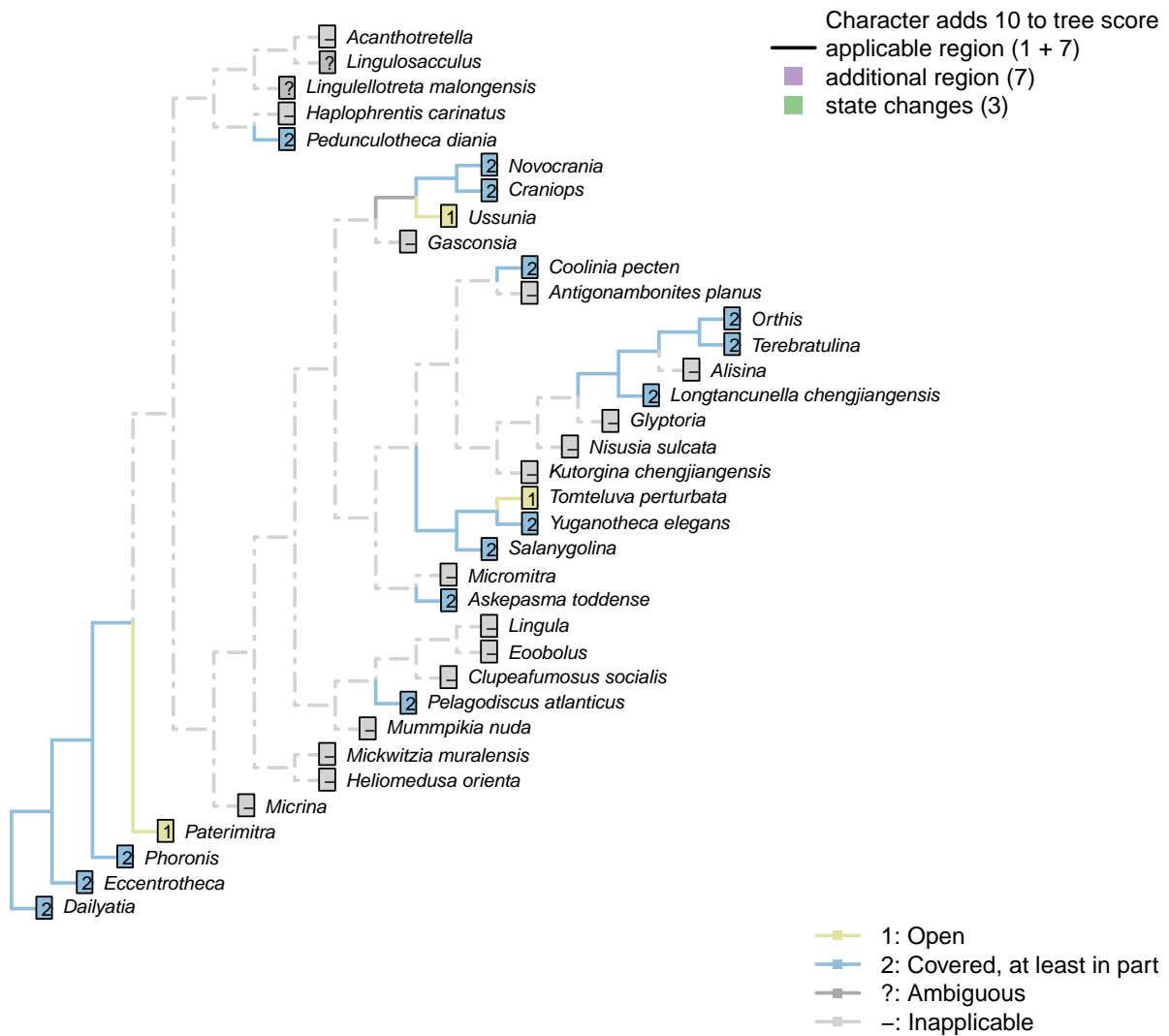
Character 35 – 'Sclerites: Ventral valve: Posterior surface: Delthyrium'

Character 36 – 'Sclerites: Ventral valve: Posterior surface: Delthyrium: Shape'



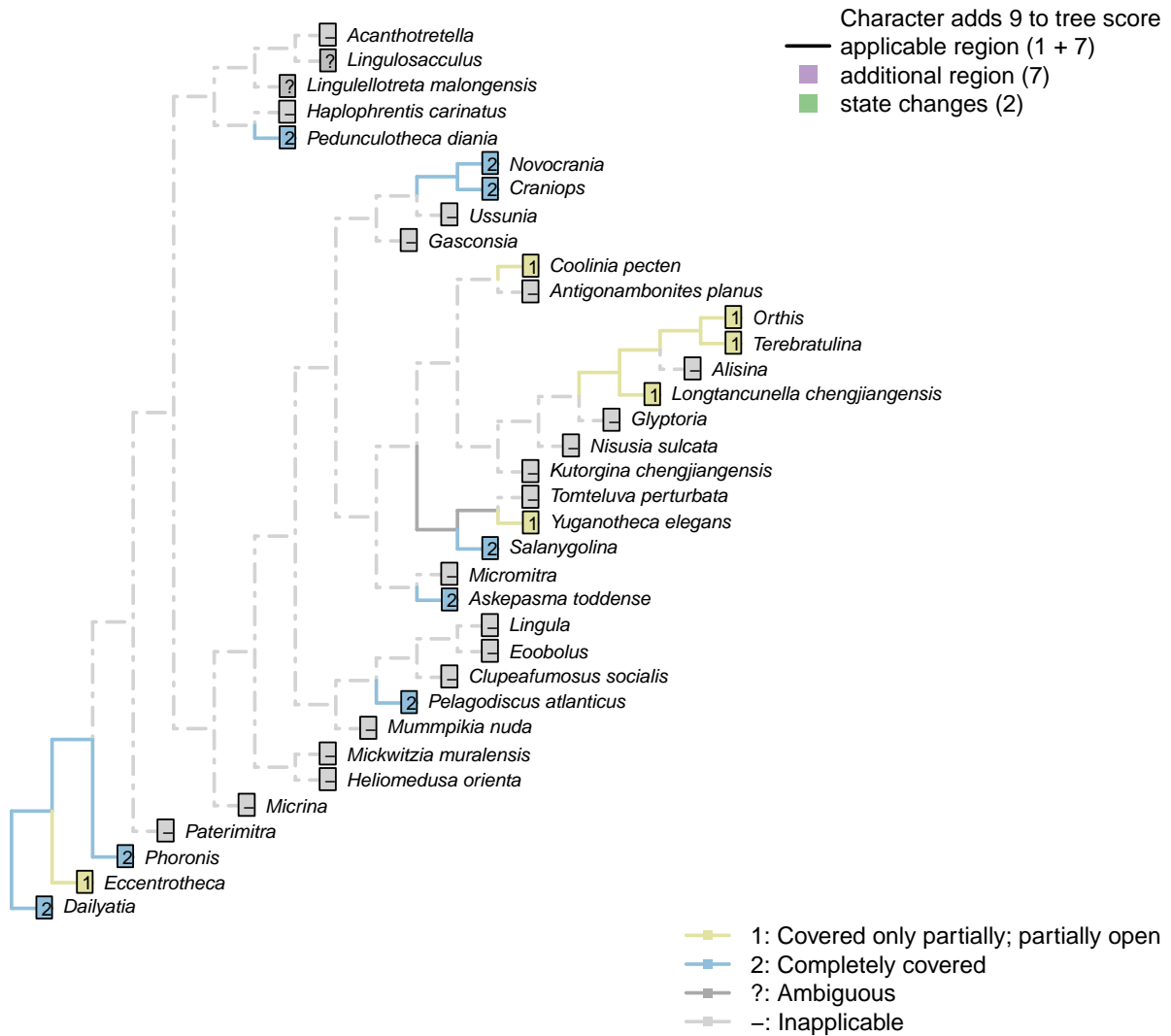
Character 36 – 'Sclerites: Ventral valve: Posterior surface: Delthyrium: Shape'

Character 37 – 'Sclerites: Ventral valve: Posterior surface: Delthyrium: Cover'



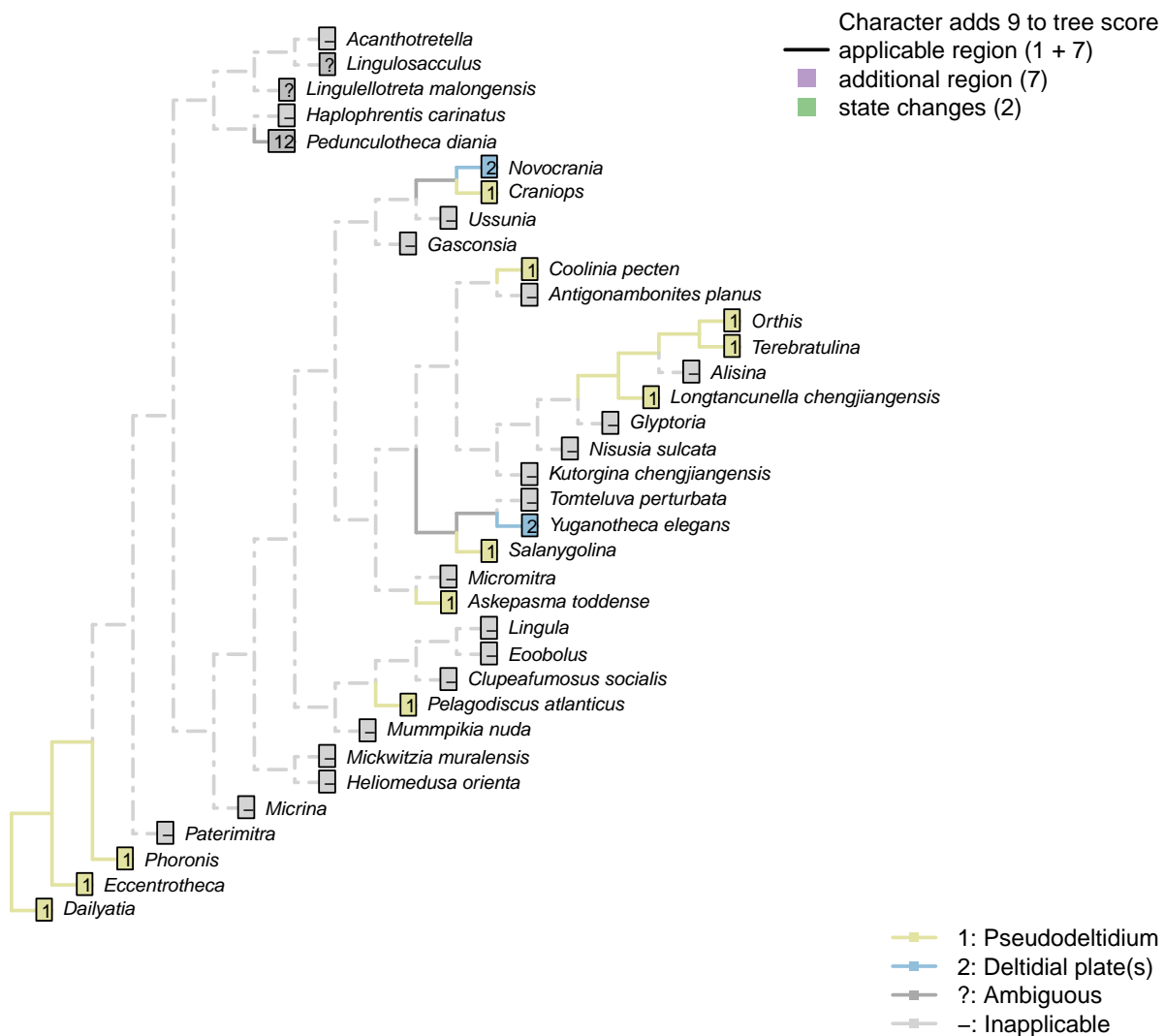
Character 37 – 'Sclerites: Ventral valve: Posterior surface: Delthyrium: Cover'

Character 38 – 'Sclerites: Ventral valve: Posterior surface: Delthyrium: Cover: Extent'



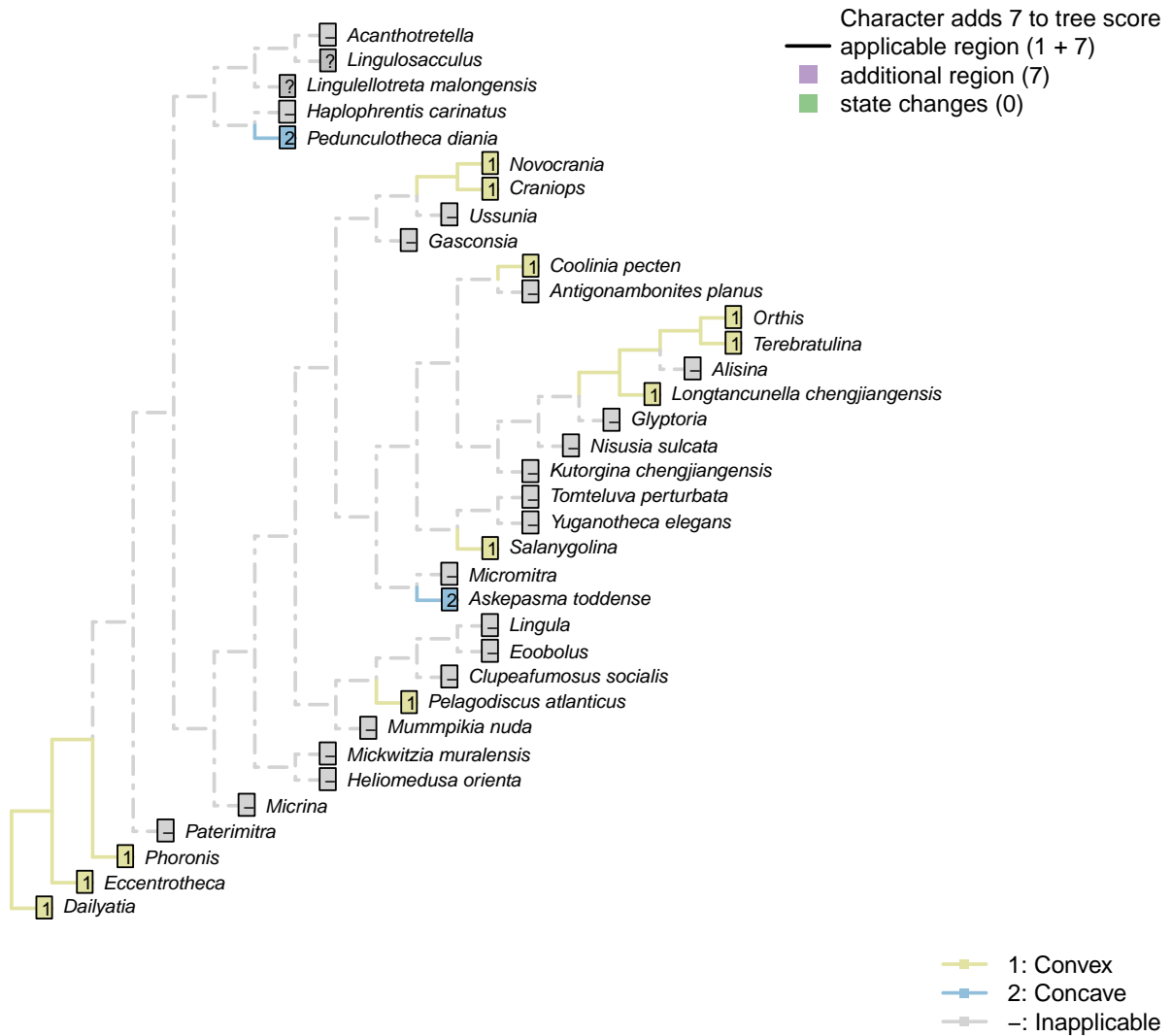
Character 38 – 'Sclerites: Ventral valve: Posterior surface: Delthyrium: Cover: Extent'

Character 39 – 'Sclerites: Ventral valve: Posterior surface: Delthyrium: Cover: Identity'



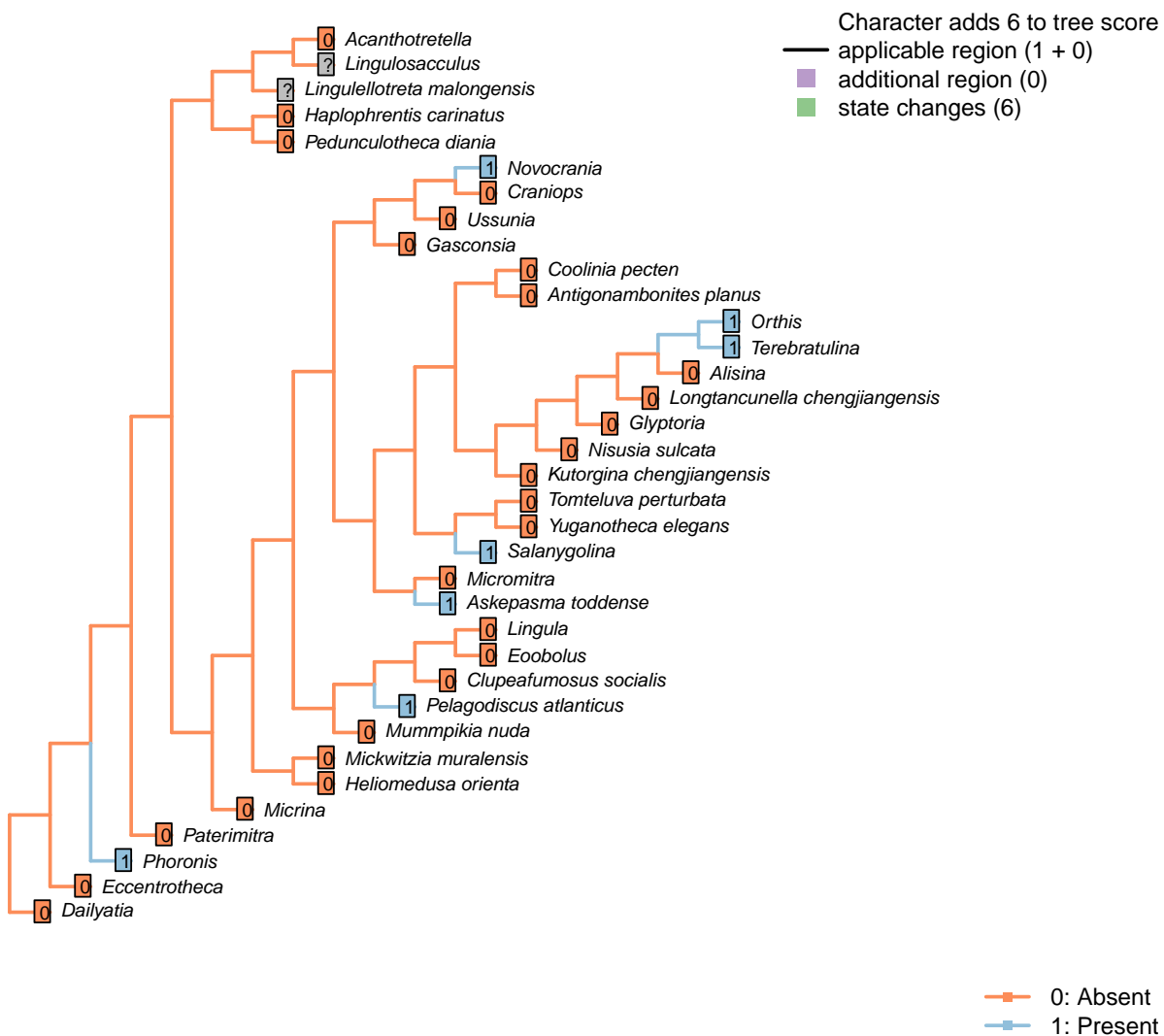
Character 39 – 'Sclerites: Ventral valve: Posterior surface: Delthyrium: Cover: Identity'

Character 40 – 'Sclerites: Ventral valve: Posterior surface: Delthyrium: Pseudodeltidium: Shape'



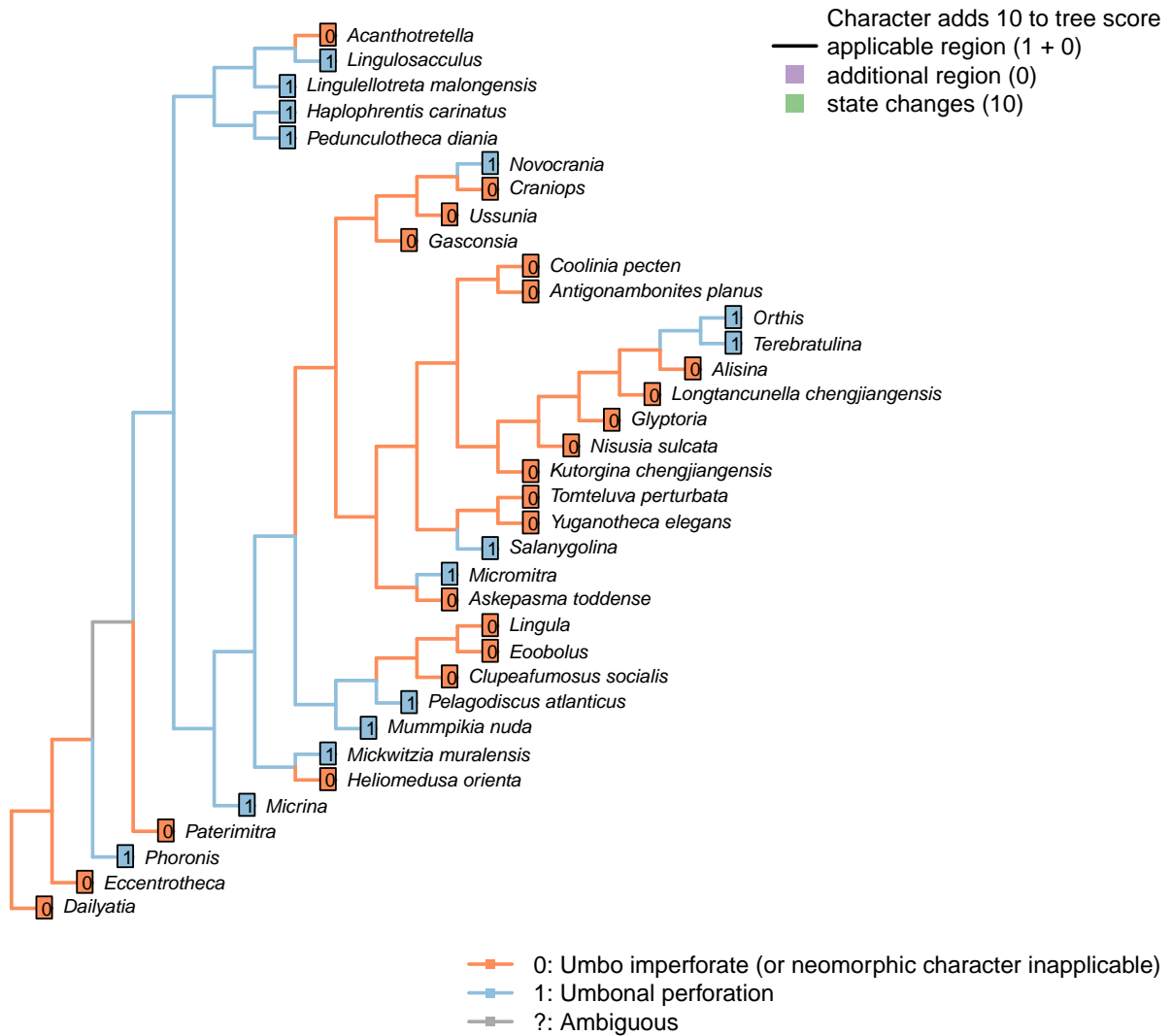
Character 40 – 'Sclerites: Ventral valve: Posterior surface: Delthyrium: Pseudodeltidium: Shape'

Character 41 – 'Sclerites: Ventral valve: Posterior surface: Delthyrium: Pseudodeltidium: Hinge furrows'



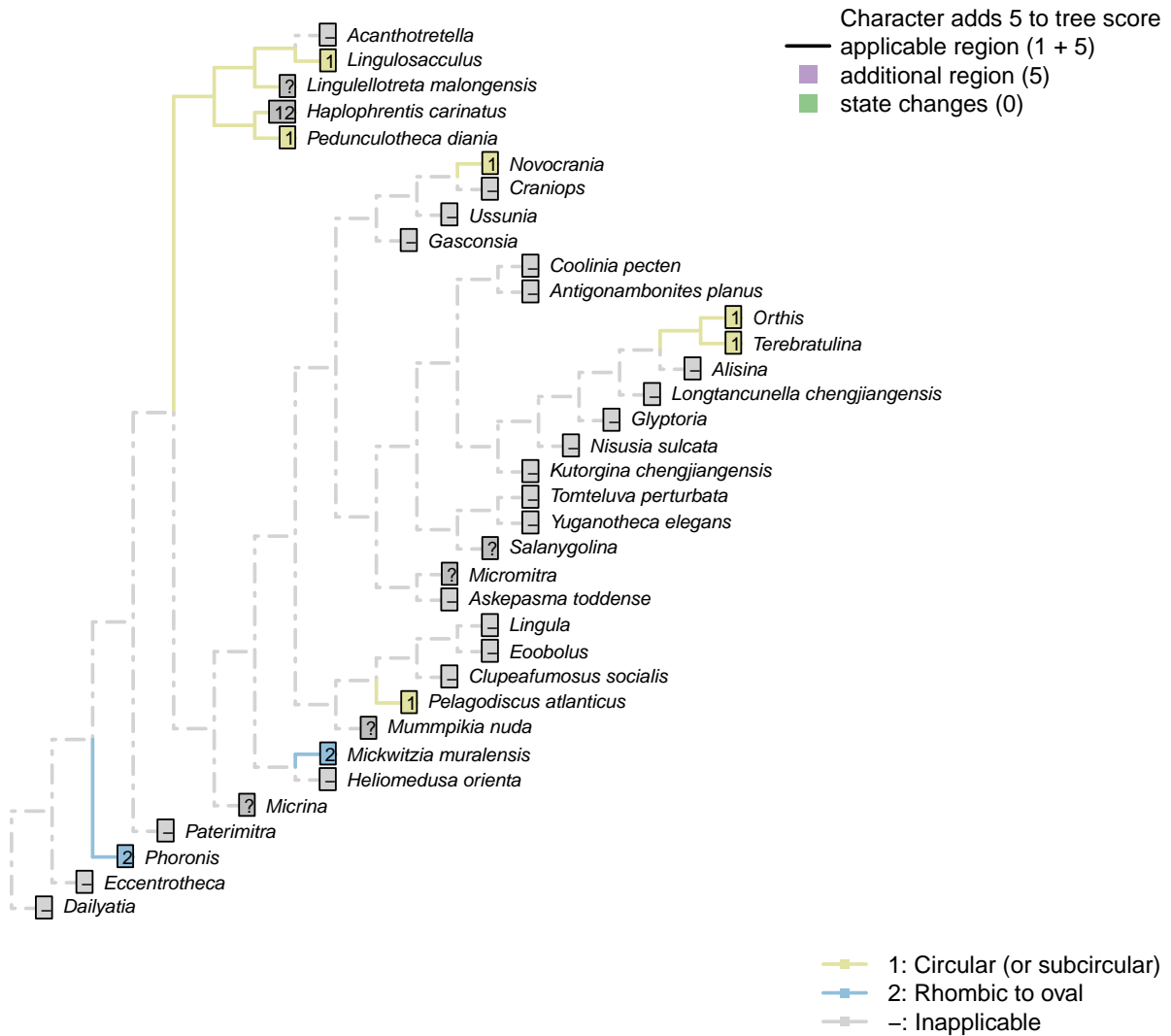
Character 41 – 'Sclerites: Ventral valve: Posterior surface: Delthyrium: Pseudodeltidium: Hinge furrows'

Character 42 – 'Sclerites: Ventral valve: Umbonal perforation'



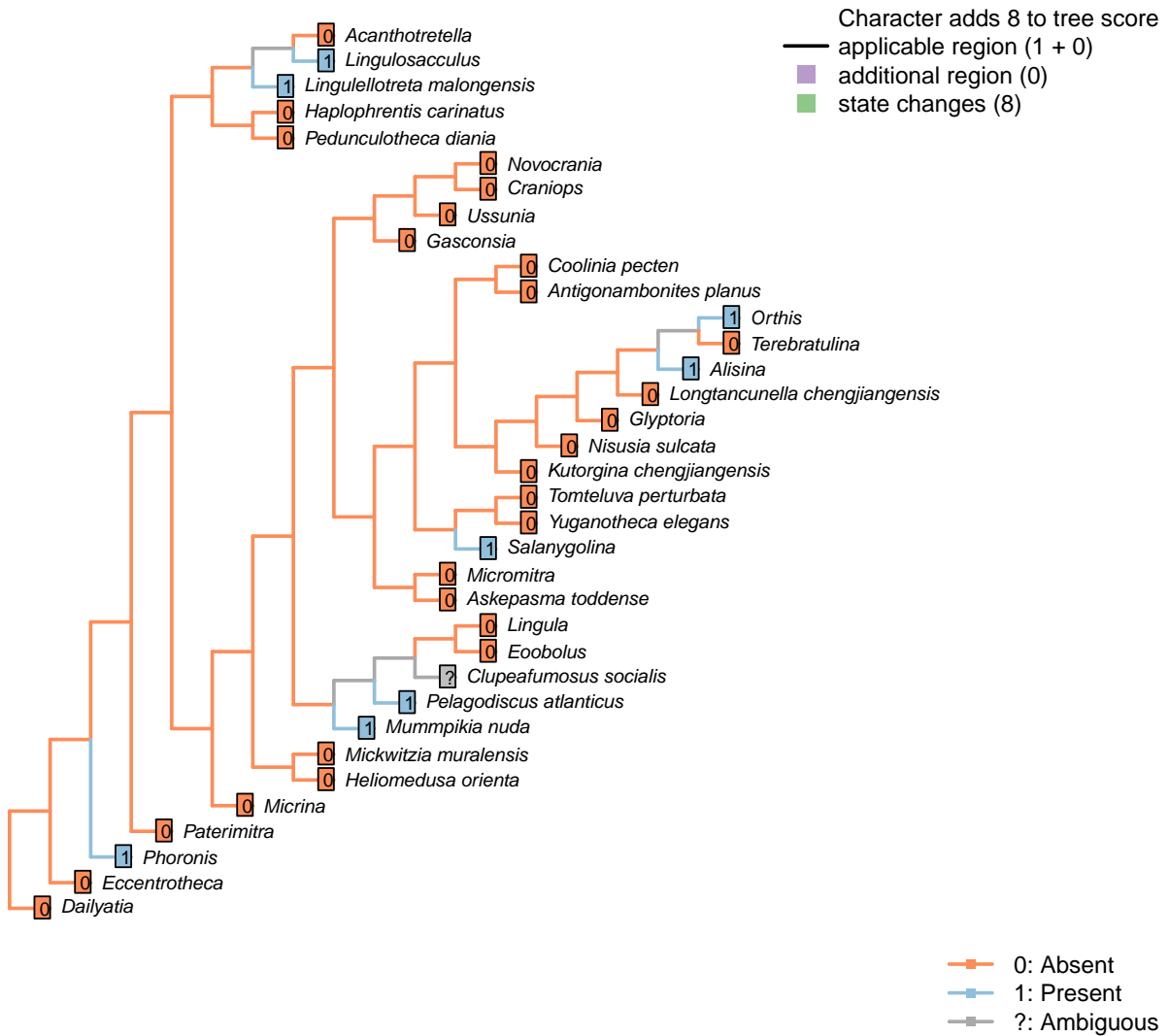
Character 42 – 'Sclerites: Ventral valve: Umbonal perforation'

Character 43 – 'Sclerites: Ventral valve: Umbonal perforation: Shape'



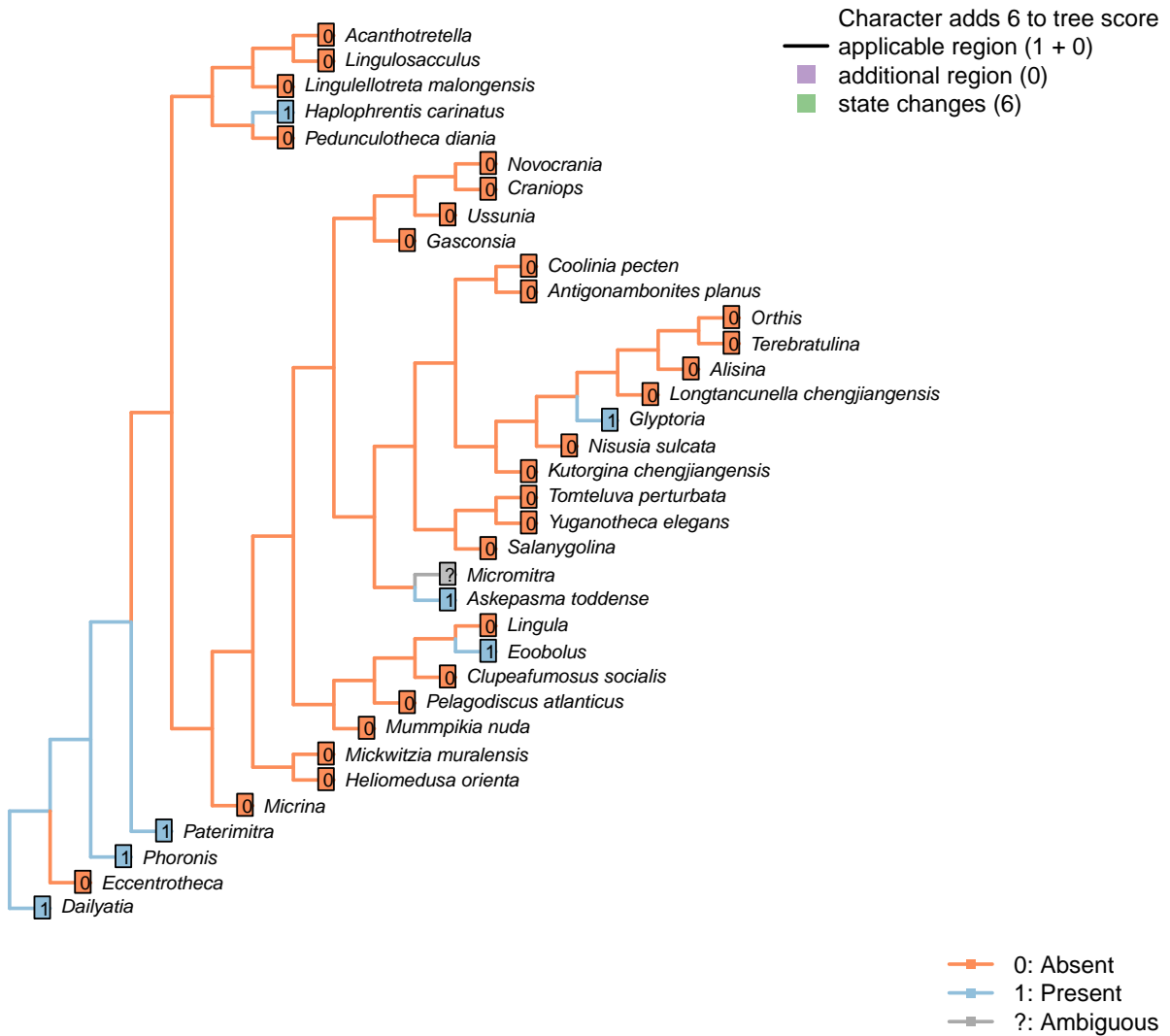
Character 43 – 'Sclerites: Ventral valve: Umbonal perforation: Shape'

Character 44 – 'Sclerites: Ventral valve: Colleplax, cicatrix or pedicle sheath'



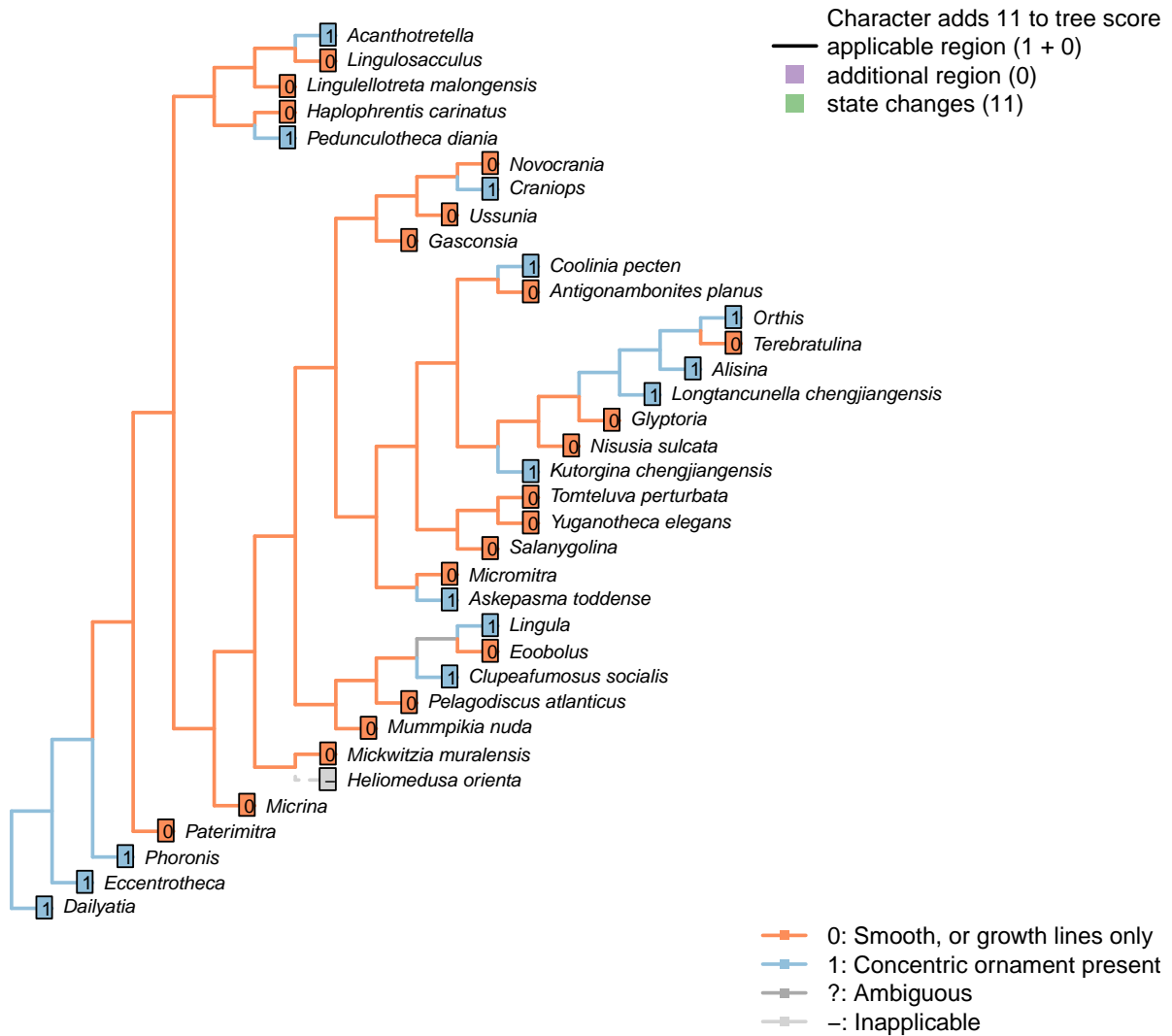
Character 44 – 'Sclerites: Ventral valve: Colleplax, cicatrix or pedicle sheath'

Character 45 – 'Sclerites: Ventral valve: Median septum'

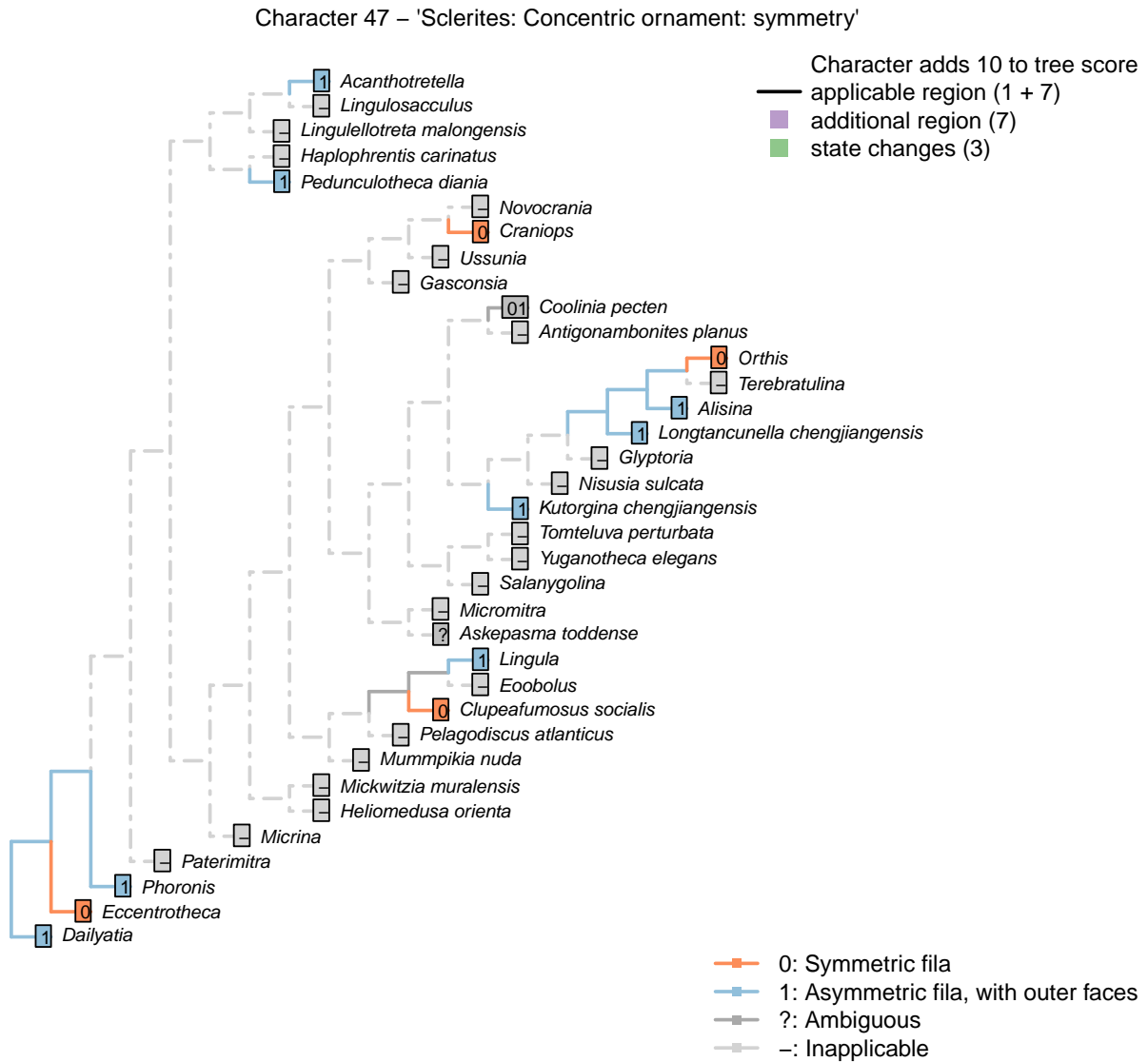


Character 45 – 'Sclerites: Ventral valve: Median septum'

Character 46 – 'Sclerites: Concentric ornament'

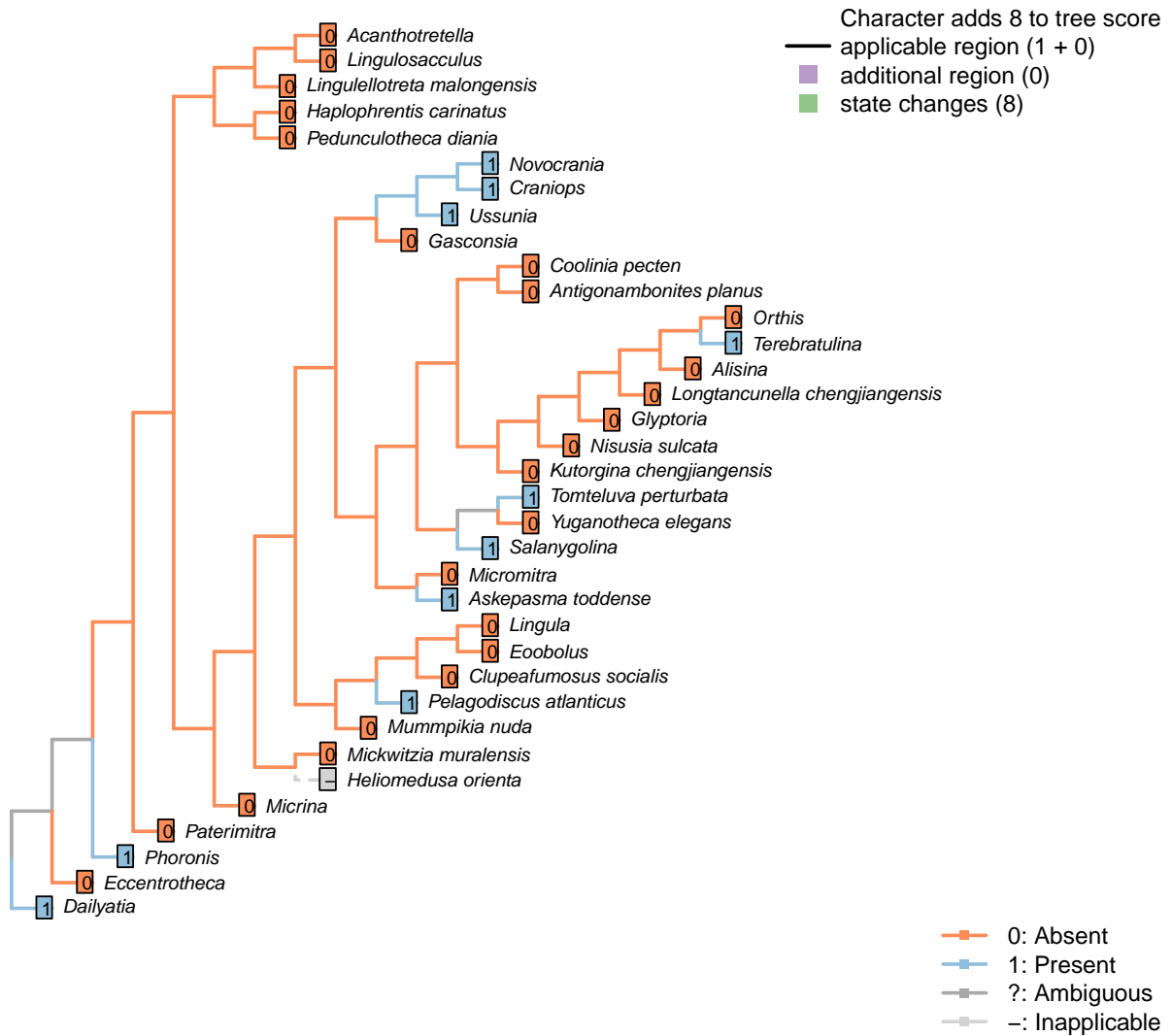


Character 46 – 'Sclerites: Concentric ornament'



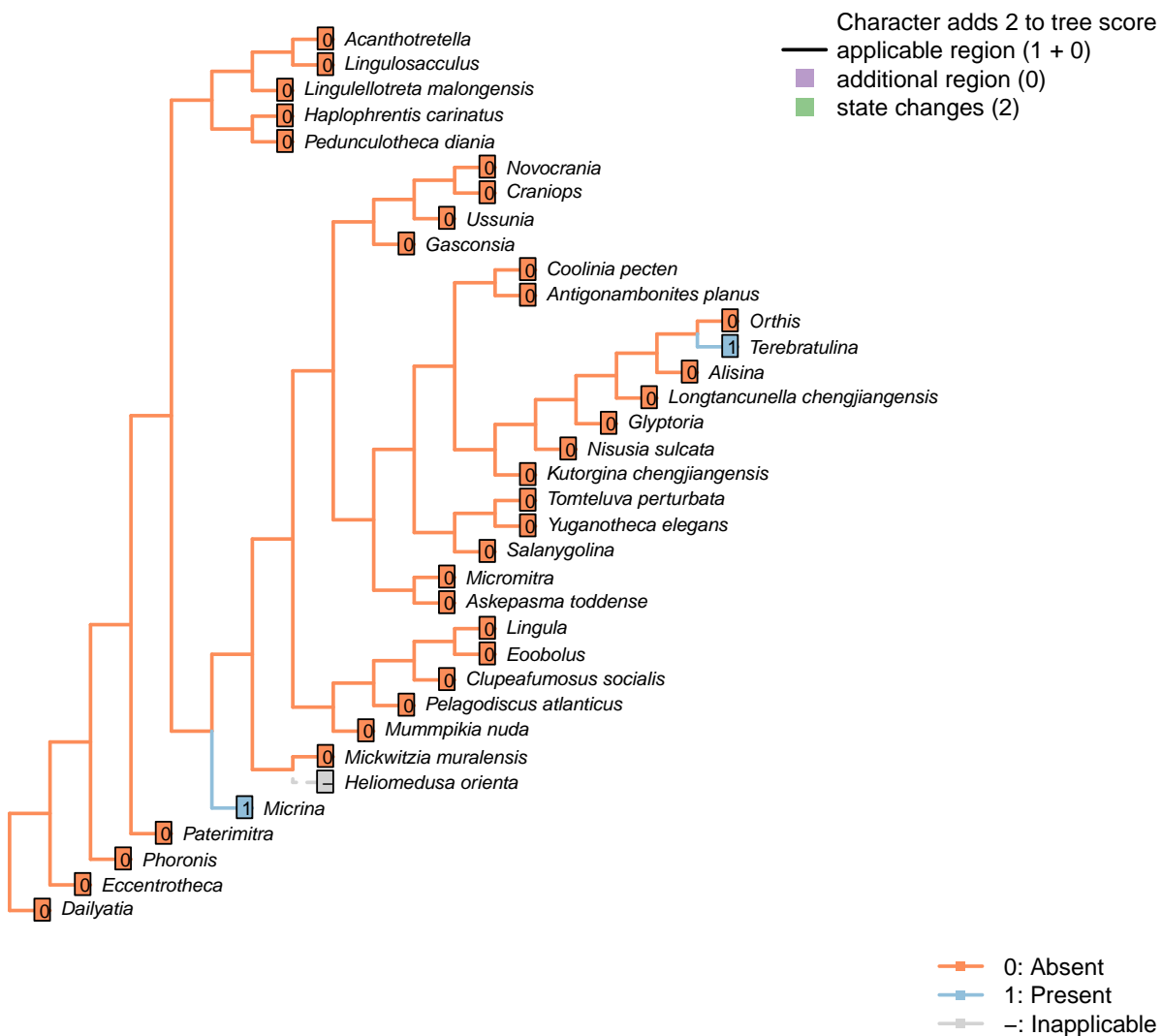
Character 47 – 'Sclerites: Concentric ornament: symmetry'

Character 48 – 'Sclerites: Radial ornament'

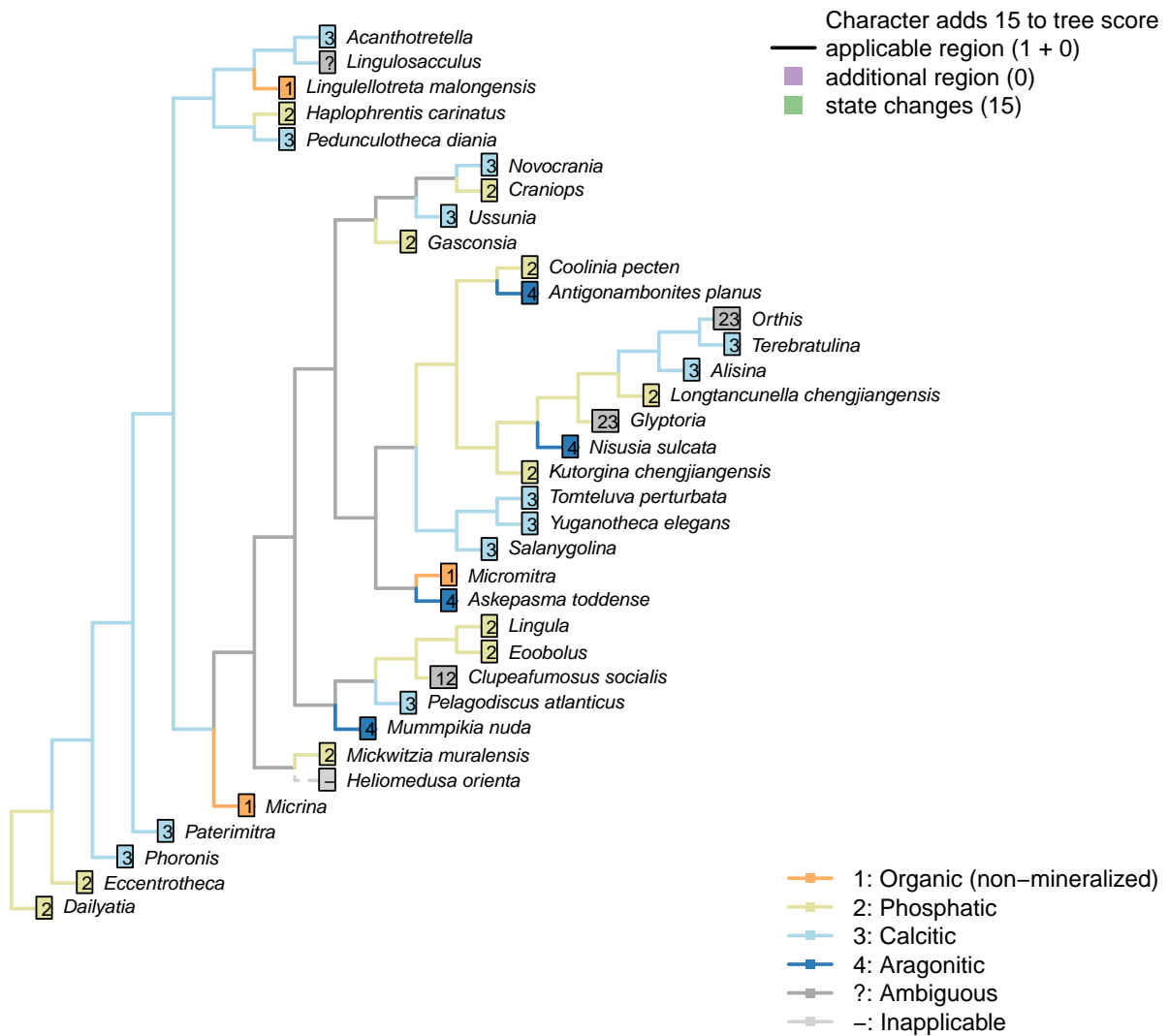


Character 48 – 'Sclerites: Radial ornament'

Character 49 – 'Sclerites: Shell-penetrating spines'

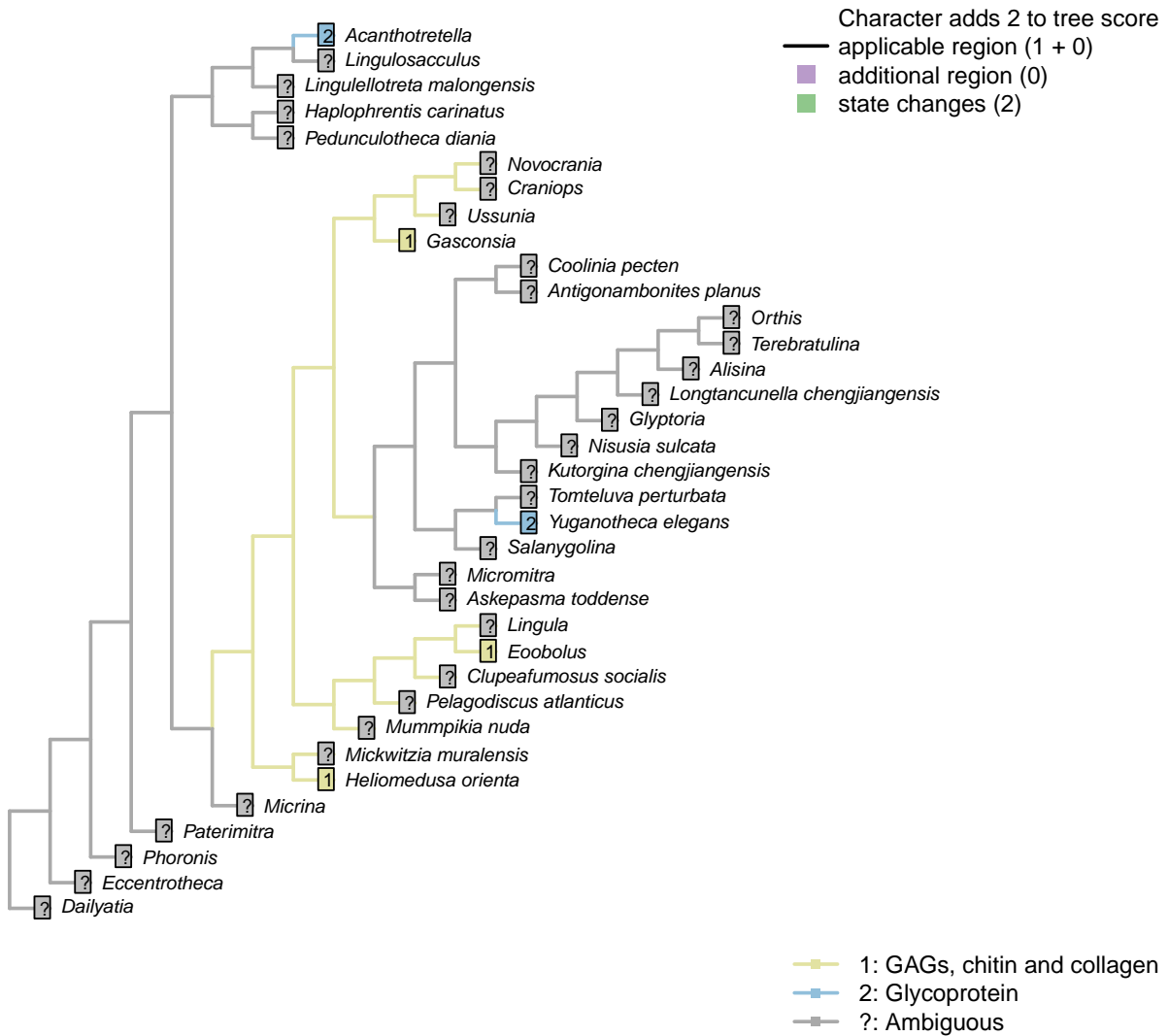


Character 50 – 'Sclerites: Mineralogy'



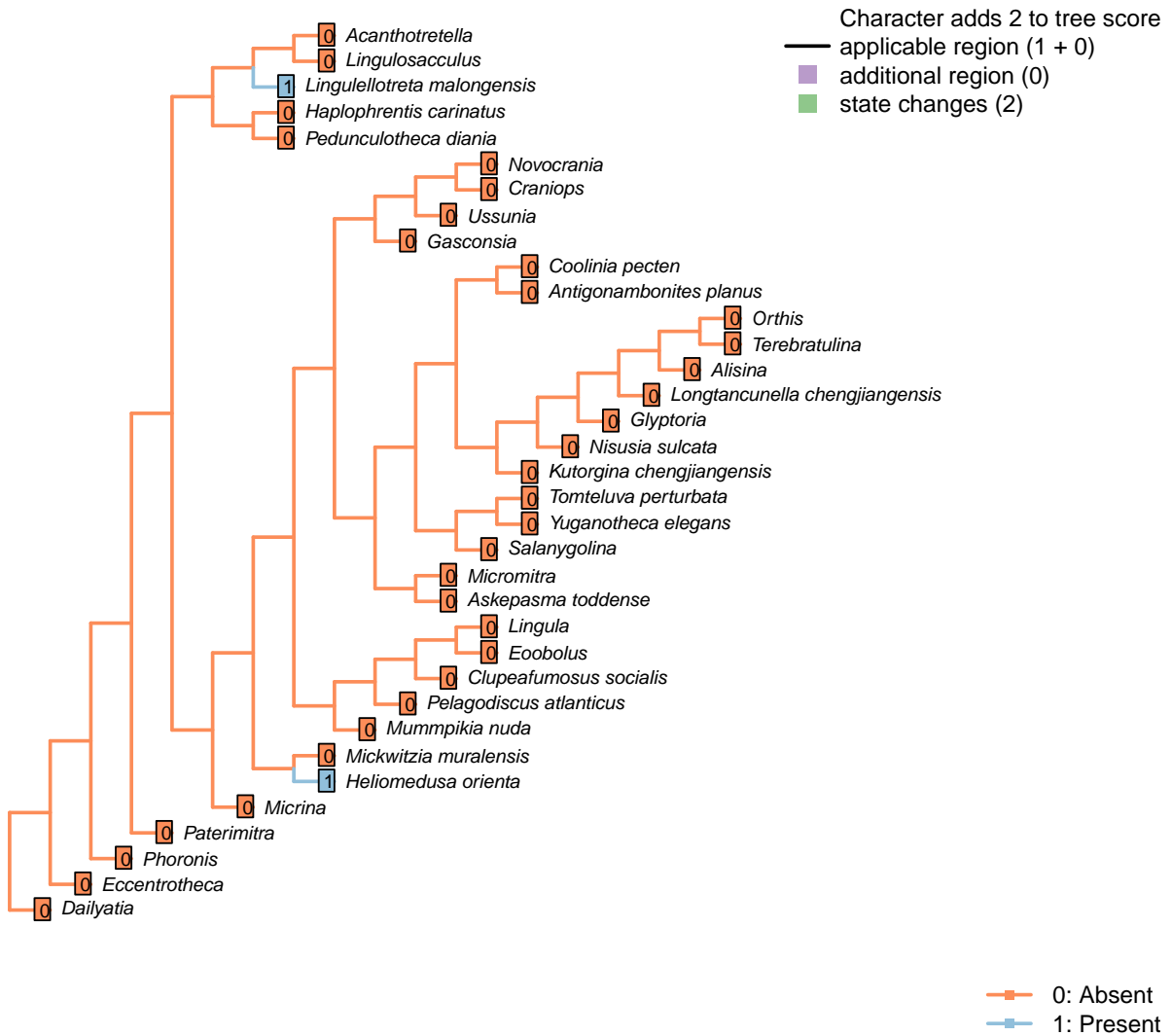
Character 50 – 'Sclerites: Mineralogy'

Character 51 – 'Sclerites: Composition of cuticle or organic matrix'



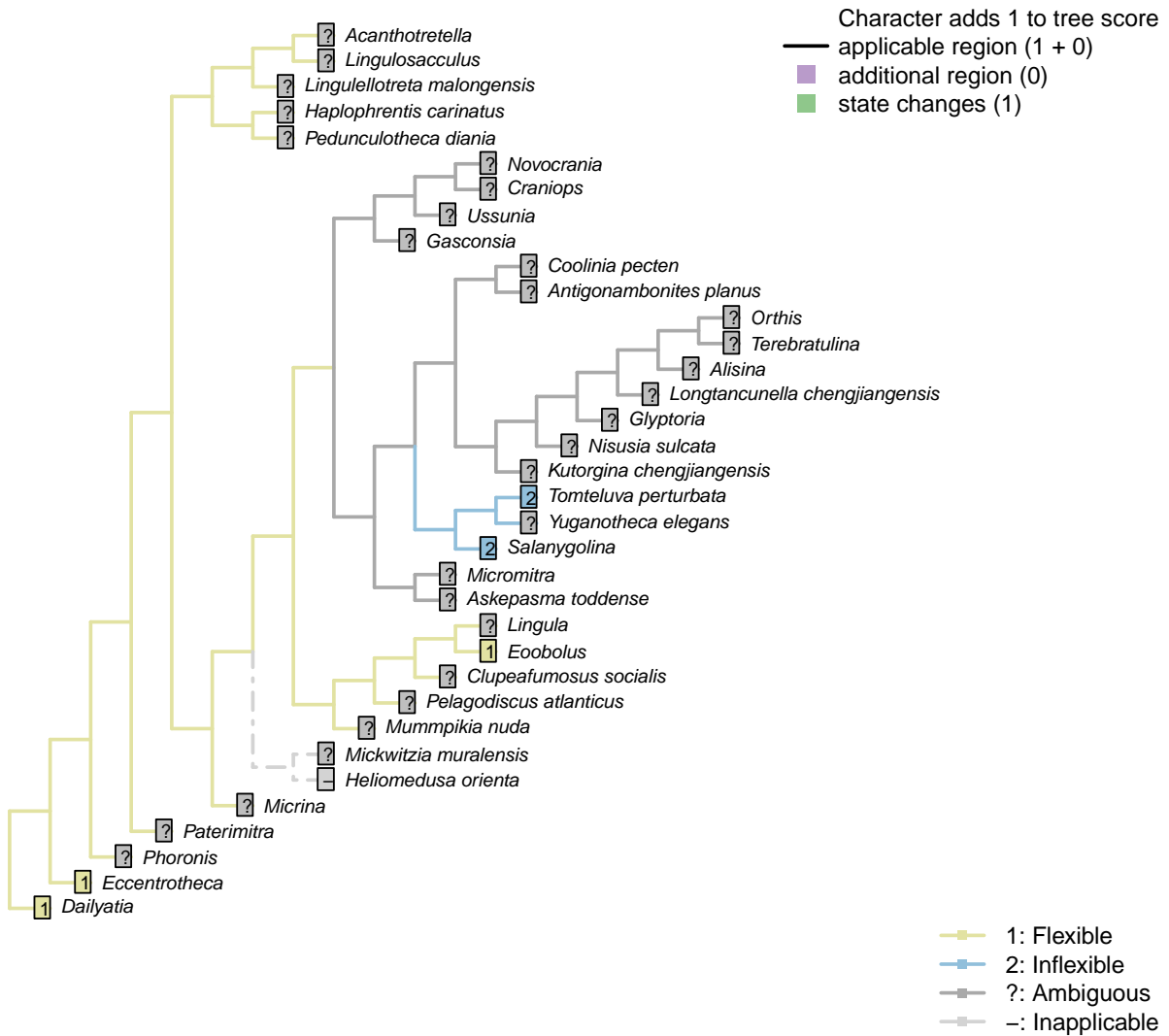
Character 51 – 'Sclerites: Composition of cuticle or organic matrix'

Character 52 – 'Sclerites: incorporation of sedimentary particles'



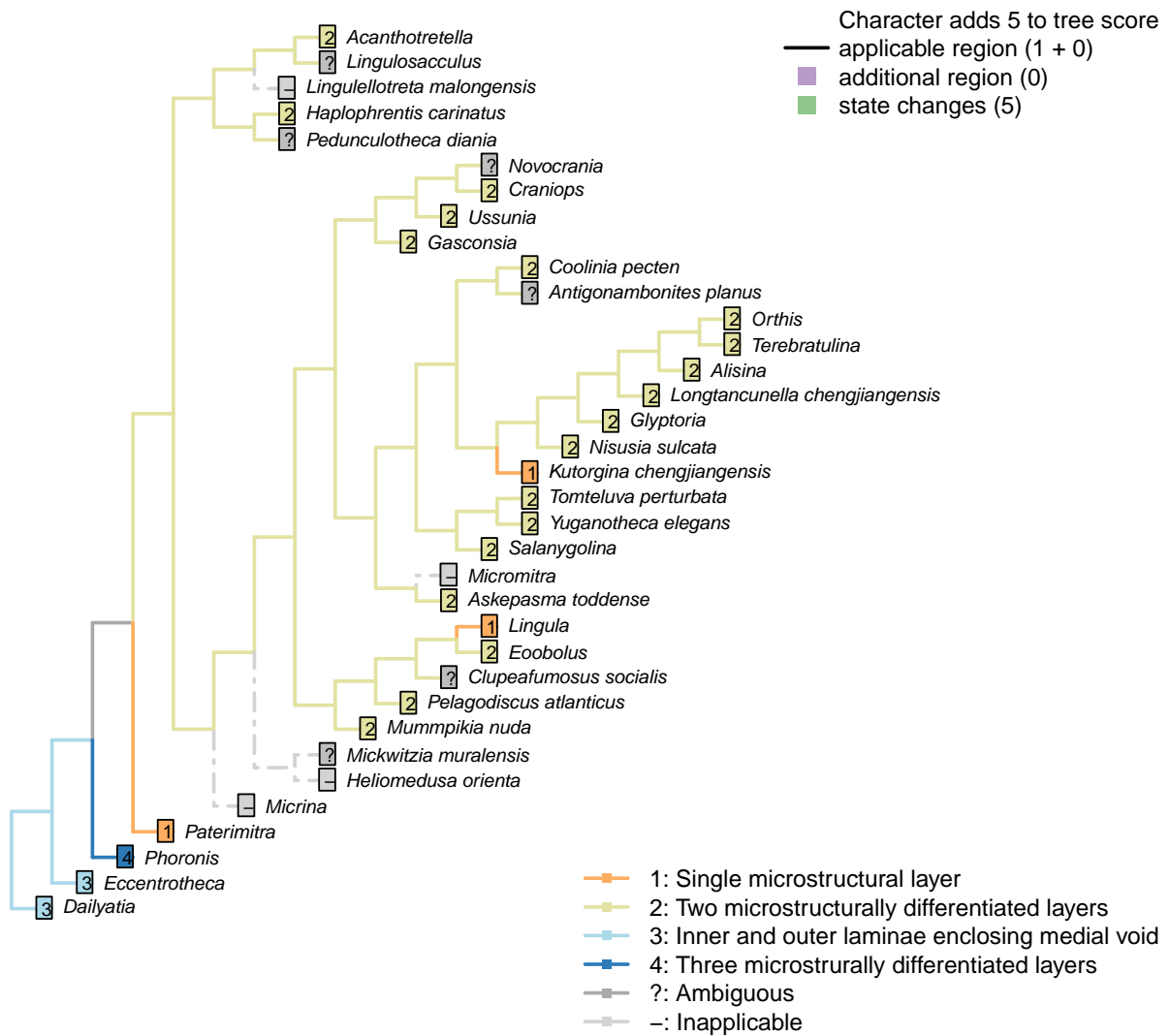
Character 52 – 'Sclerites: incorporation of sedimentary particles'

Character 53 – 'Sclerites: Periostracum: Flexibility'



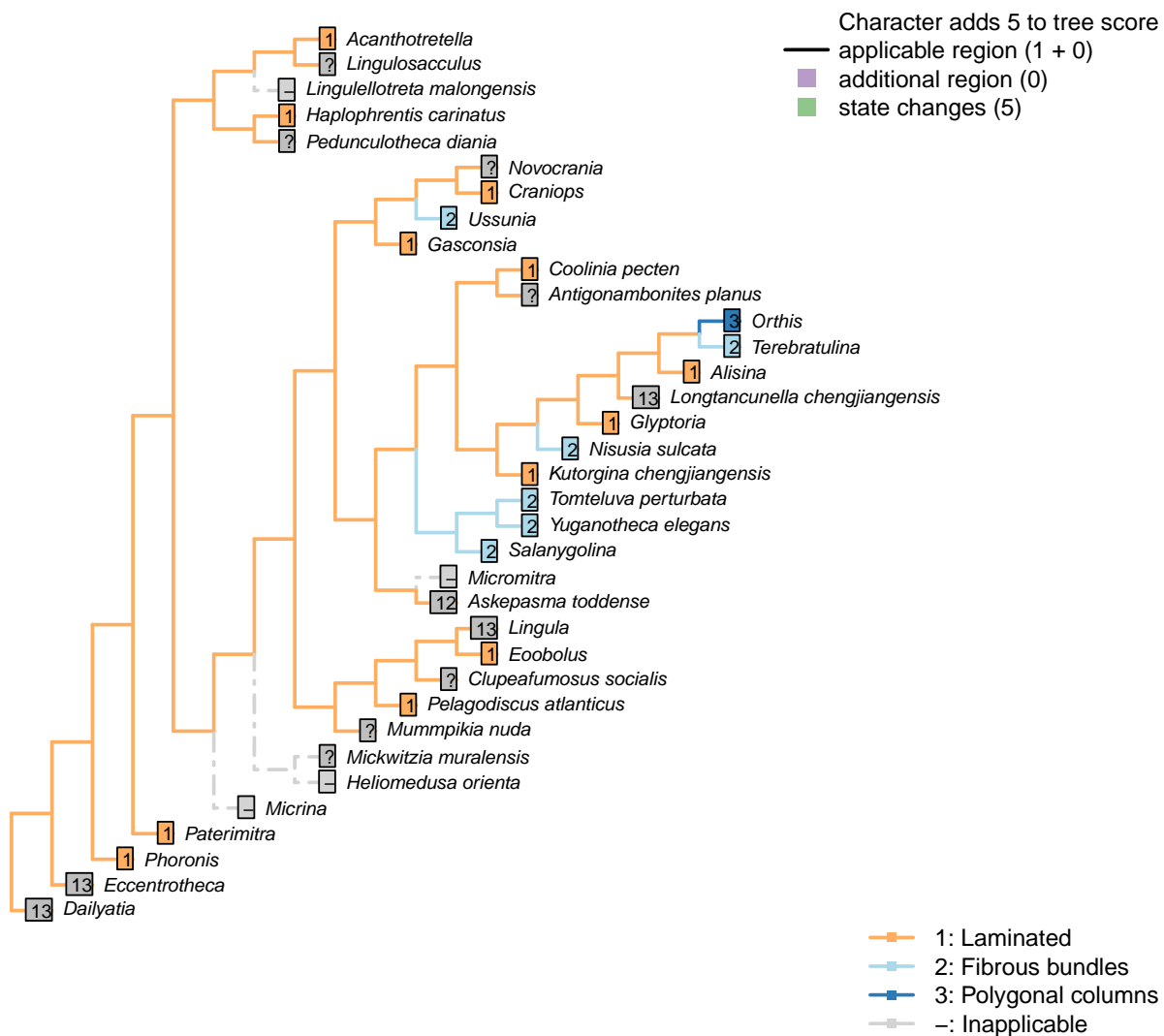
Character 53 – 'Sclerites: Periostracum: Flexibility'

Character 54 – 'Sclerites: Microstructure: Layers'



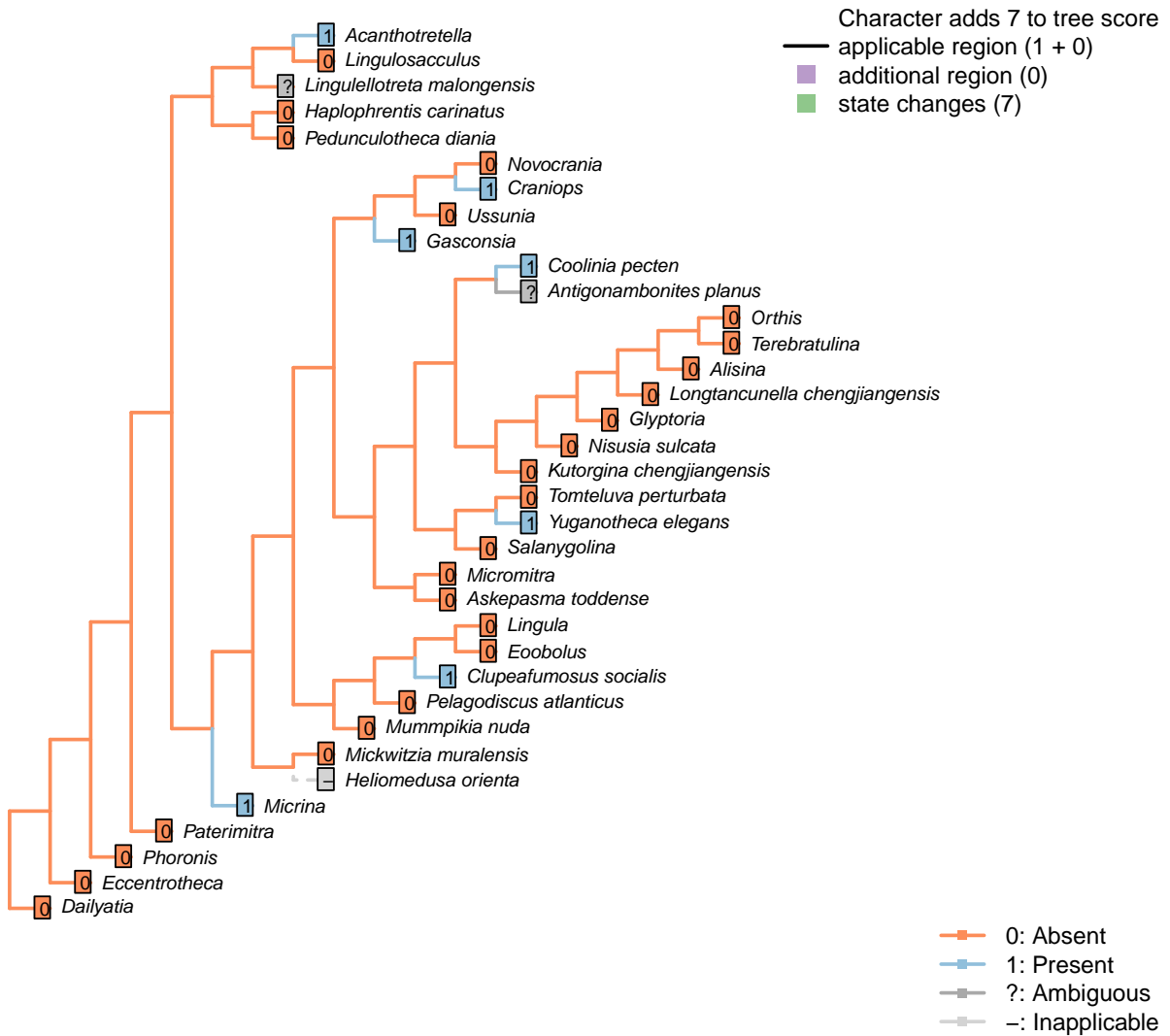
Character 54 – 'Sclerites: Microstructure: Layers'

Character 55 – 'Sclerites: Microstructure: Crystal format'



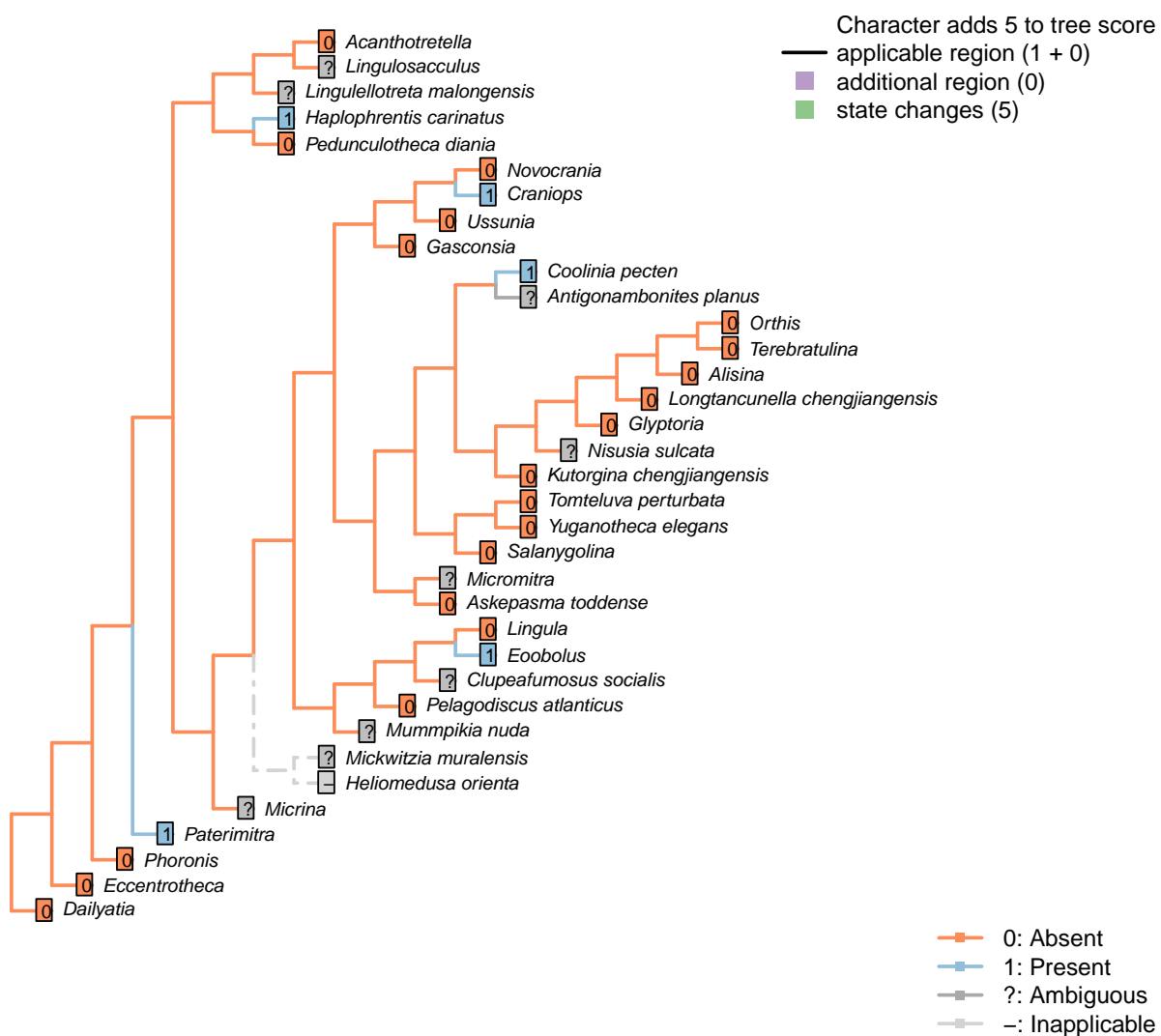
Character 55 – 'Sclerites: Microstructure: Crystal format'

Character 56 – 'Sclerites: Microstructure: Punctae'



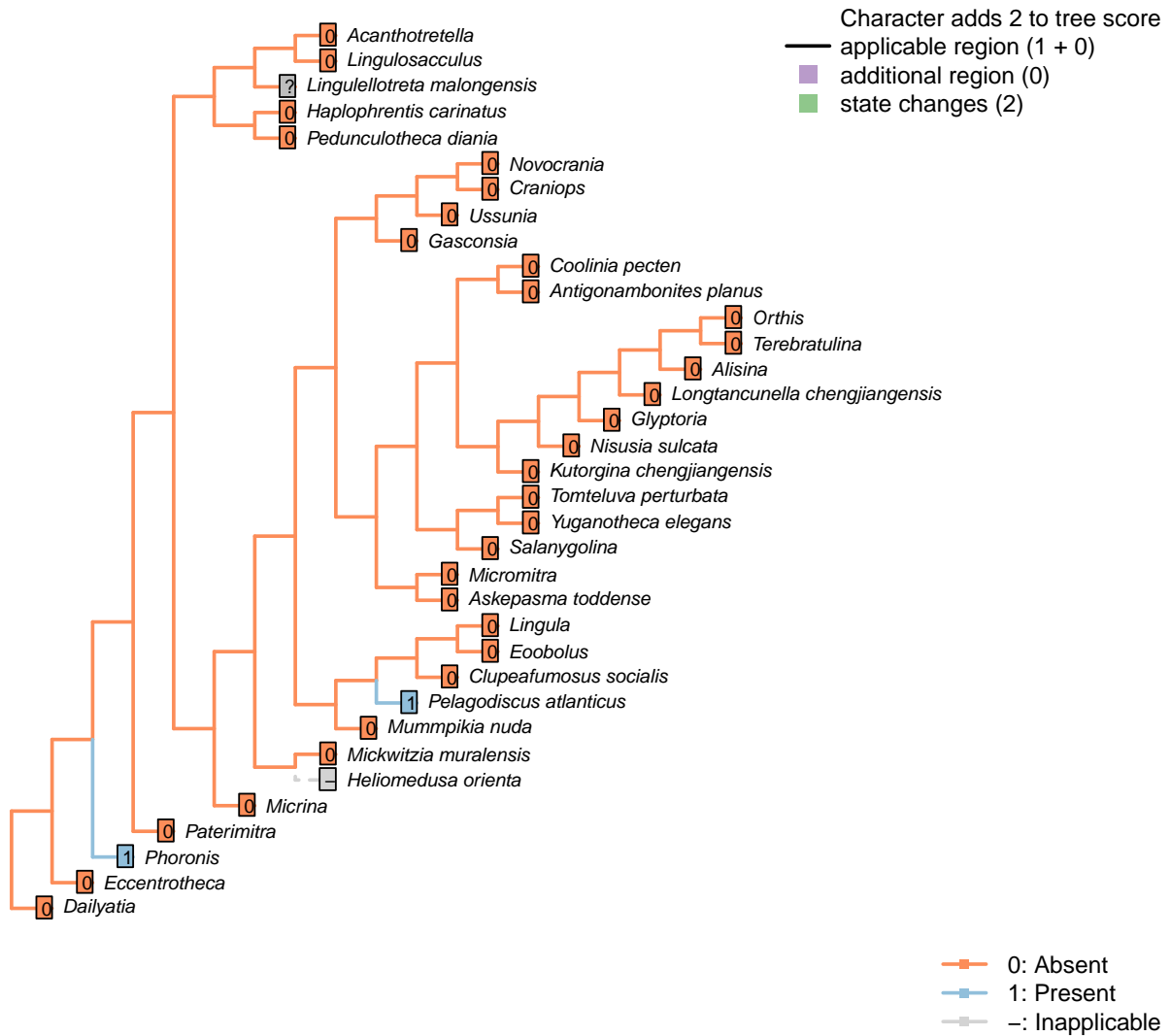
Character 56 – 'Sclerites: Microstructure: Punctae'

Character 57 – 'Sclerites: Microstructure: Canals'



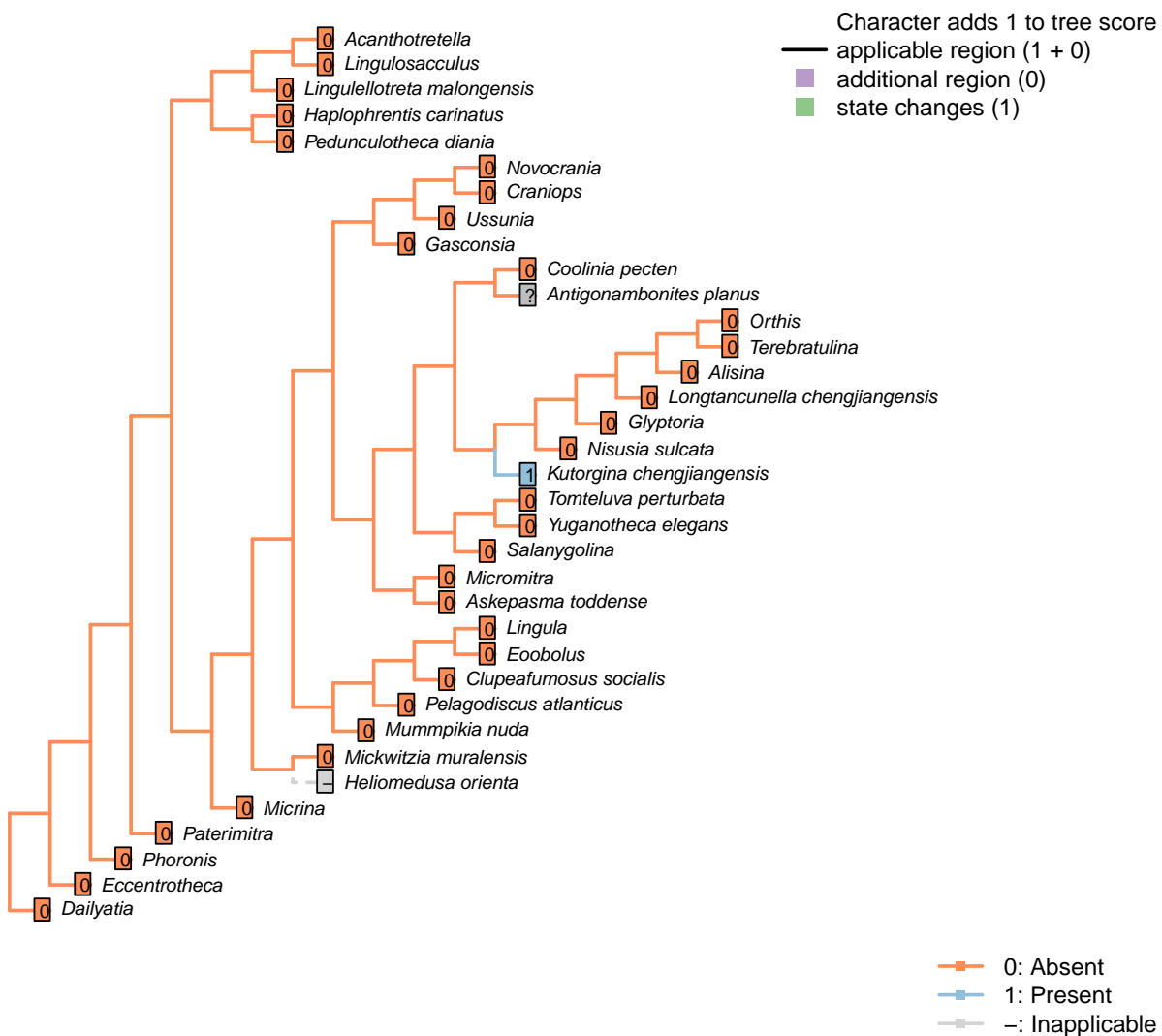
Character 57 – 'Sclerites: Microstructure: Canals'

Character 58 – 'Sclerites: Microstructure: Pseudopunctae'



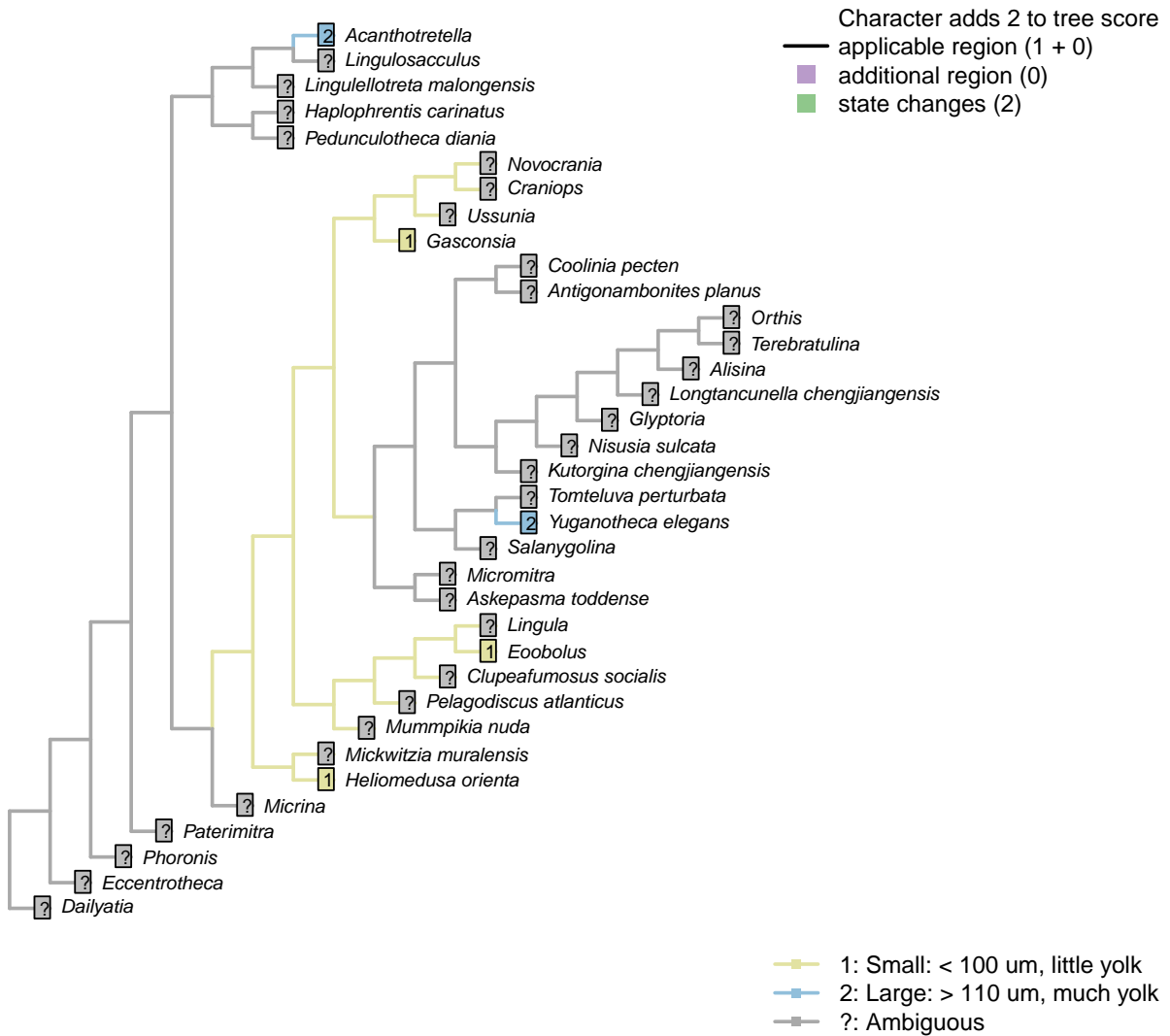
Character 58 – 'Sclerites: Microstructure: Pseudopunctae'

Character 59 – 'Sclerites: Microstructure: External polygonal ornament'



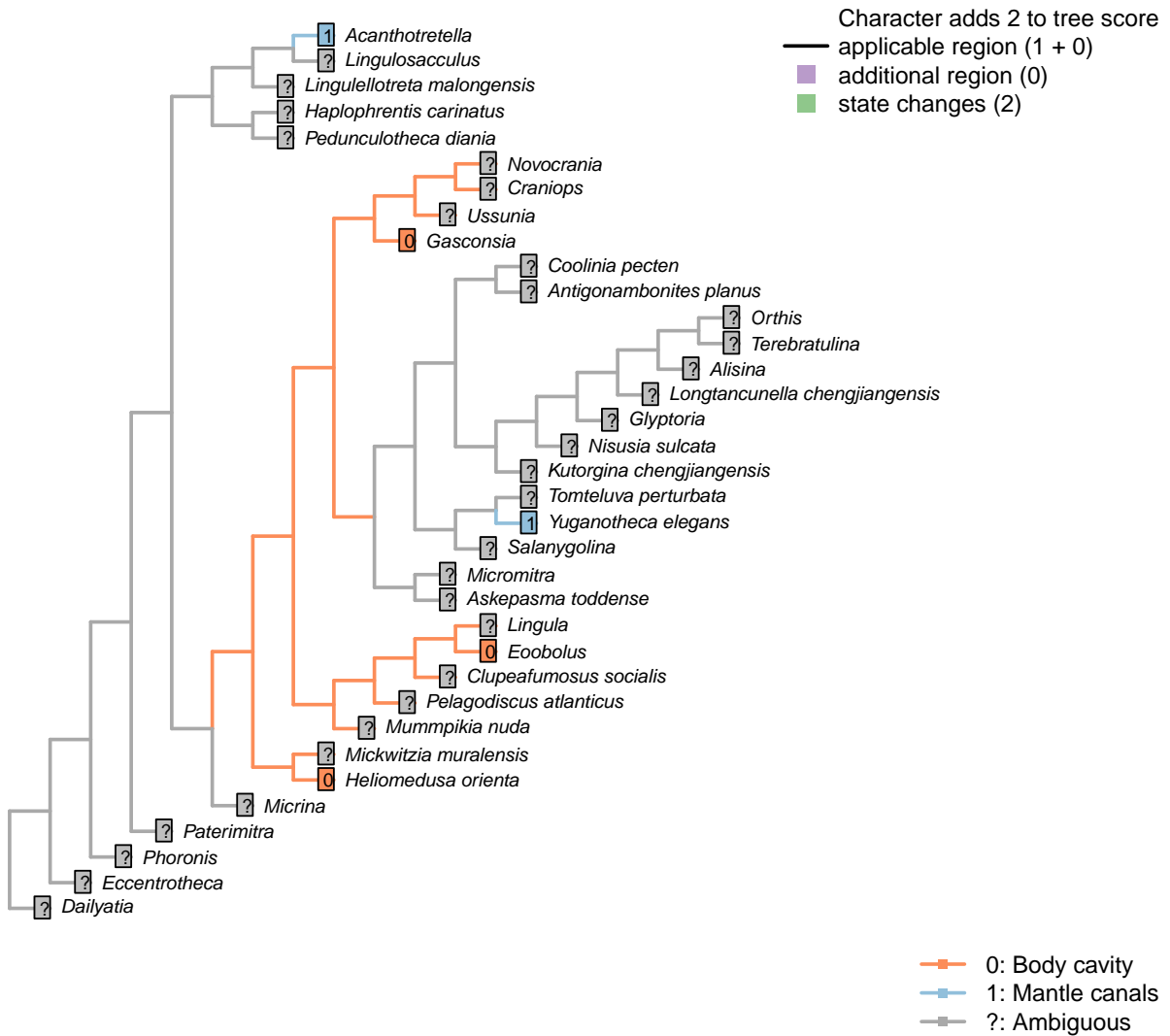
Character 59 – 'Sclerites: Microstructure: External polygonal ornament'

Character 60 – 'Egg size'

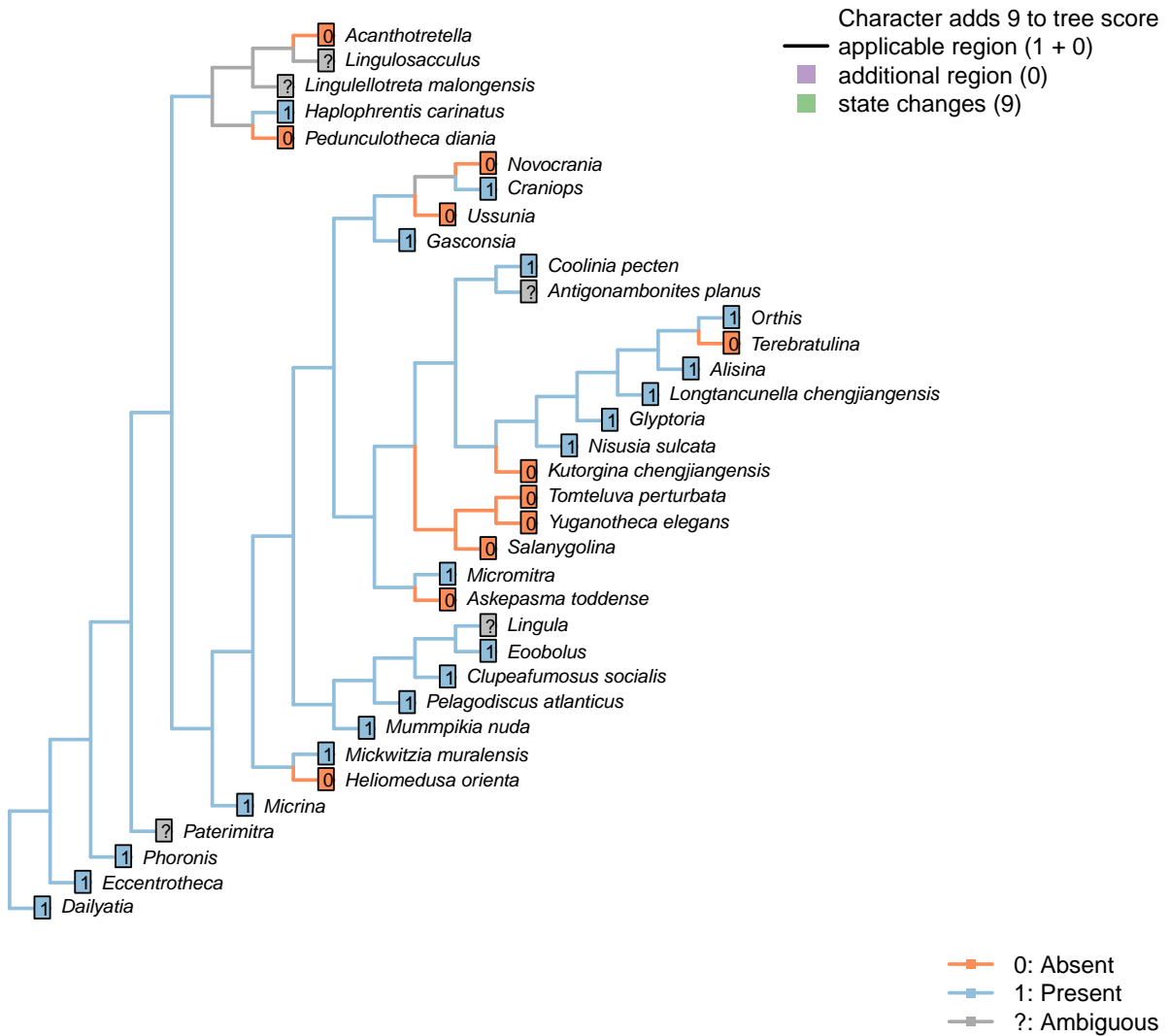


Character 60 – 'Egg size'

Character 61 – 'Site of gamete maturation'

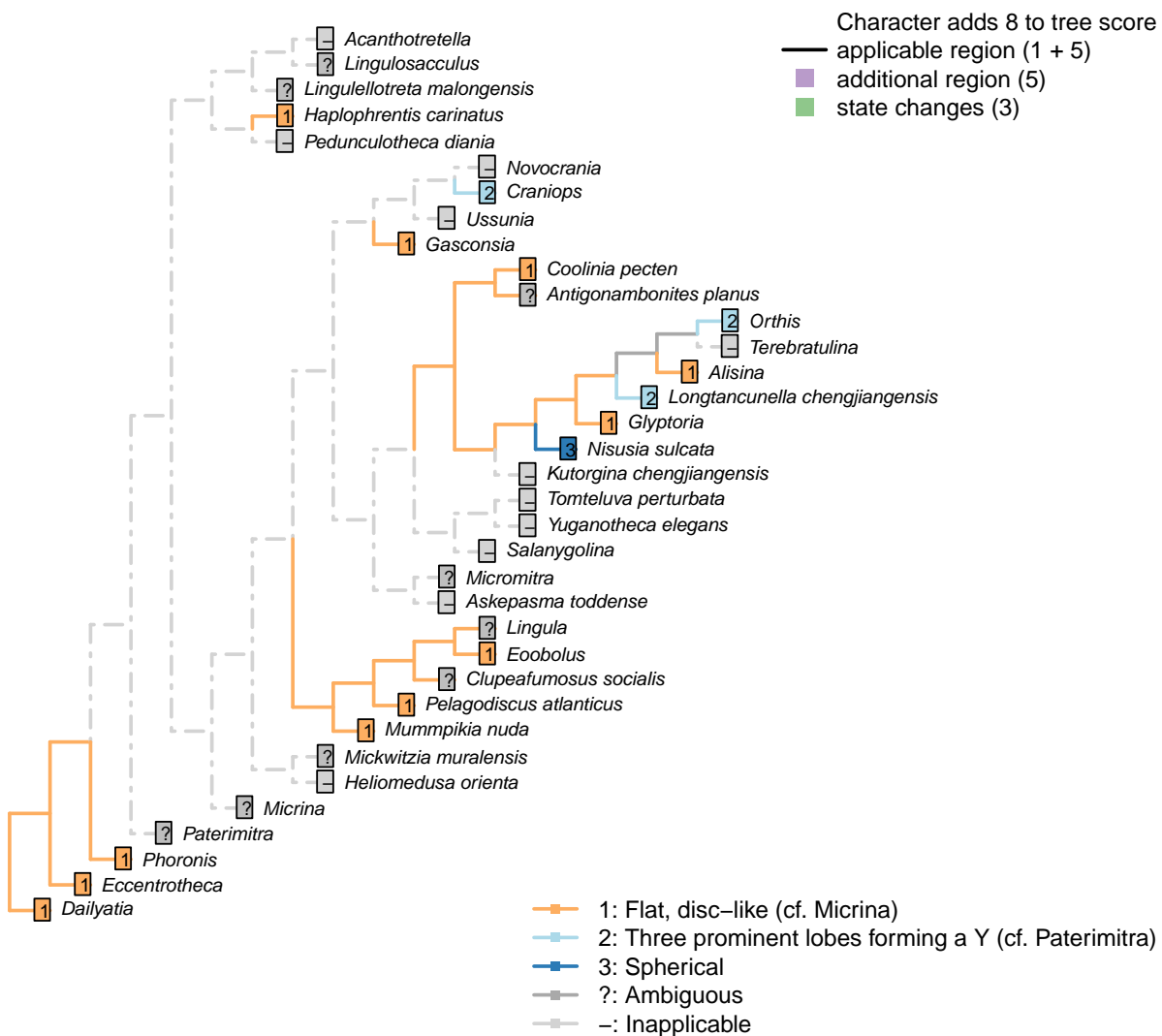


Character 62 – 'Embryonic shell'



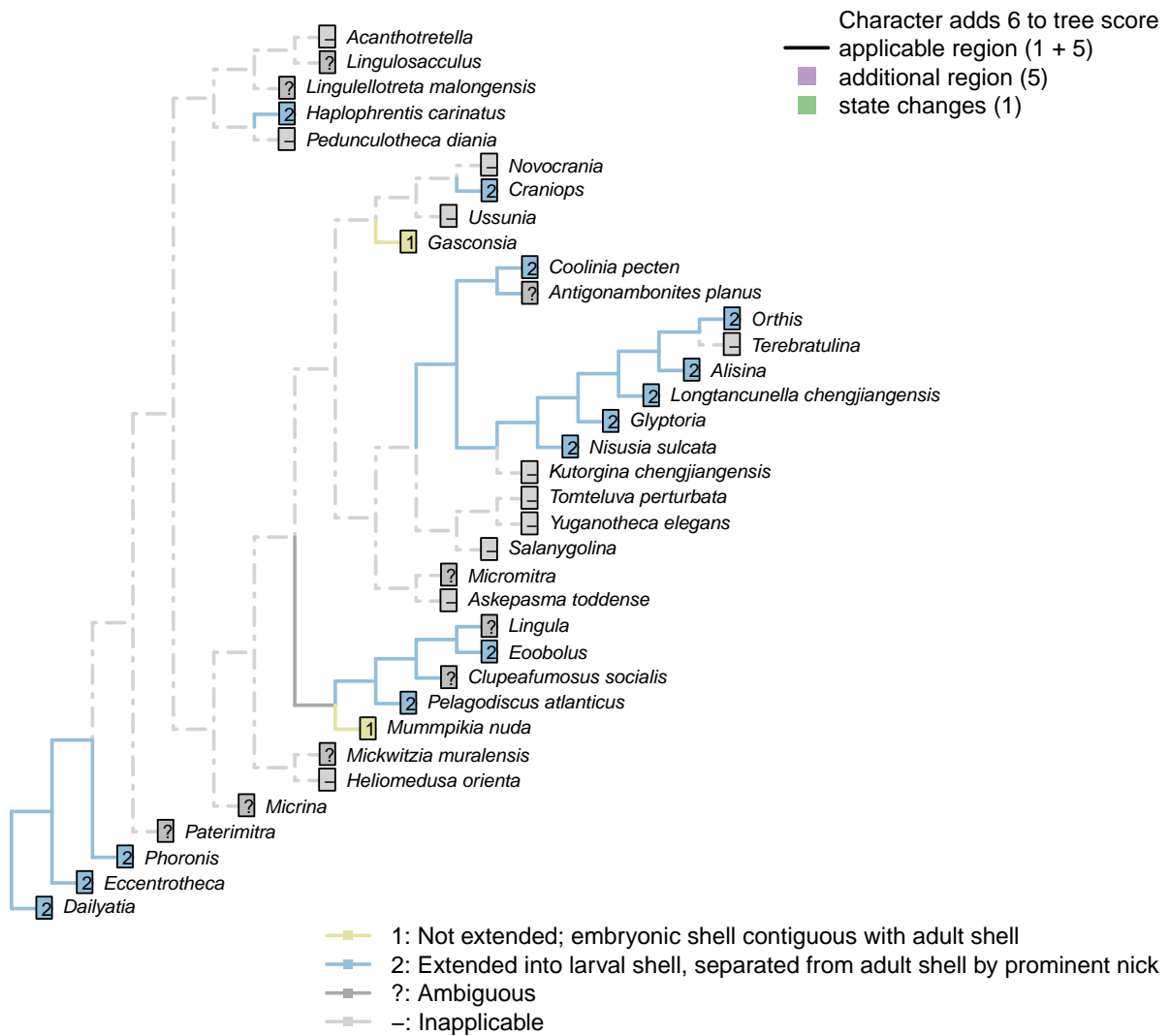
Character 62 – 'Embryonic shell'

Character 63 – 'Embryonic shell: Morphology'



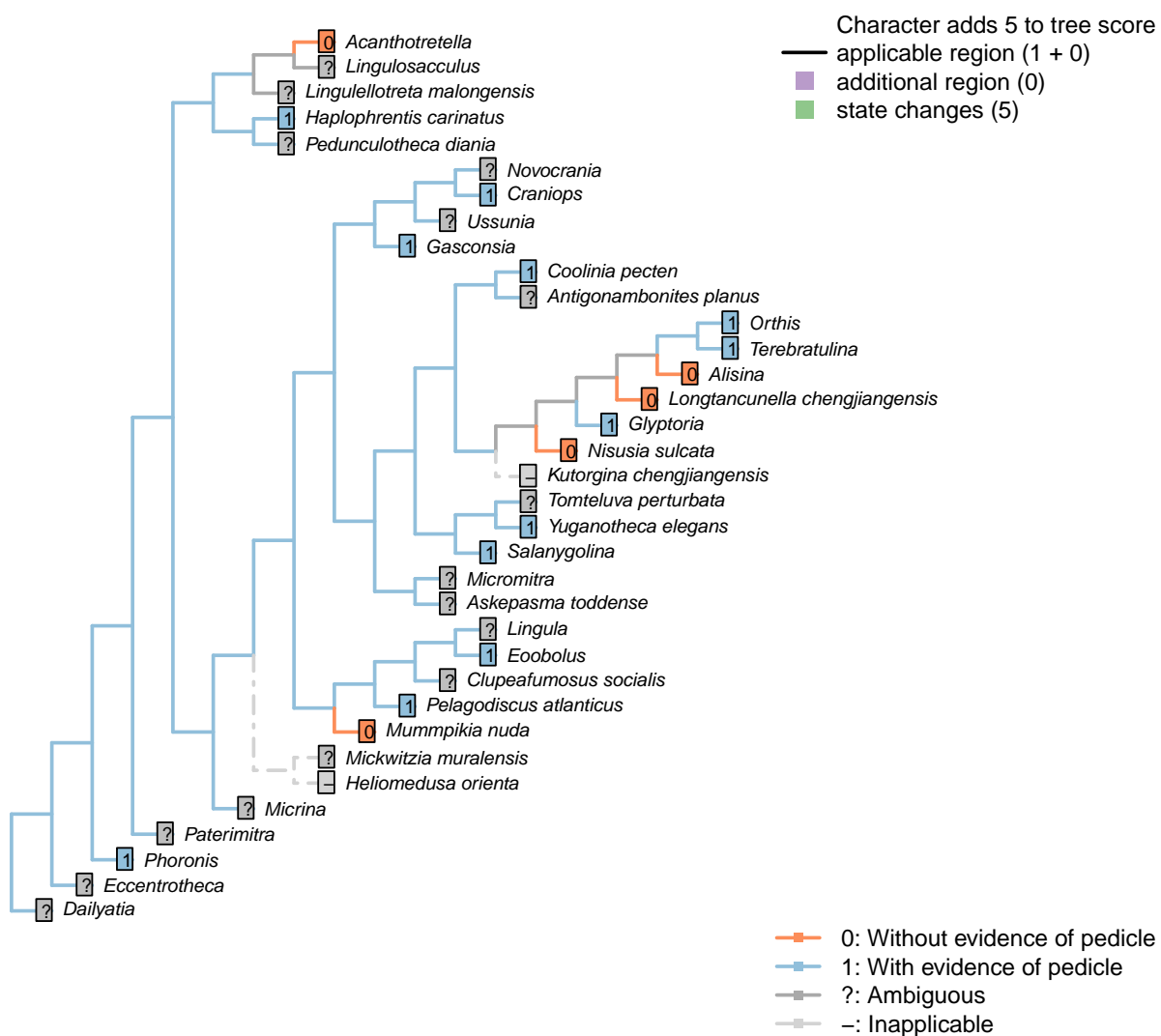
Character 63 – 'Embryonic shell: Morphology'

Character 64 – 'Embryonic shell: Extended in larvae'



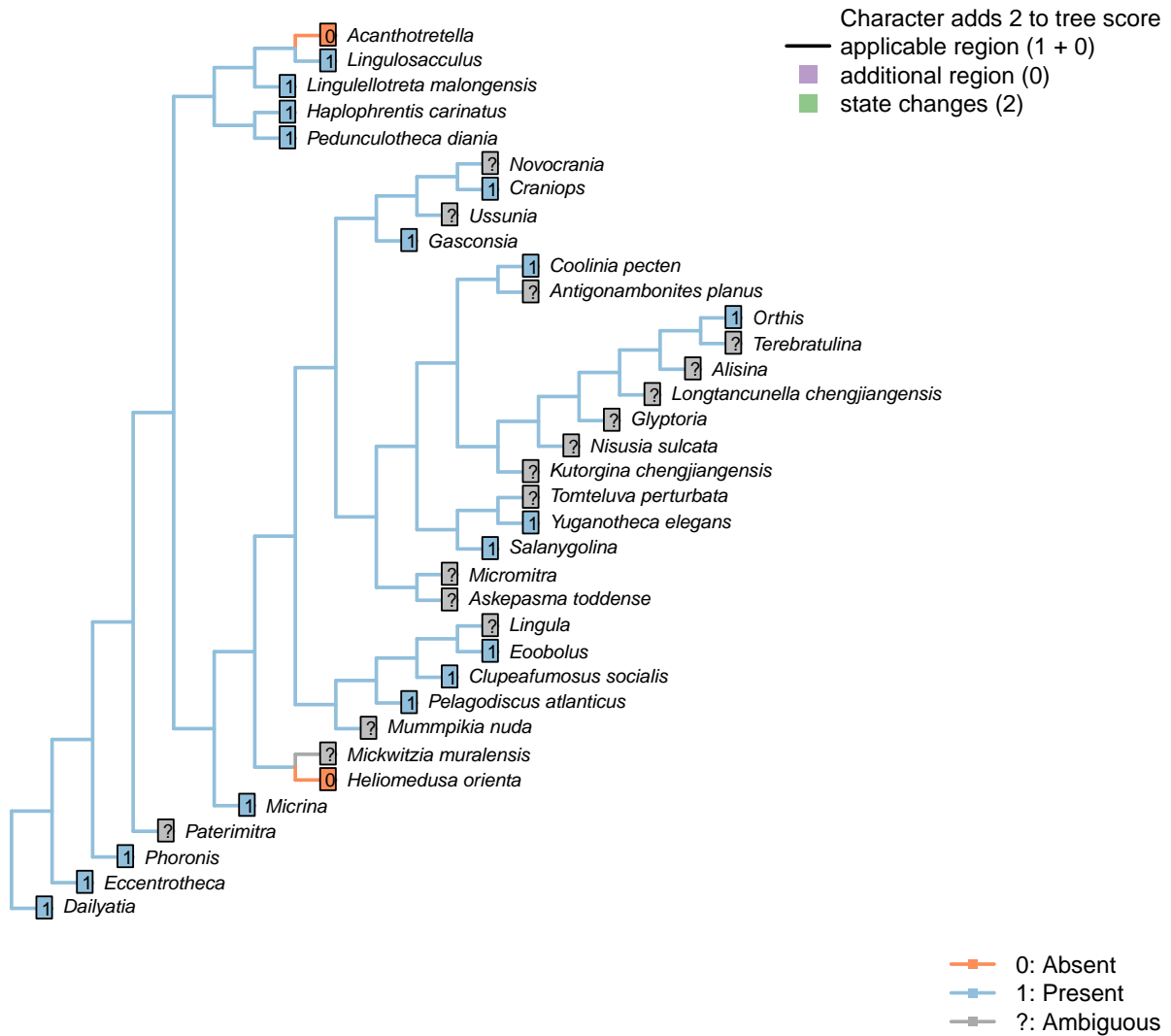
Character 64 – 'Embryonic shell: Extended in larvae'

Character 65 – 'Larval attachment structure'



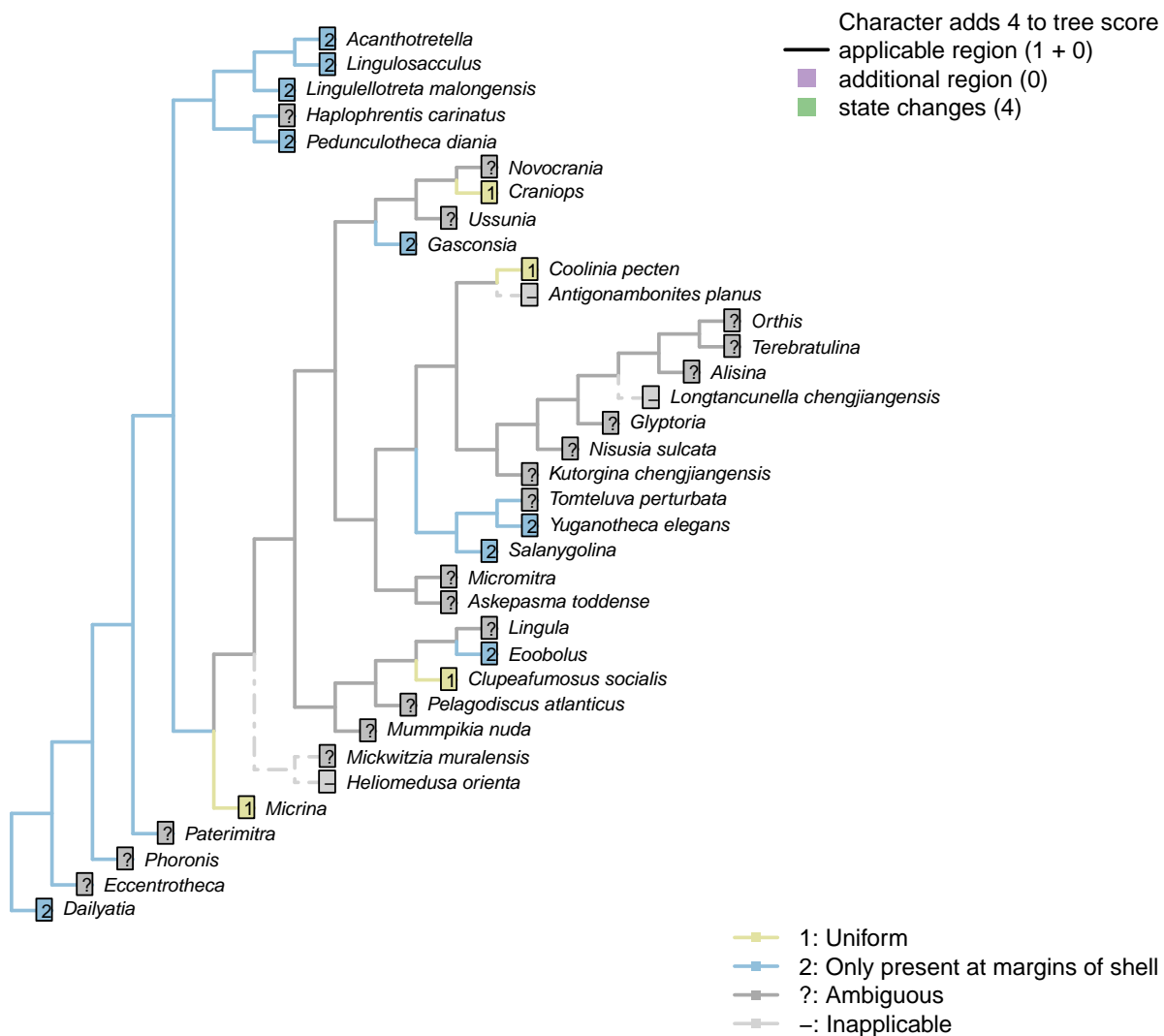
Character 65 – 'Larval attachment structure'

Character 66 – 'Setae in adults'



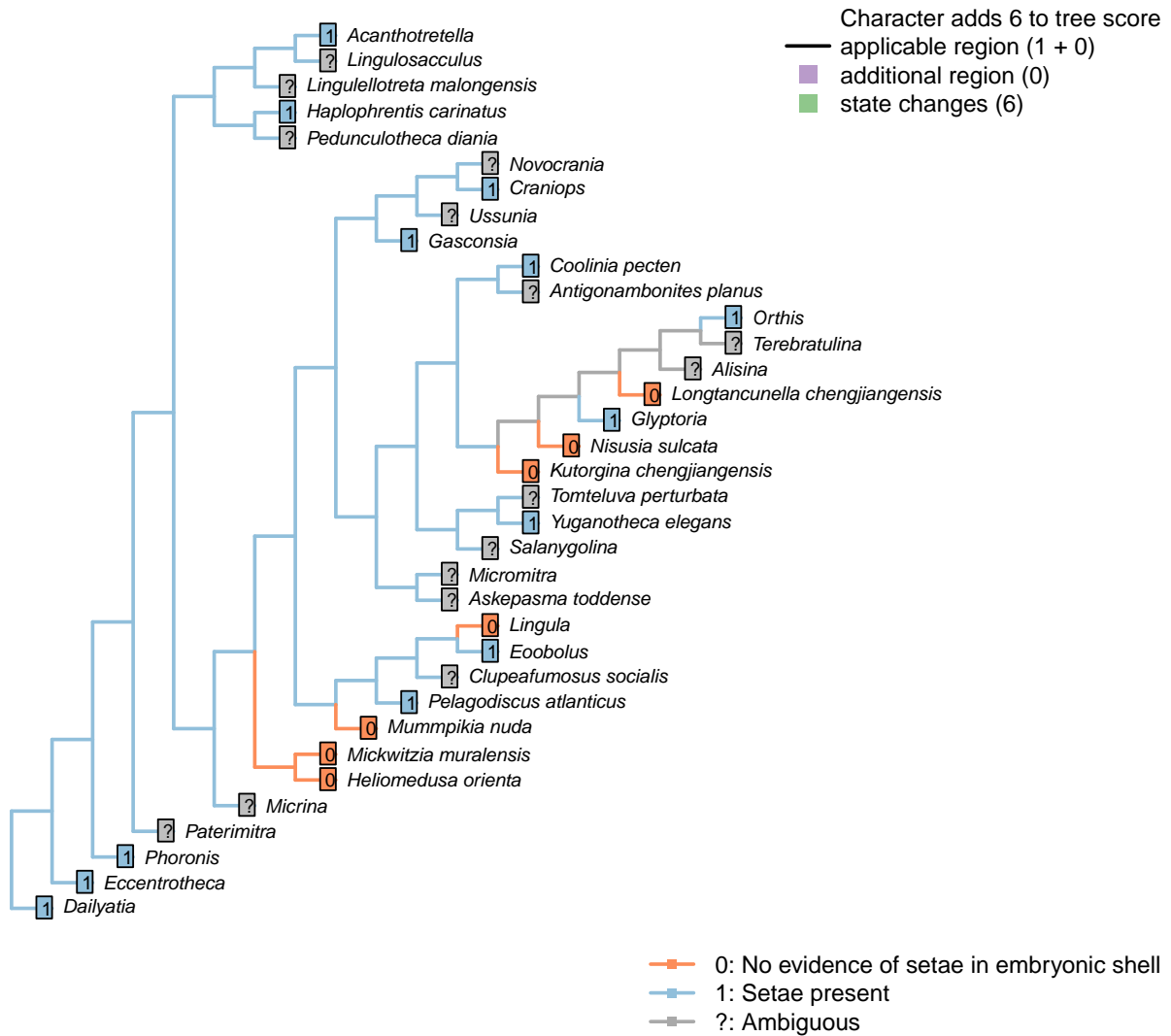
Character 66 – 'Setae in adults'

Character 67 – 'Setae: Distribution'



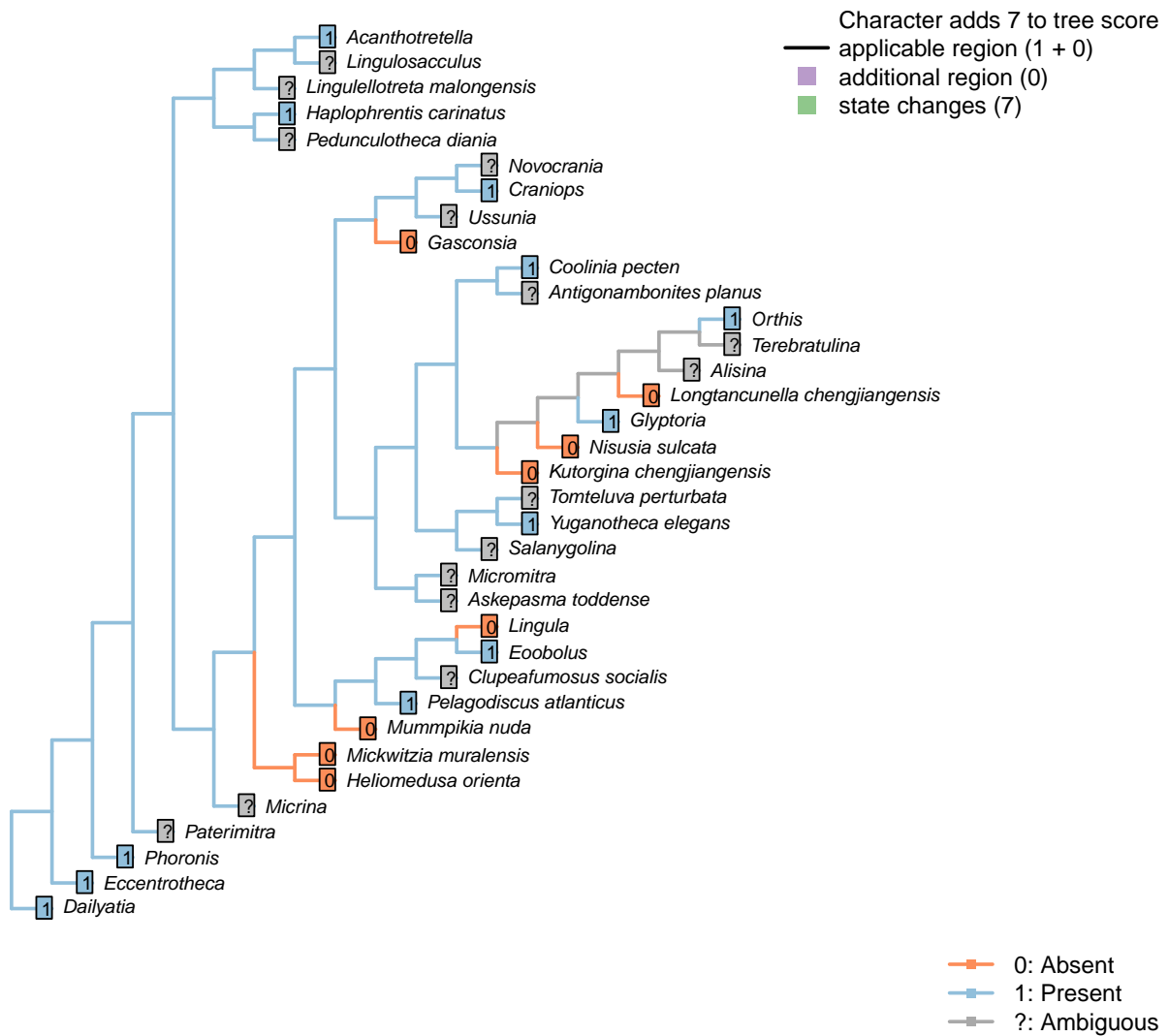
Character 67 – 'Setae: Distribution'

Character 68 – 'Setae: present in larva'



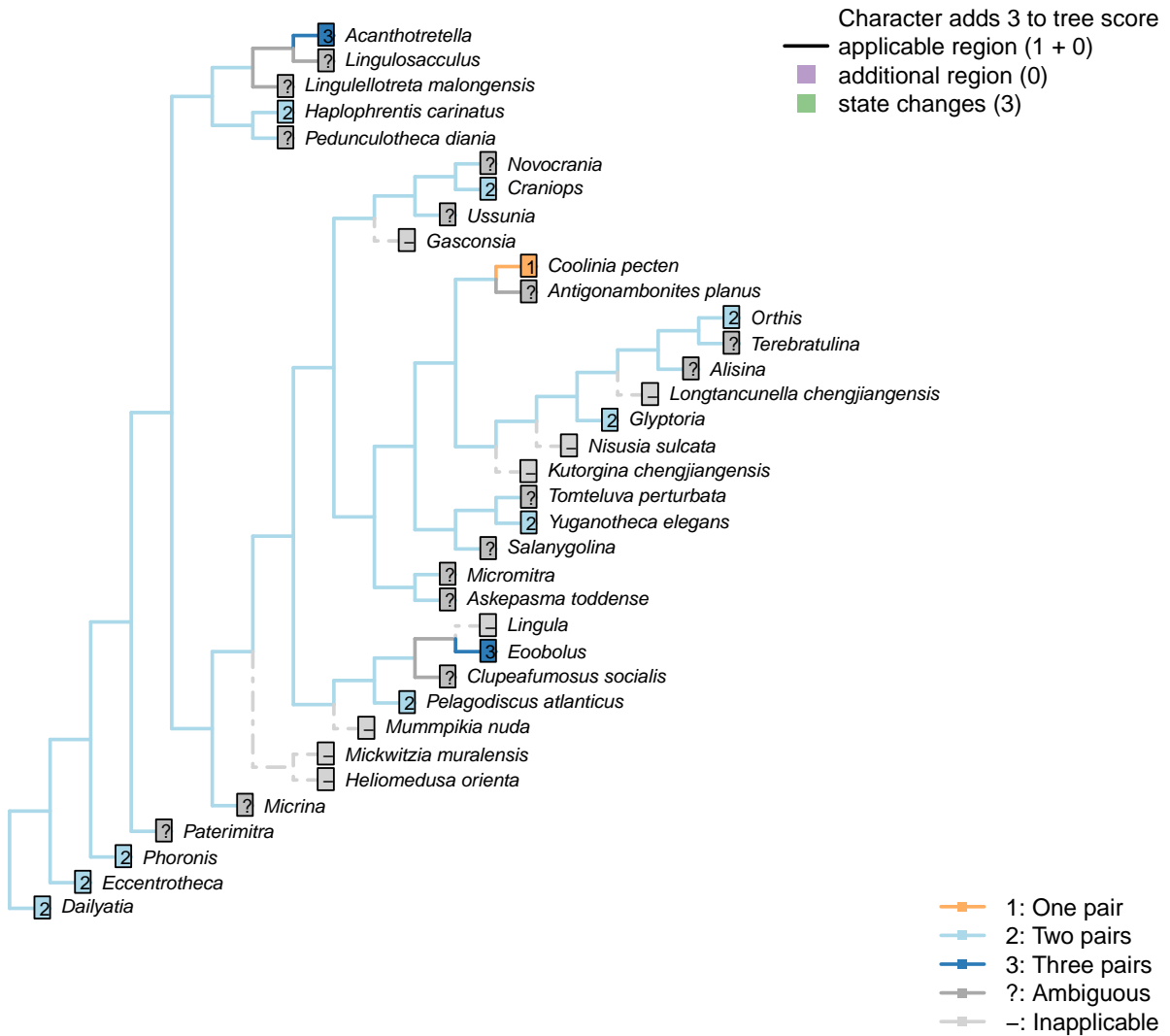
Character 68 – 'Setae: present in larva'

Character 69 – 'Setae: Embryonic: Setal sacs'



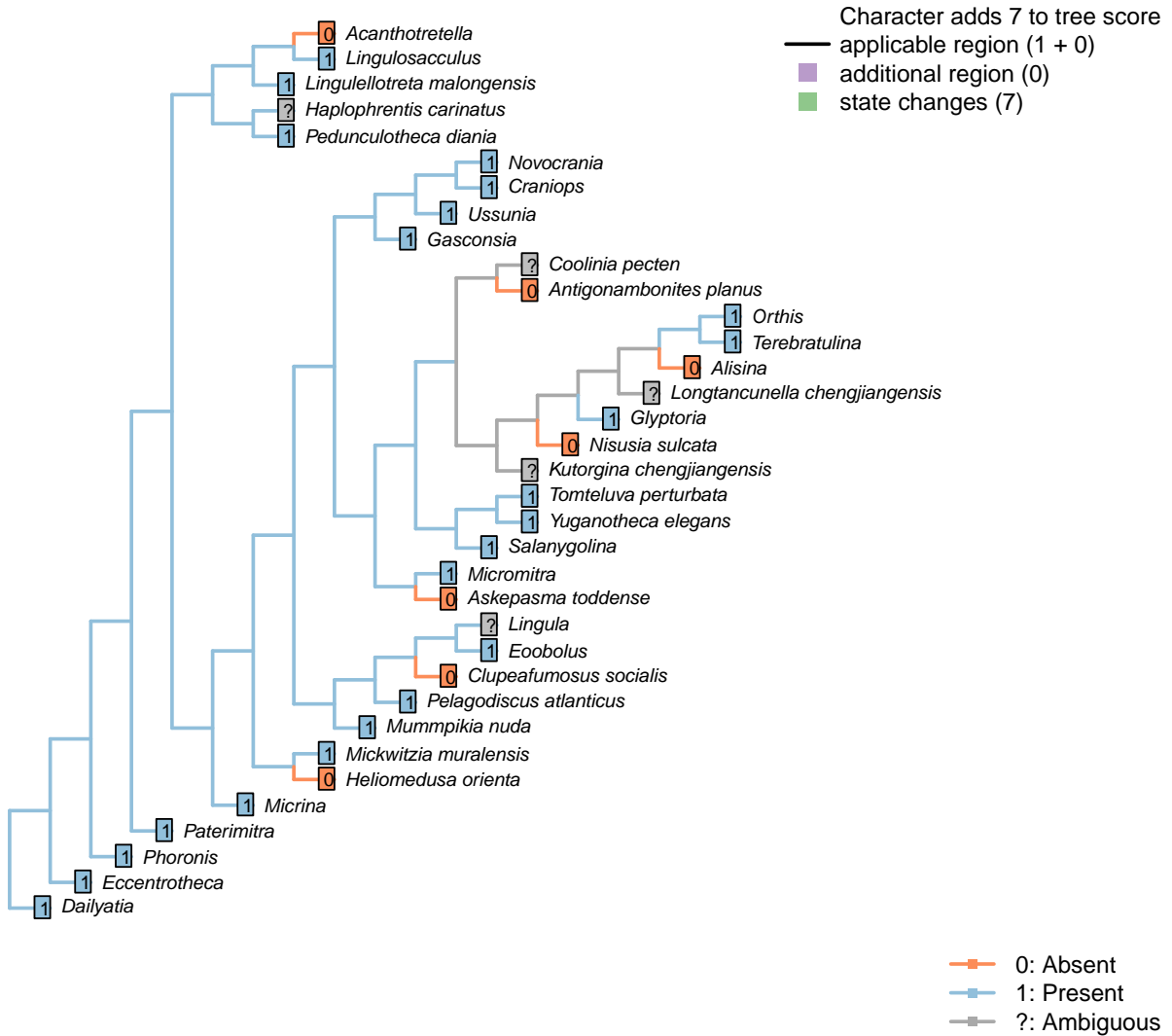
Character 69 – 'Setae: Embryonic: Setal sacs'

Character 70 – 'Setae: Embryonic: Setal sacs: Number'



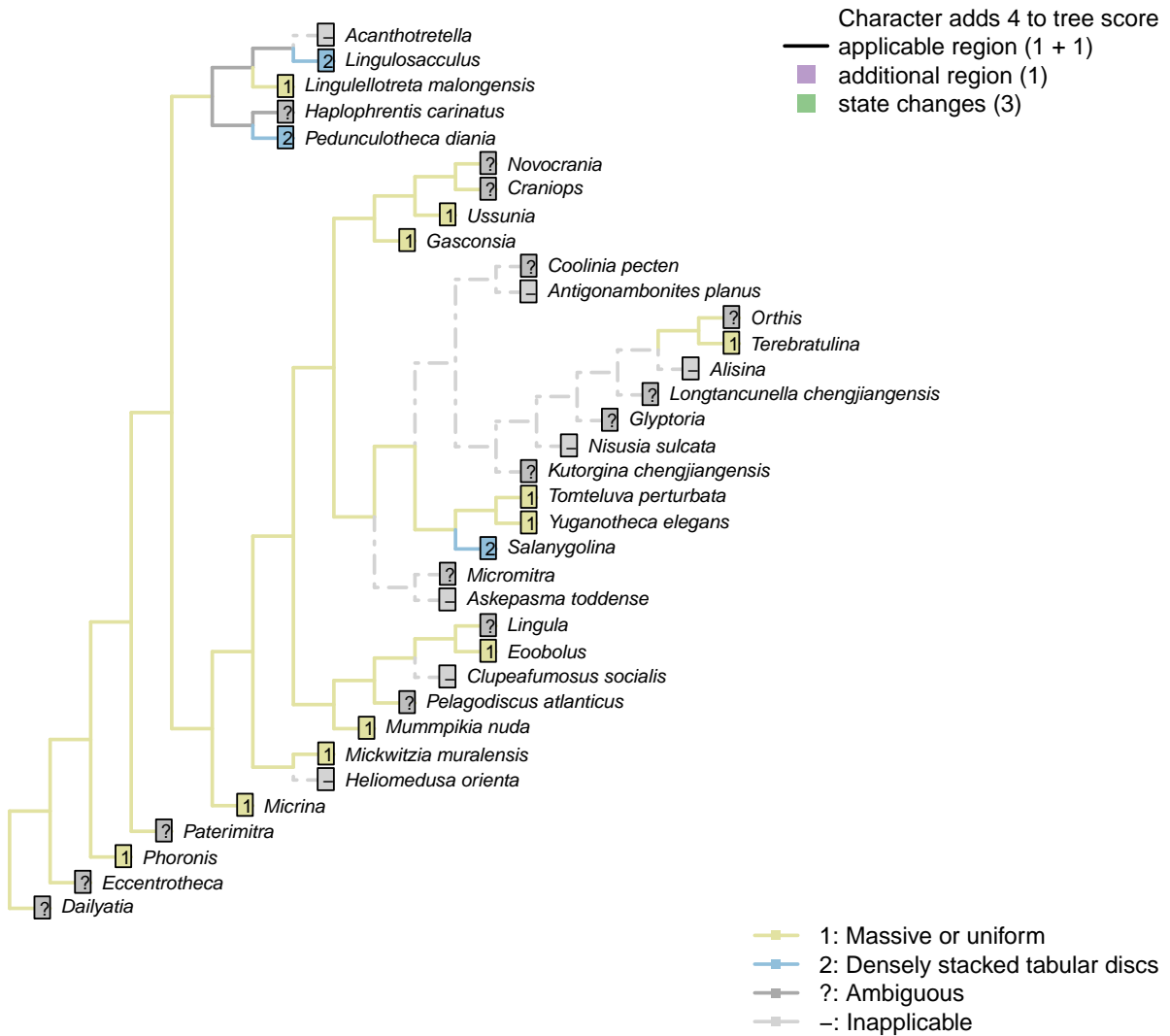
Character 70 – 'Setae: Embryonic: Setal sacs: Number'

Character 71 – 'Pedicel'



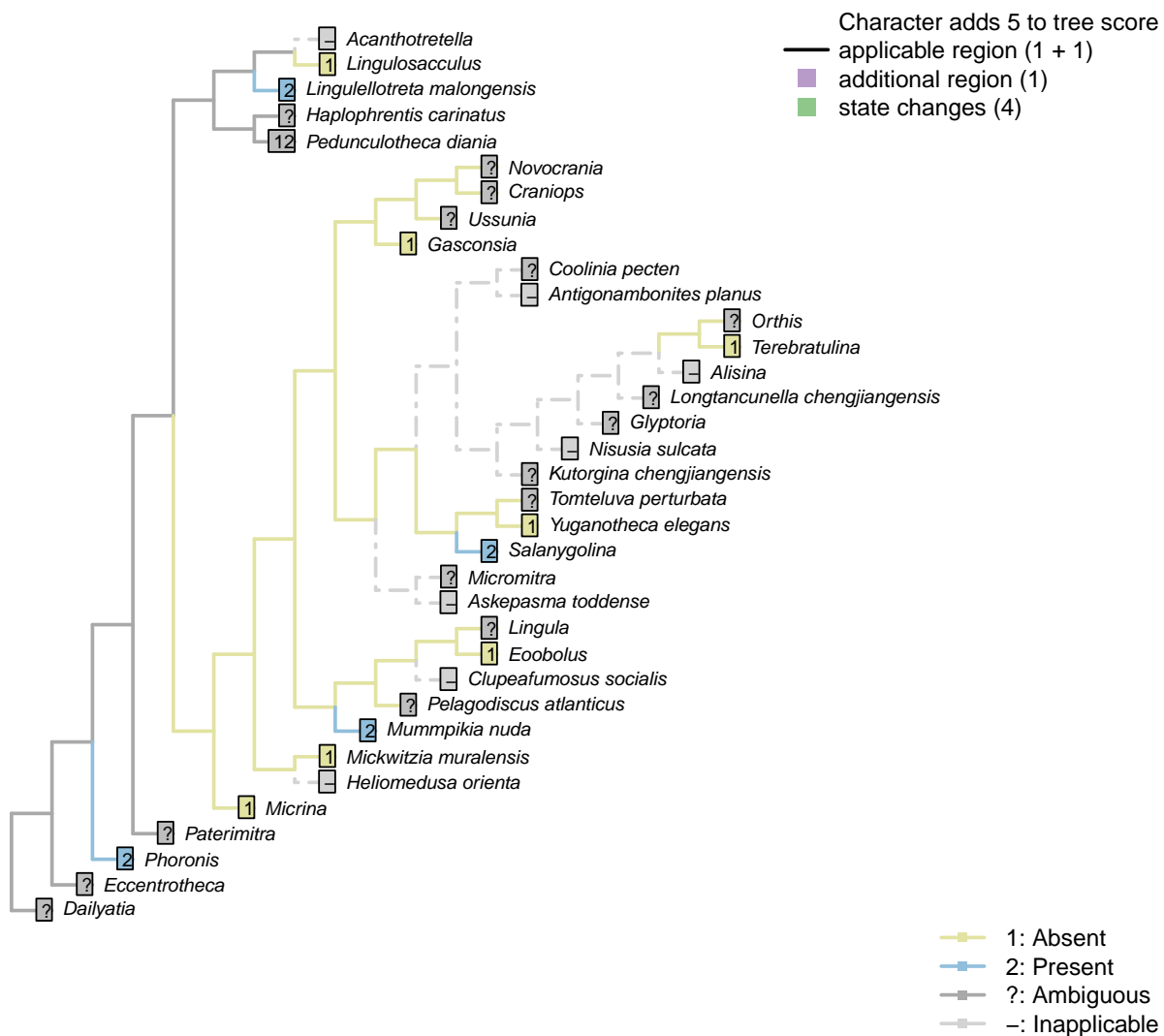
Character 71 – 'Pedicel'

Character 72 – 'Pedicel: Constitution'



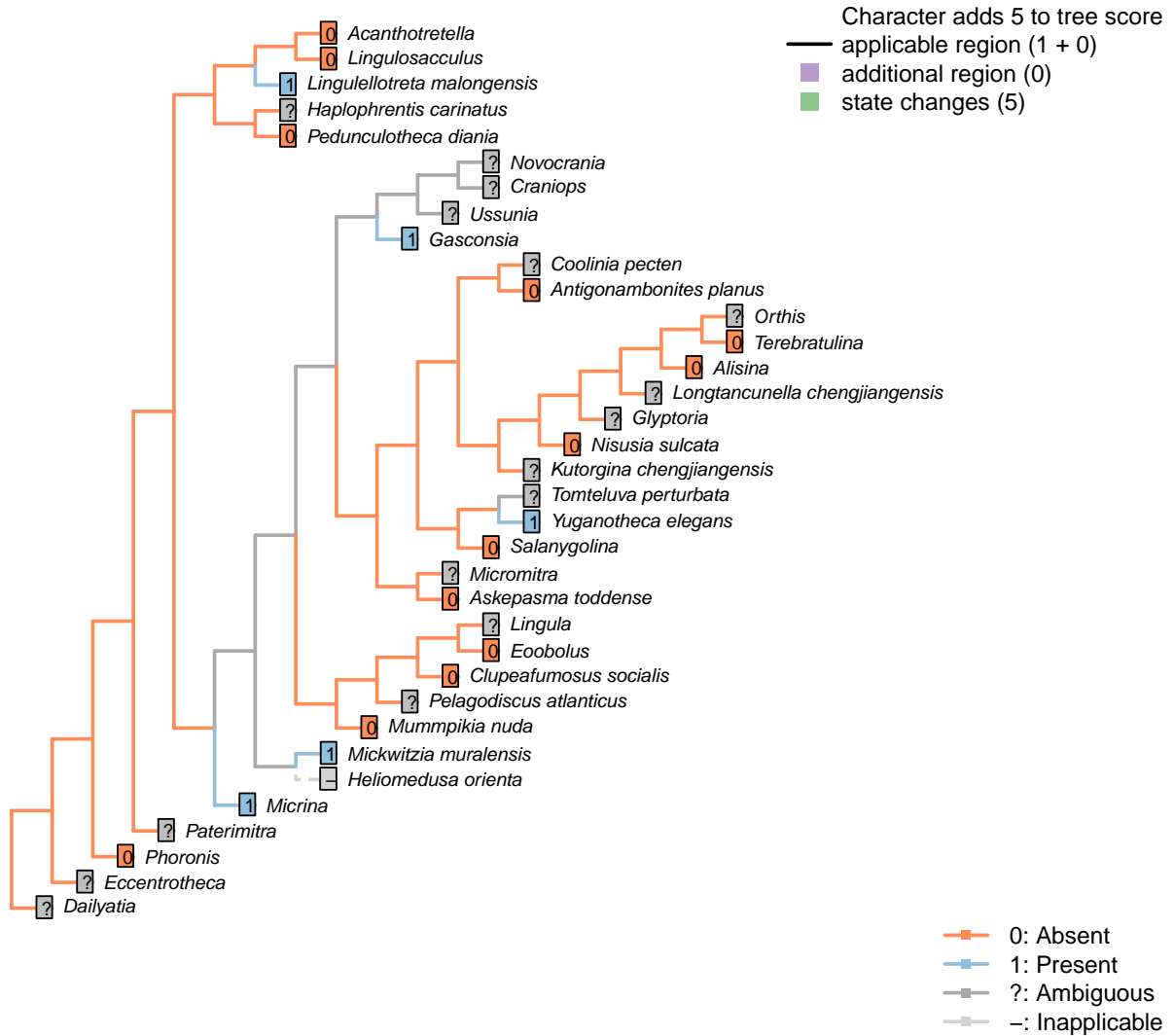
Character 72 – 'Pedicel: Constitution'

Character 73 – 'Pedicle: Biomineralization'



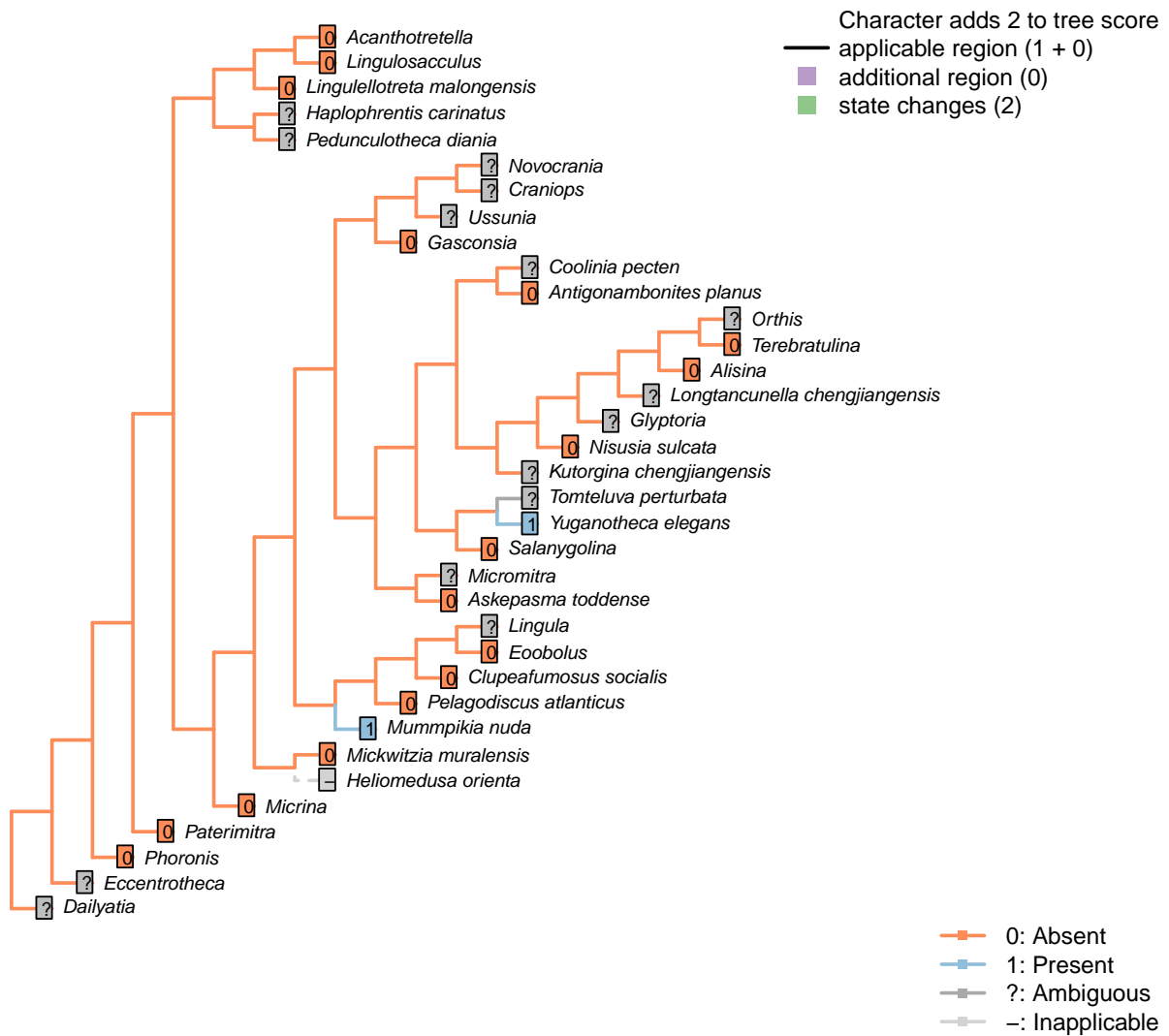
Character 73 – 'Pedicle: Biomineralization'

Character 74 – 'Pedicel: Bulb'

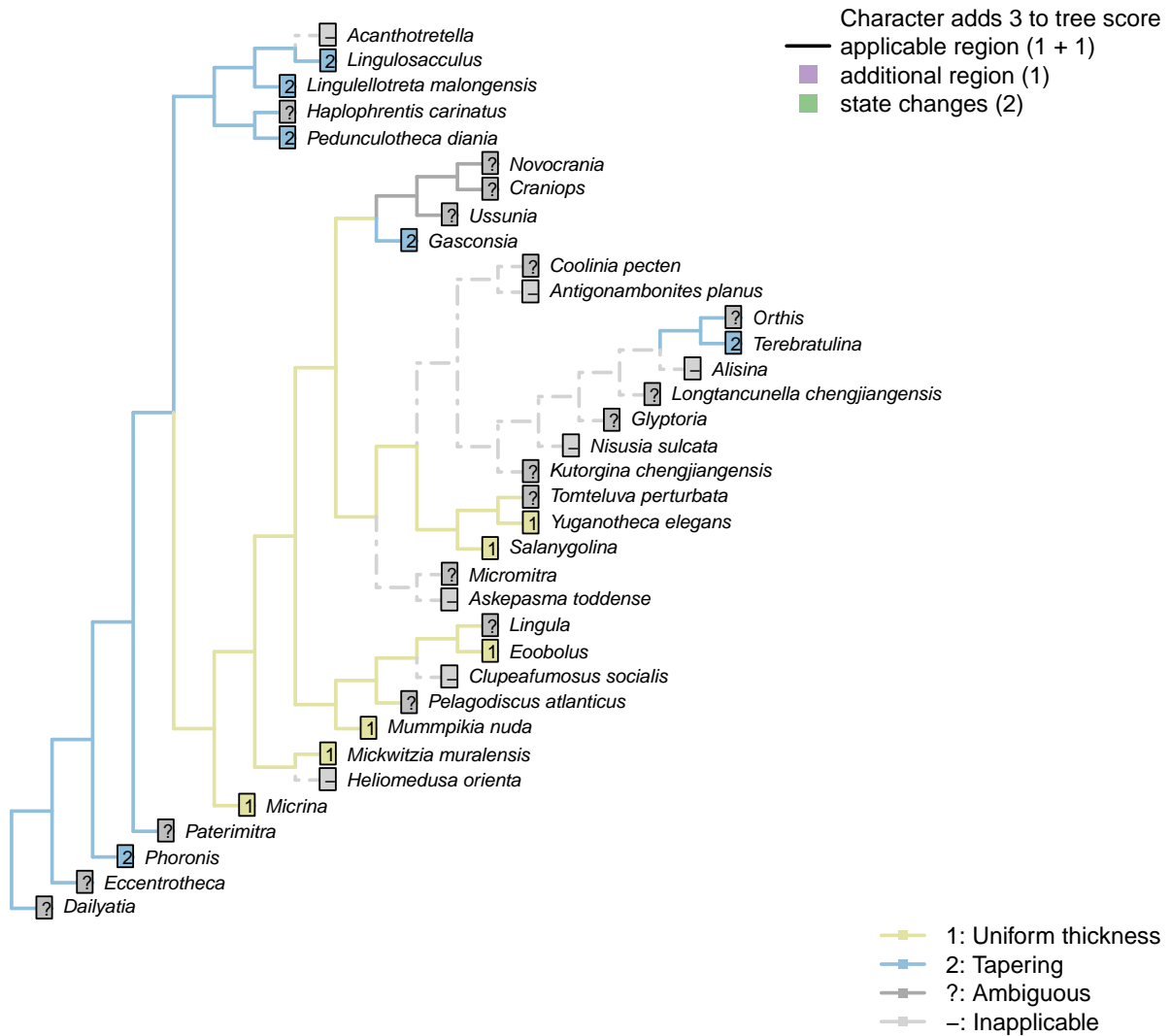


Character 74 – 'Pedicel: Bulb'

Character 75 – 'Pedicel: Distal rootlets'

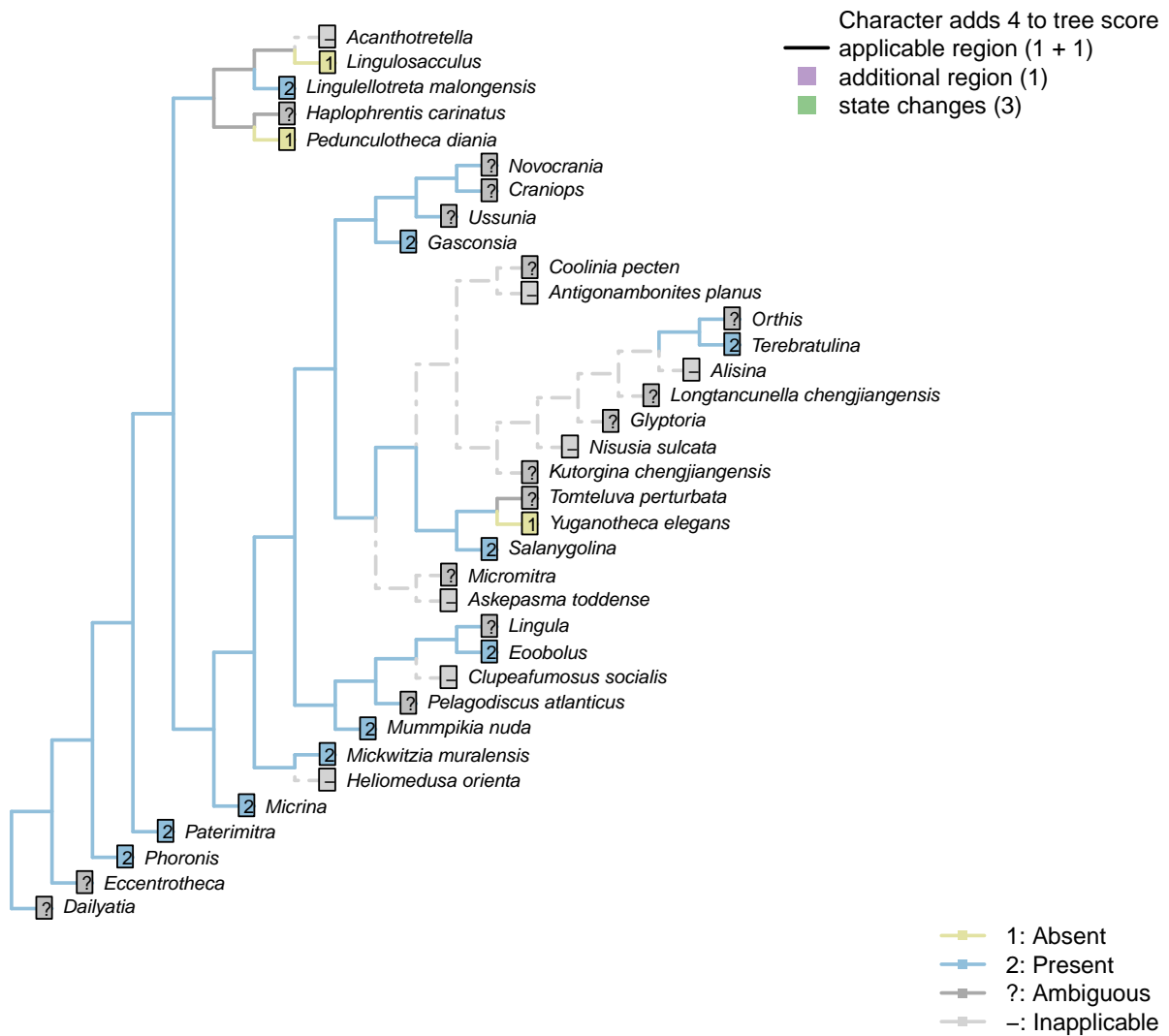


Character 76 – 'Pedicel: Tapering'



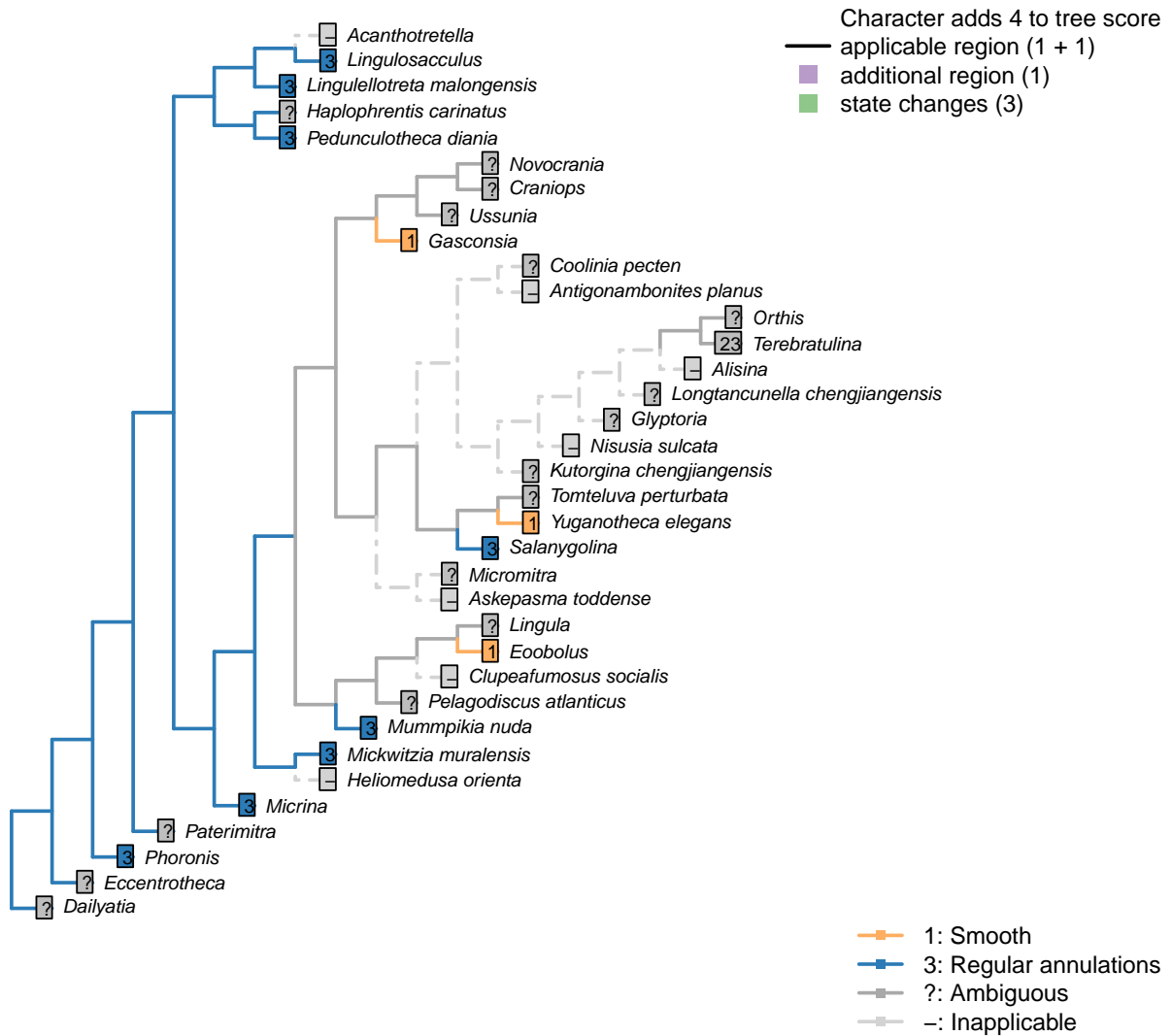
Character 76 – 'Pedicel: Tapering'

Character 77 – 'Pedicel: Coelomic region'



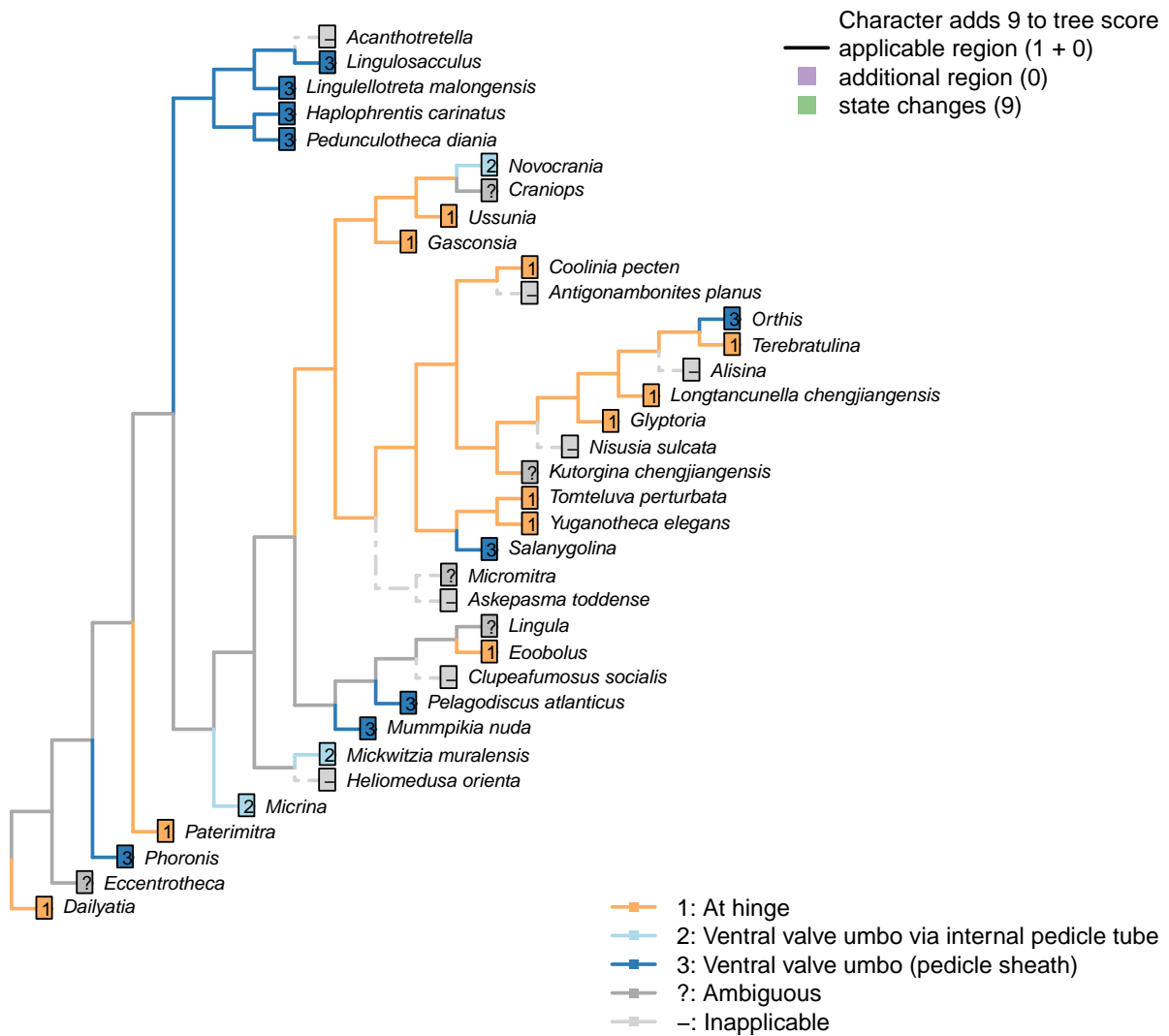
Character 77 – 'Pedicel: Coelomic region'

Character 78 – 'Pedicel: Surface ornament'



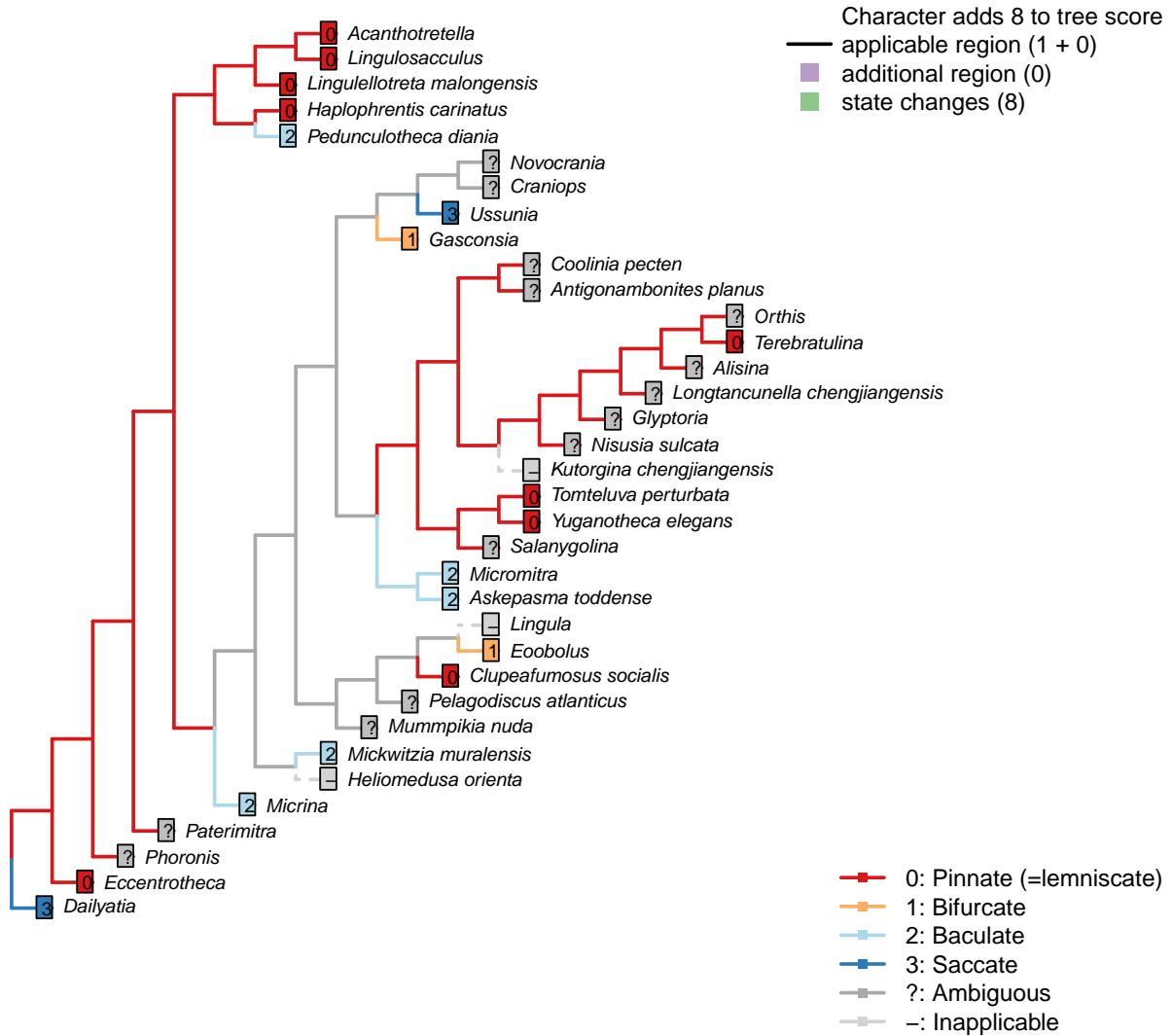
Character 78 – 'Pedicel: Surface ornament'

Character 79 – 'Pedicel: position'



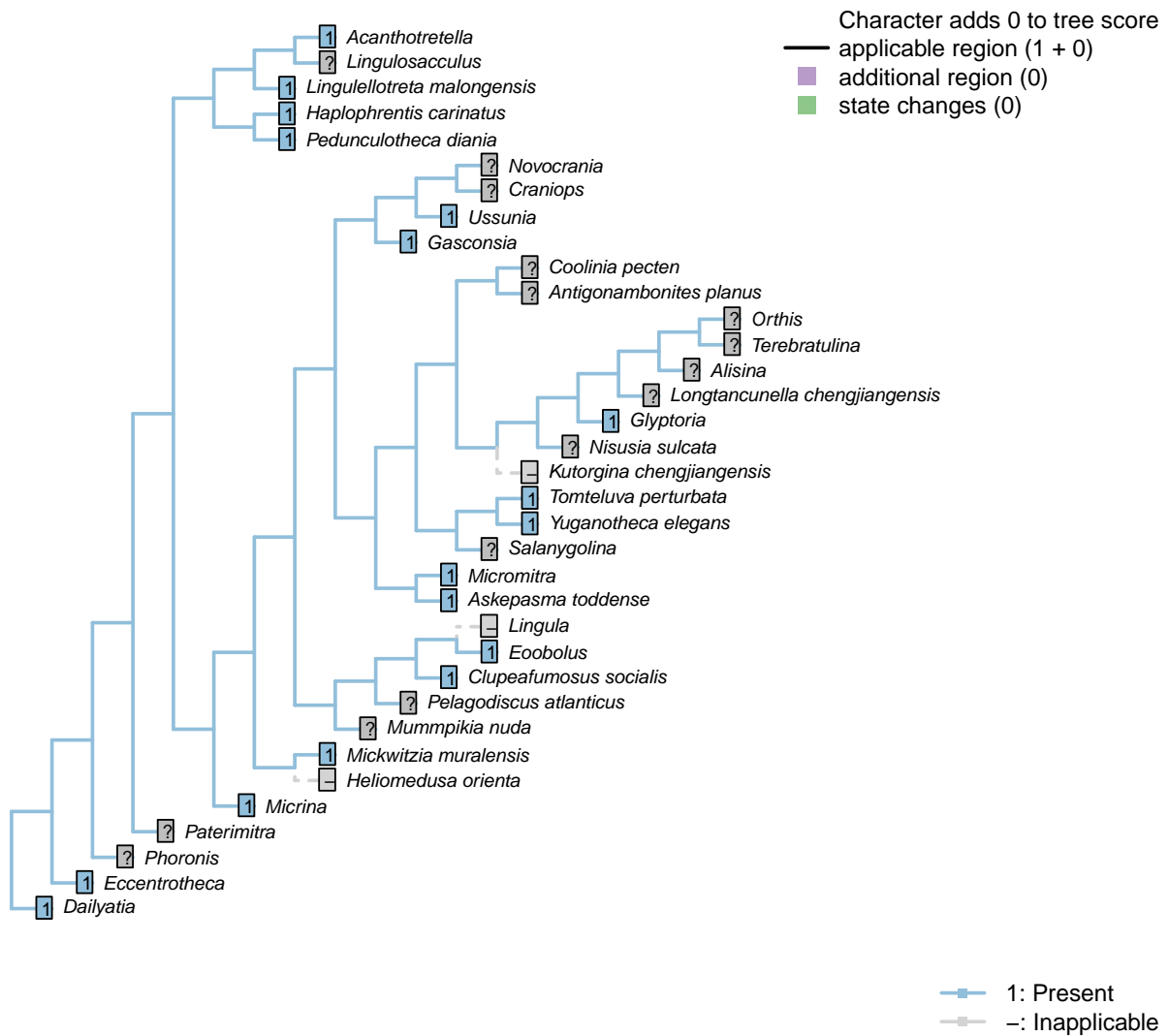
Character 79 – 'Pedicel: position'

Character 80 – 'Mantle canals: Morphology'



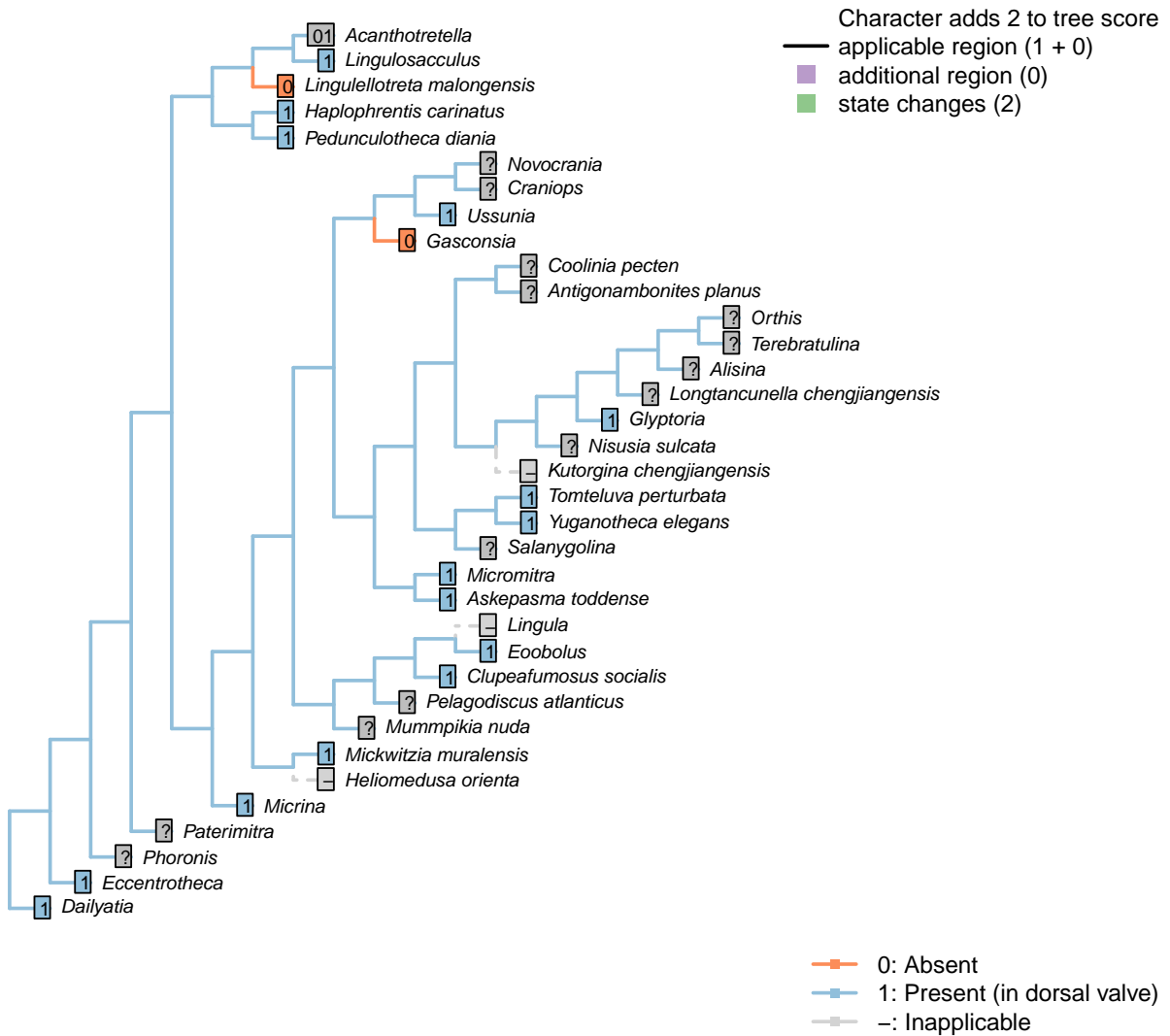
Character 80 – 'Mantle canals: Morphology'

Character 81 – 'Mantle canals: vascula lateralia'



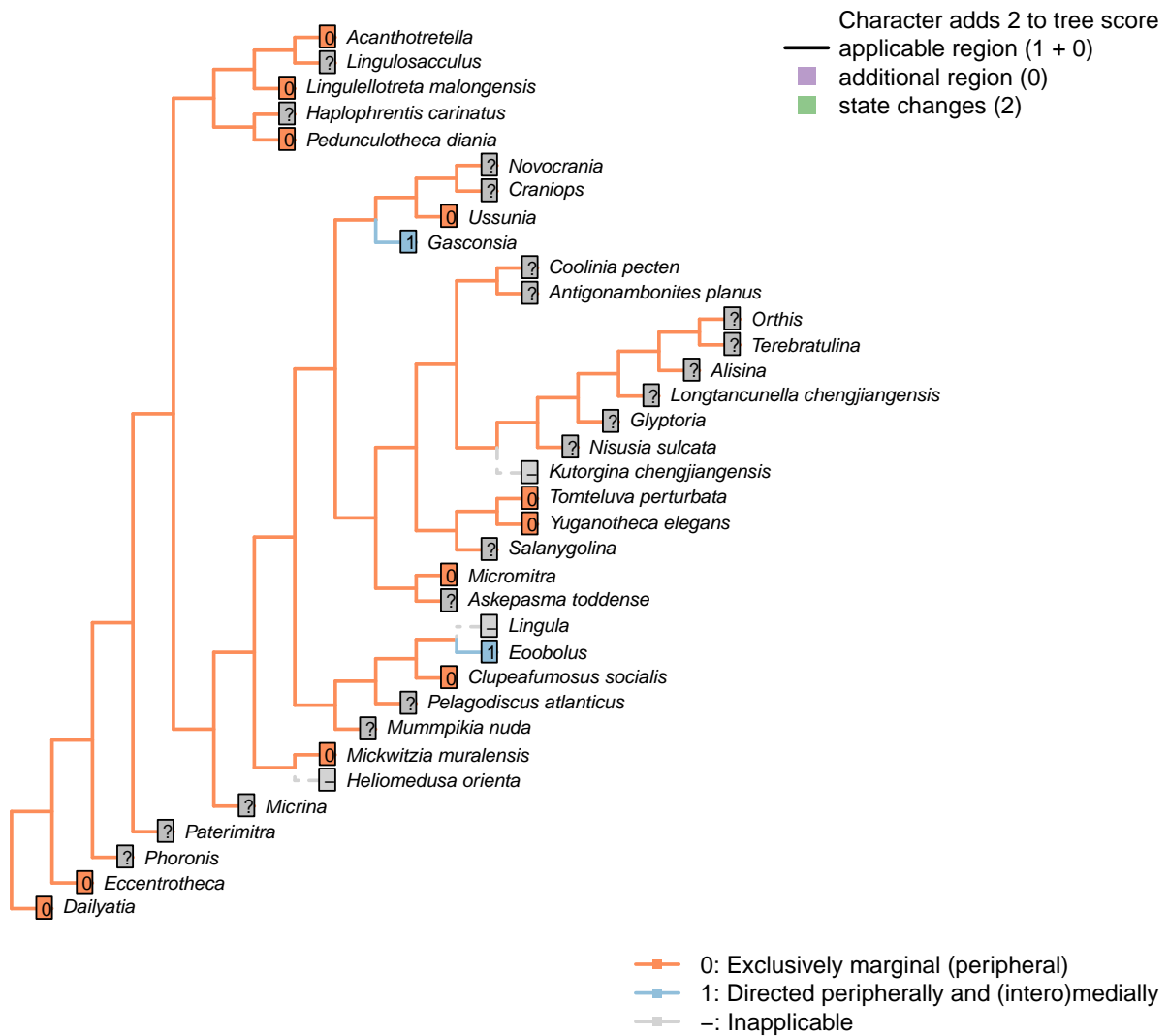
Character 81 – 'Mantle canals: vascula lateralia'

Character 82 – 'Mantle canals: vascula media'



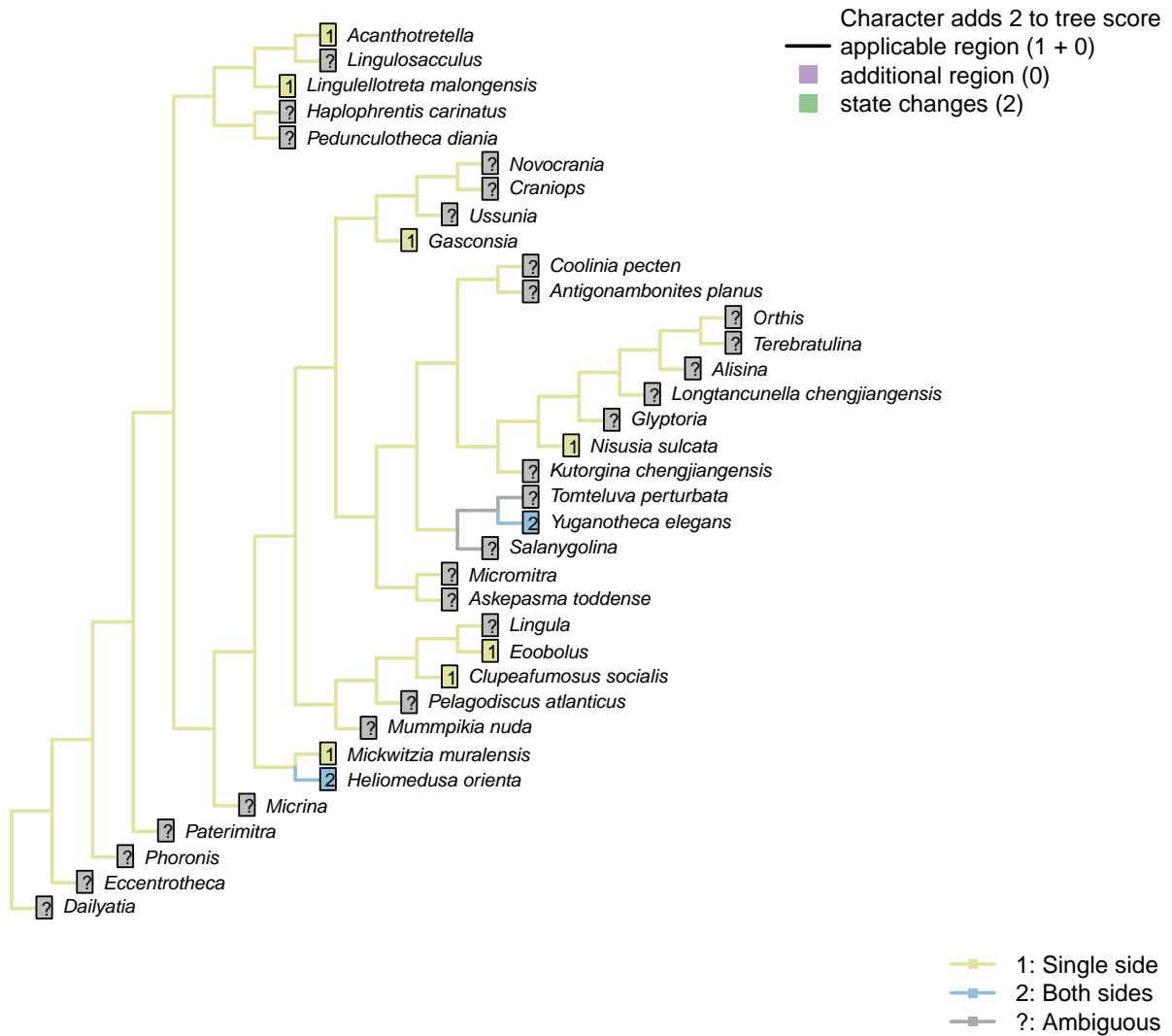
Character 82 – 'Mantle canals: vascula media'

Character 83 – 'Mantle canals: vascula terminalia'



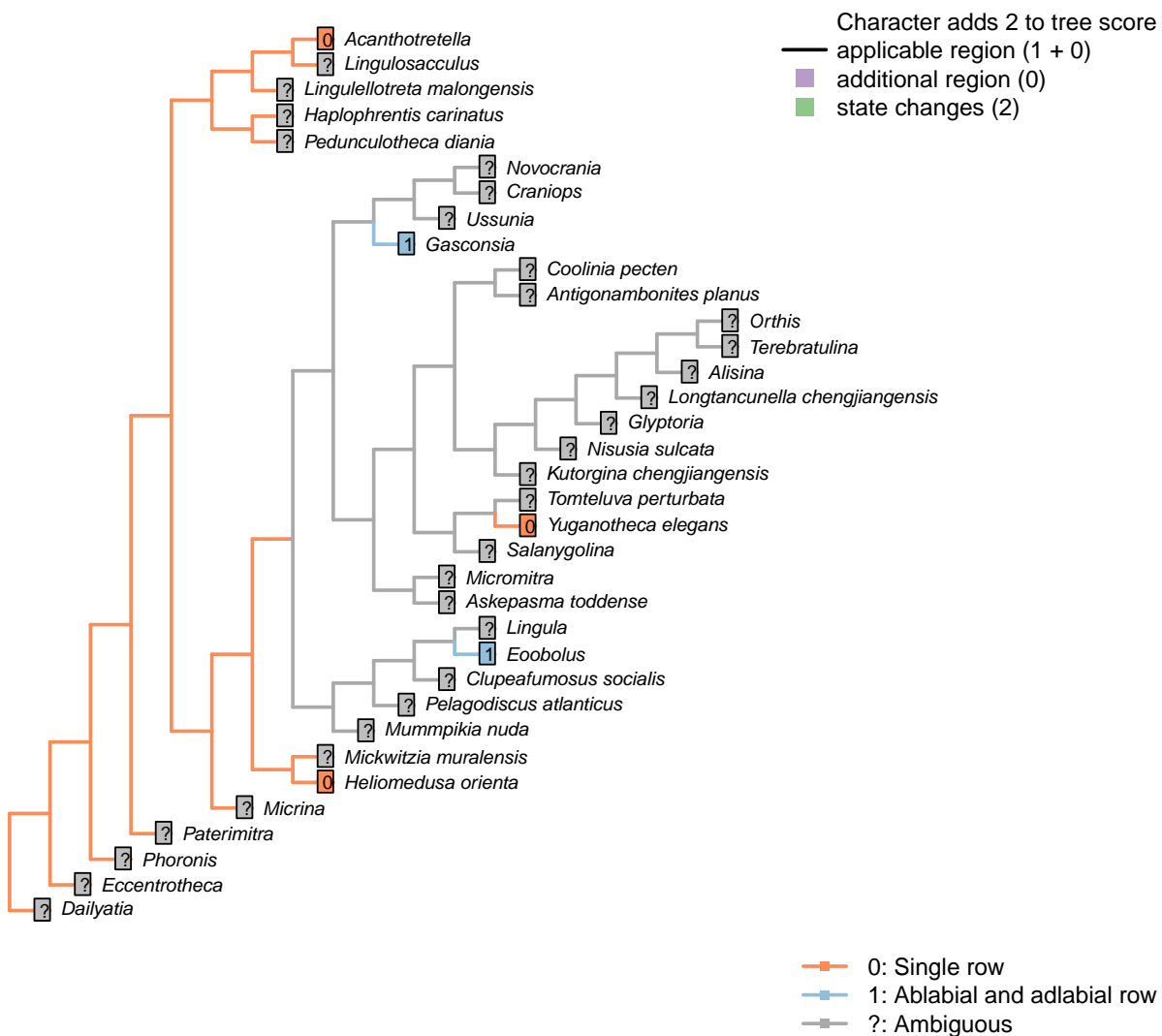
Character 83 – 'Mantle canals: vascula terminalia'

Character 84 – 'Lophophore: tentacle disposition'



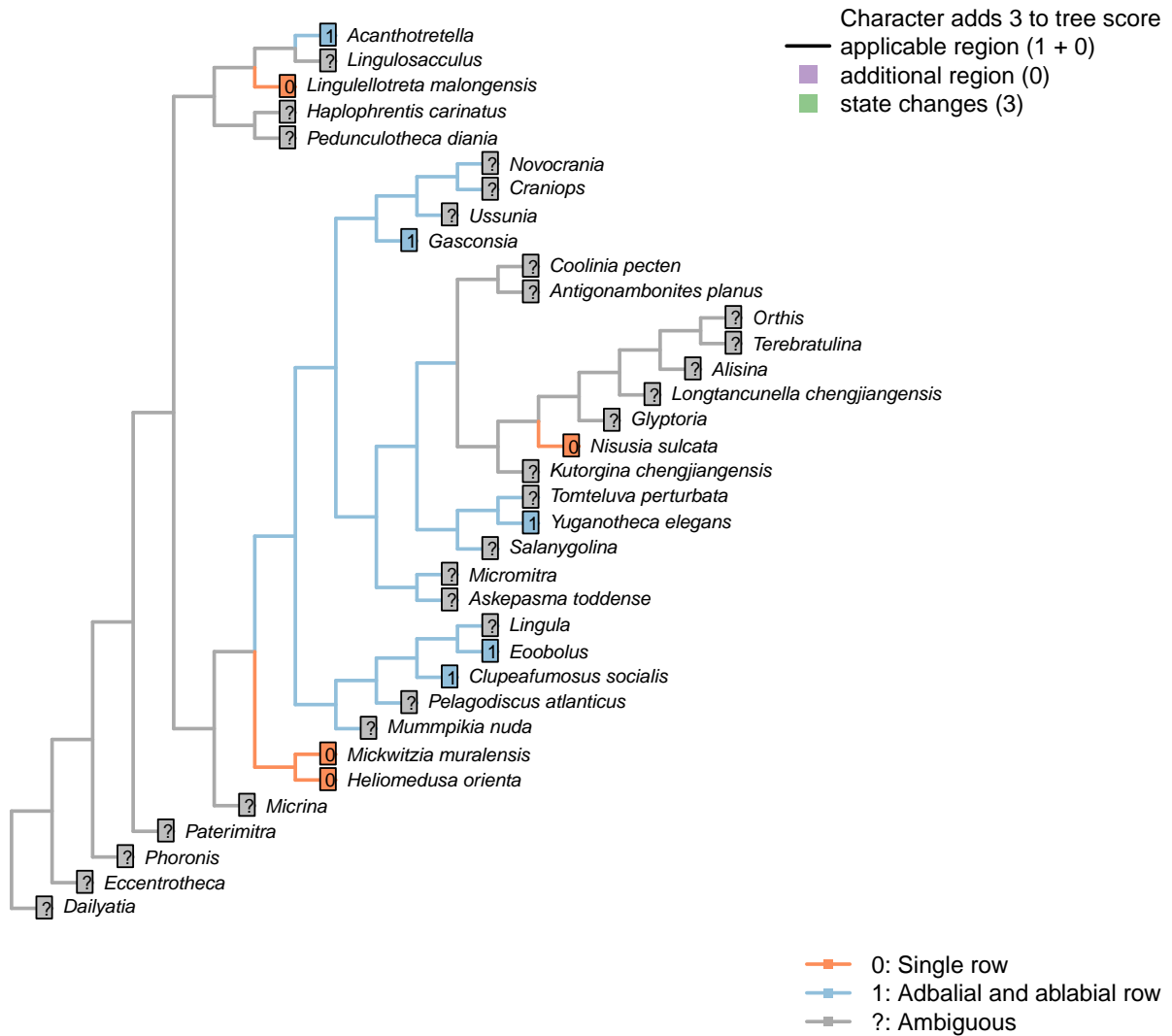
Character 84 – 'Lophophore: tentacle disposition'

Character 85 – 'Lophophore: tentacle rows per side: trocholophe stage'



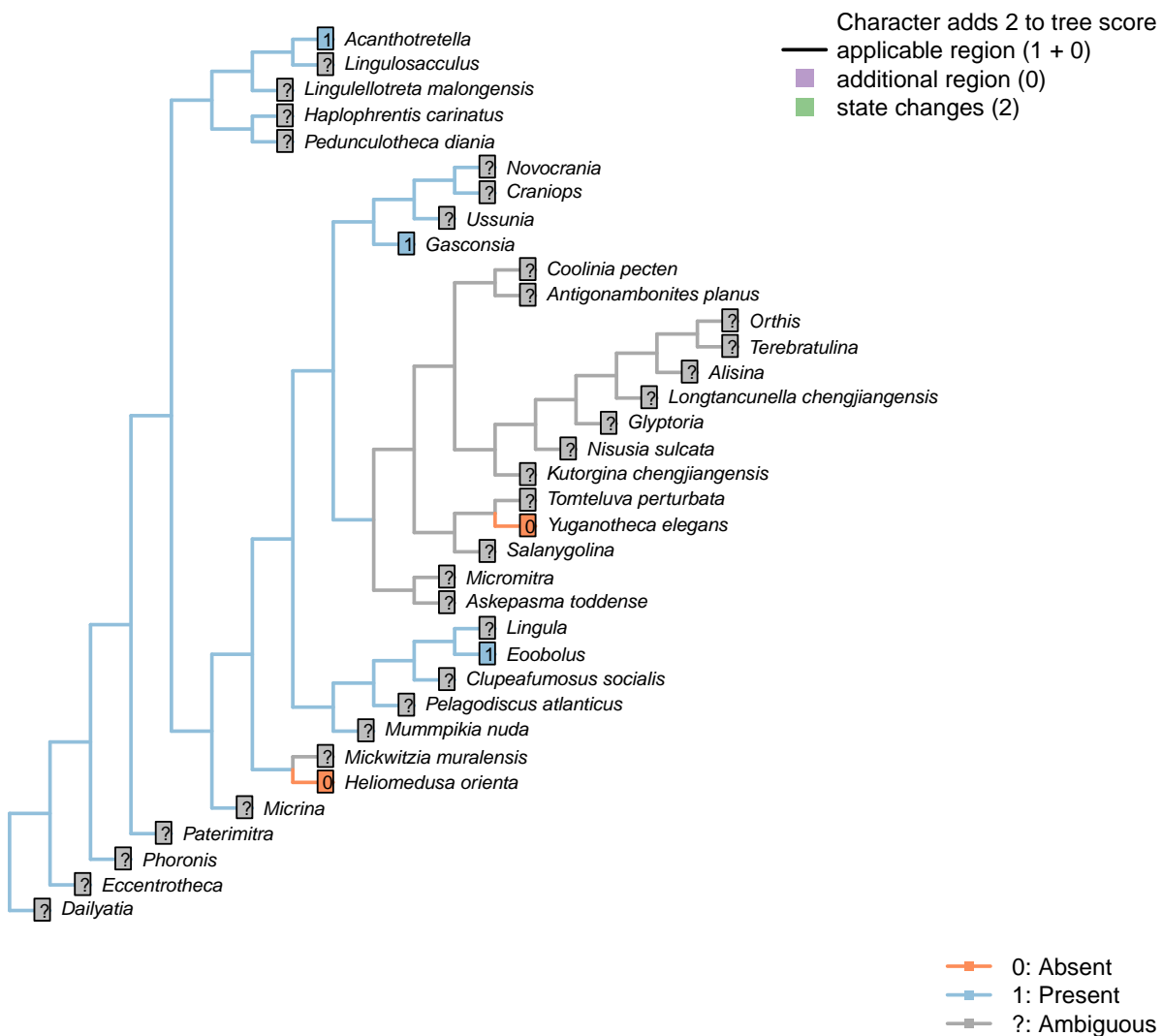
Character 85 – 'Lophophore: tentacle rows per side: trocholophe stage'

Character 86 – 'Lophophore: tentacle rows per side: post–trocholophe stage'



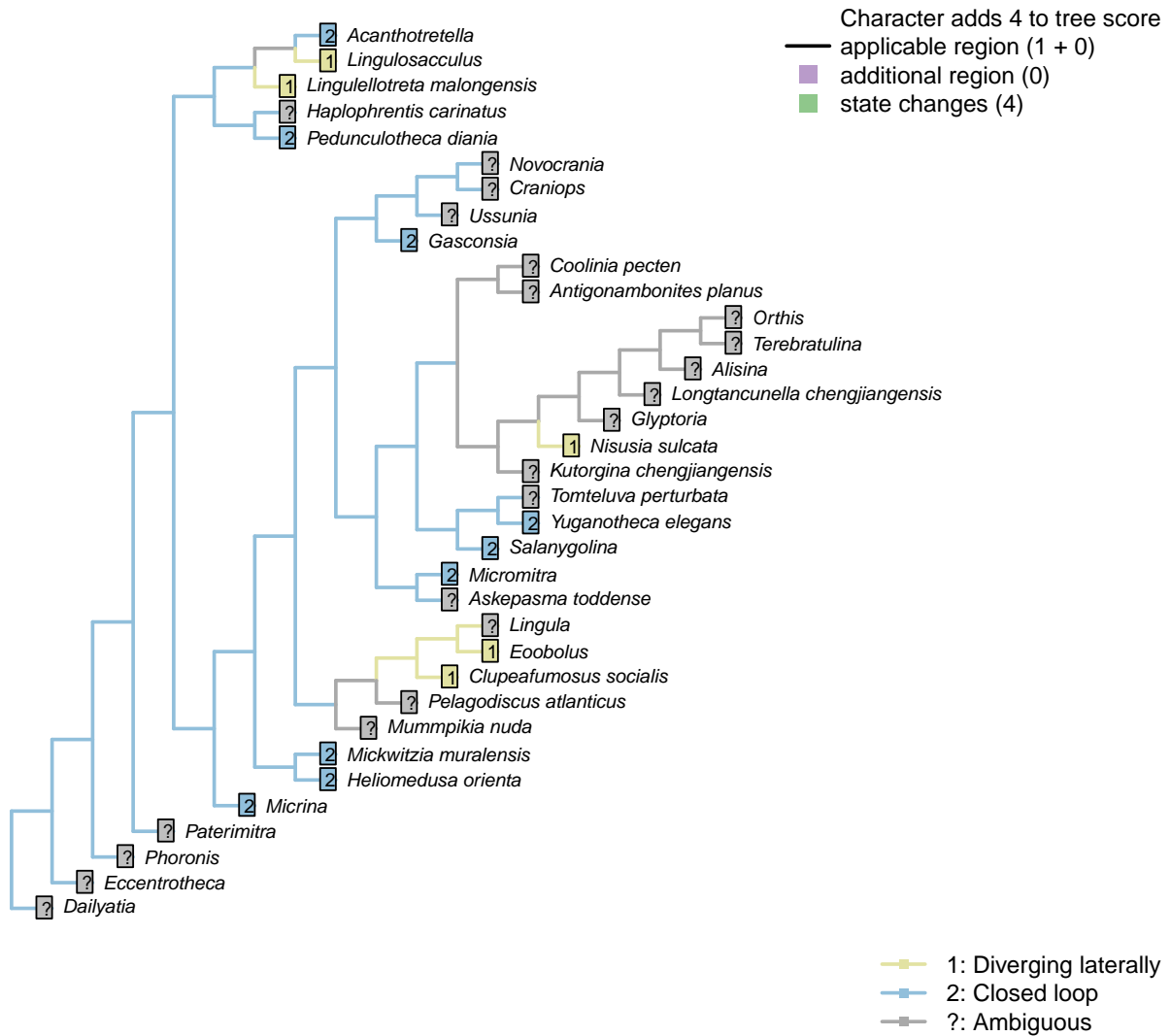
Character 86 – 'Lophophore: tentacle rows per side: post–trocholophe stage'

Character 87 – 'Lophophore: Median tentacle in early development'



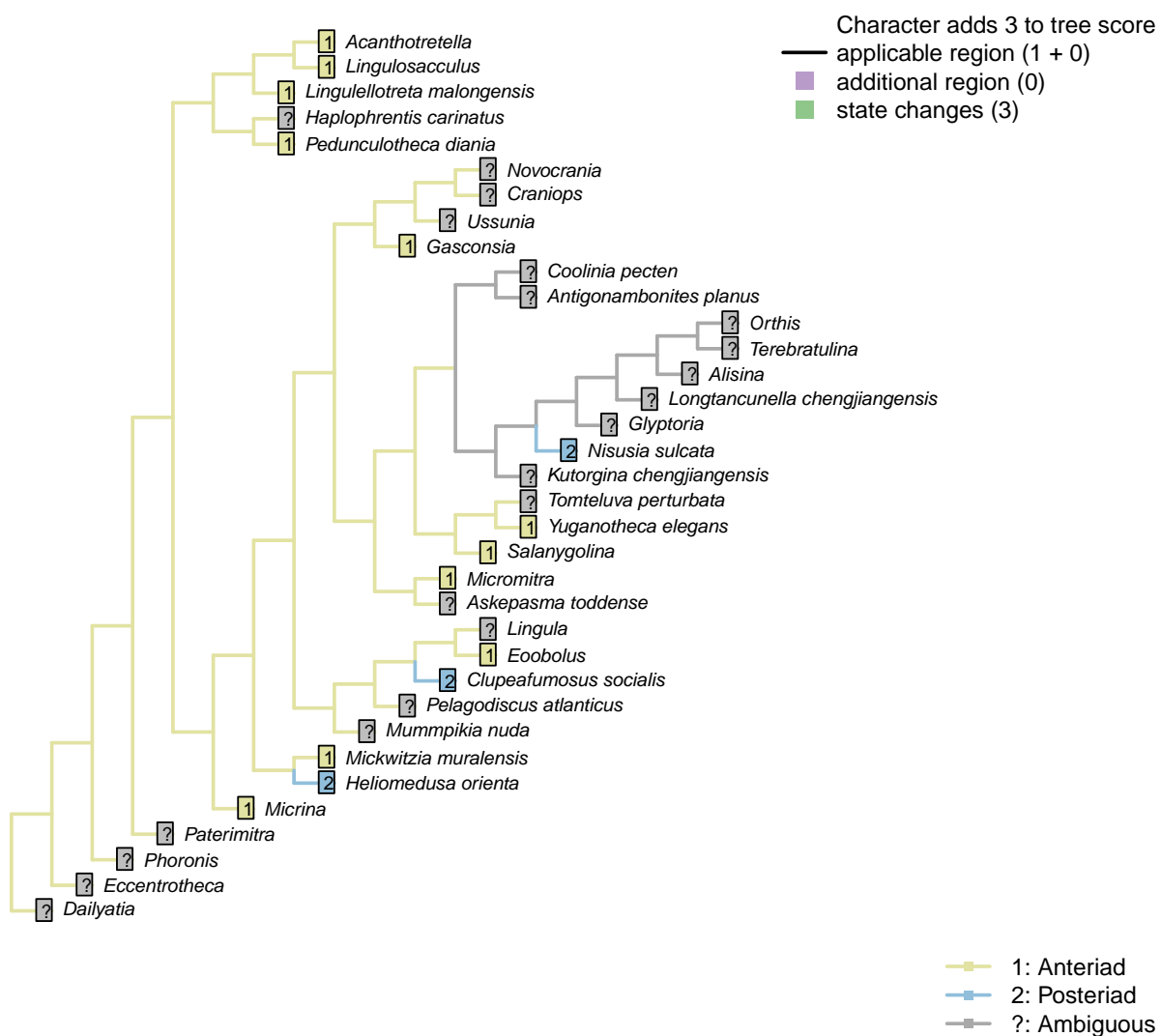
Character 87 – 'Lophophore: Median tentacle in early development'

Character 88 – 'Lophophore: forms closed loop'



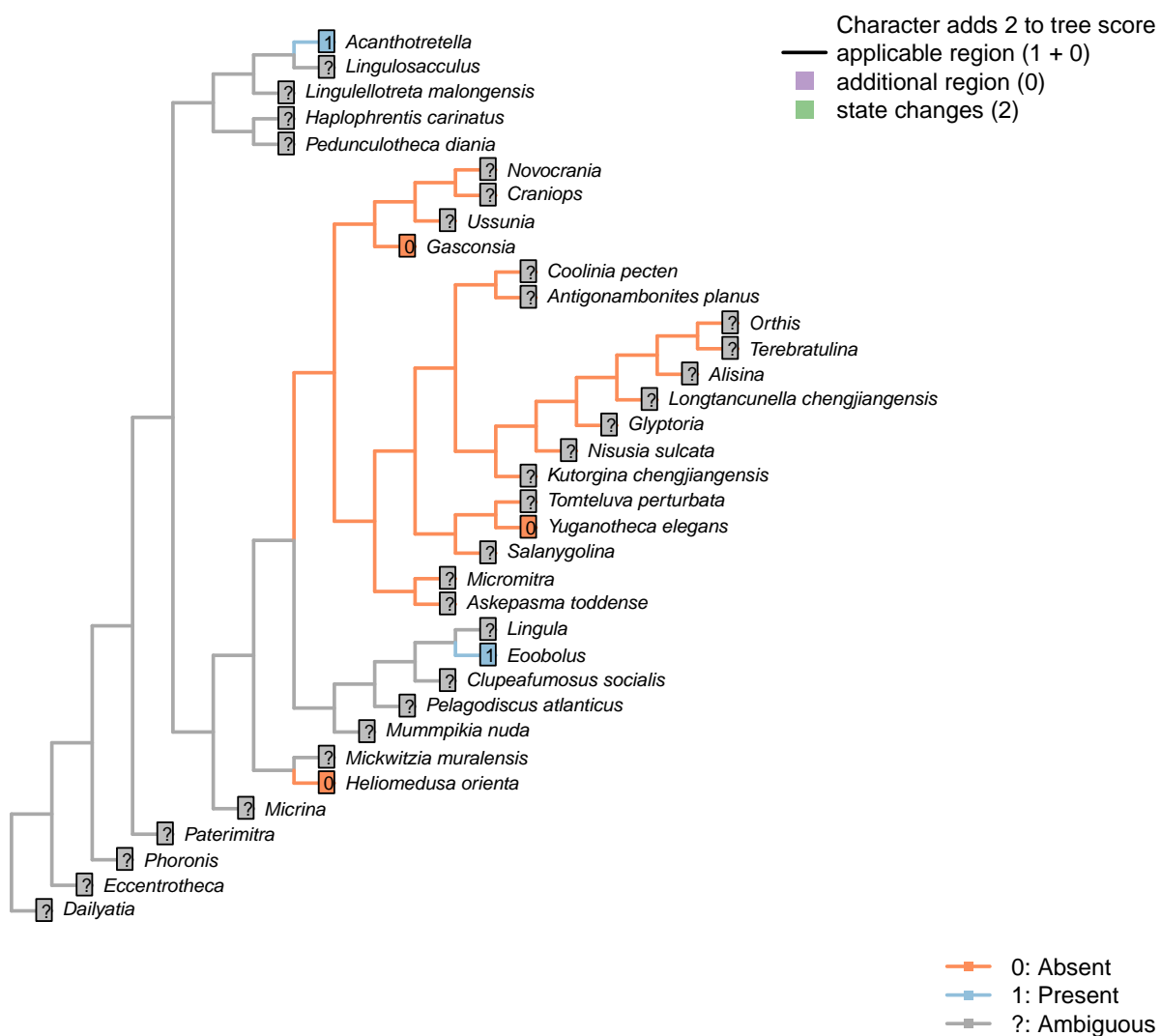
Character 88 – 'Lophophore: forms closed loop'

Character 89 – 'Lophophore: coiling direction'



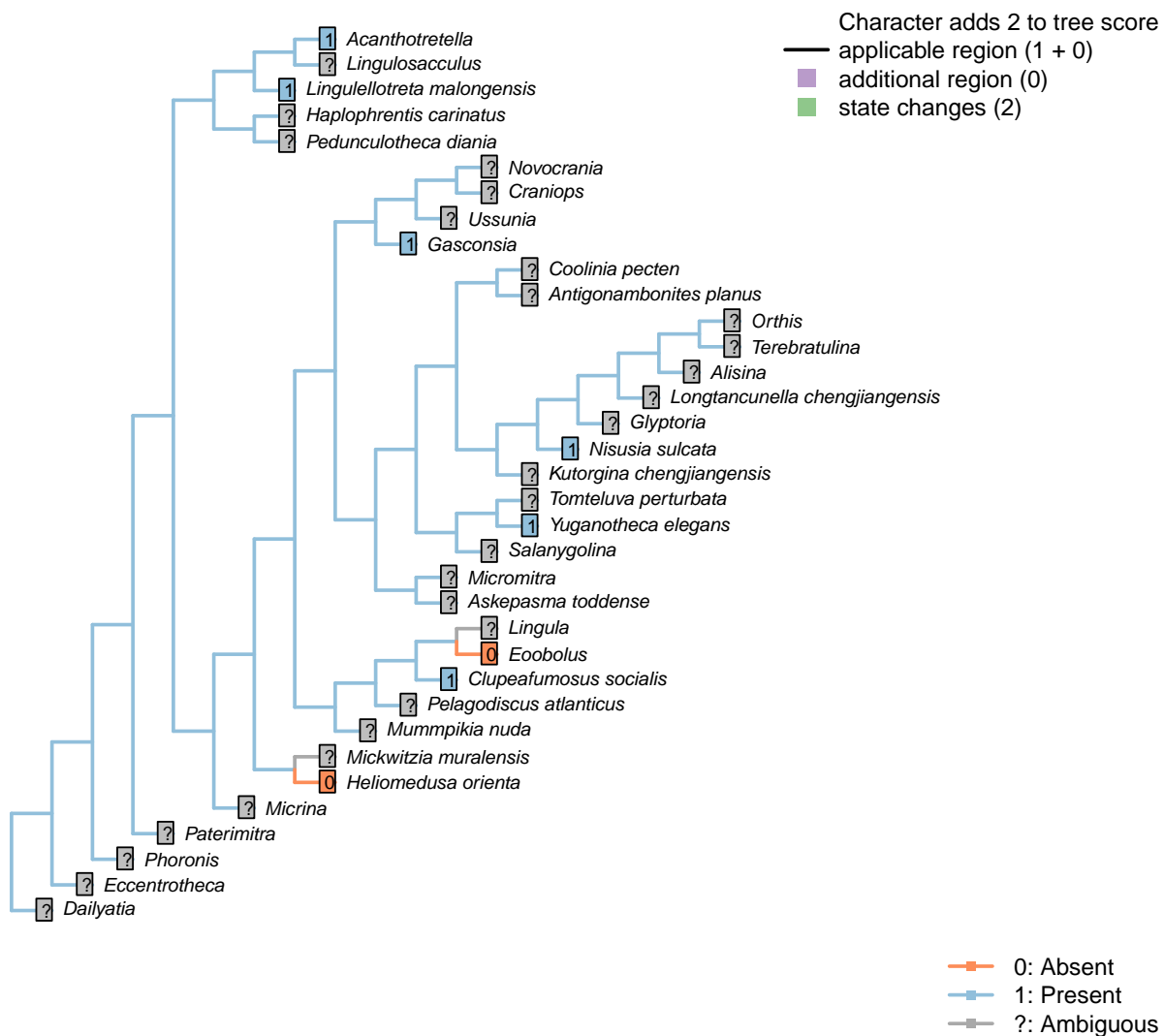
Character 89 – 'Lophophore: coiling direction'

Character 90 – 'Lophophore: adjustor muscle'



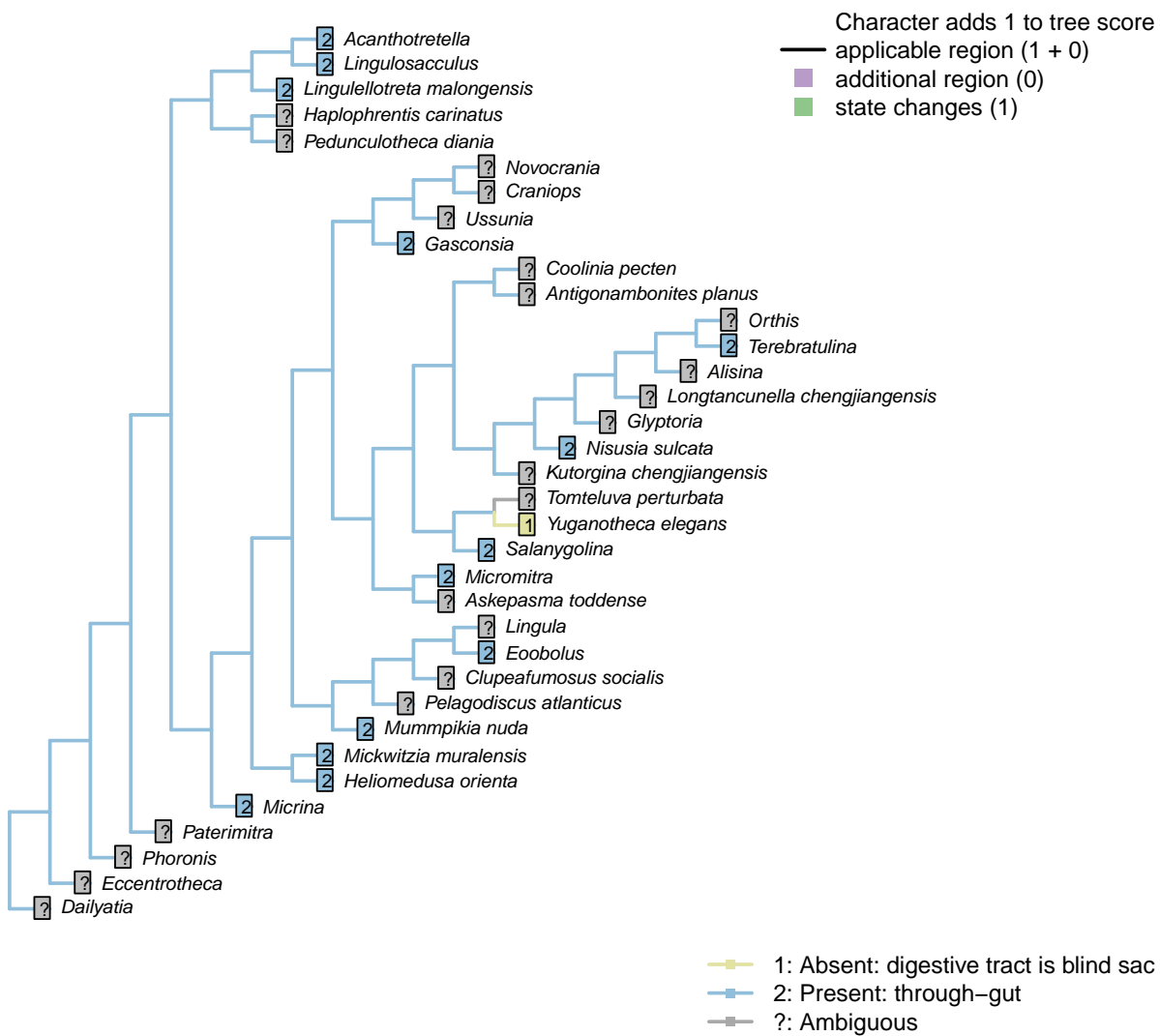
Character 90 – 'Lophophore: adjustor muscle'

Character 91 – 'Prominent pharynx'

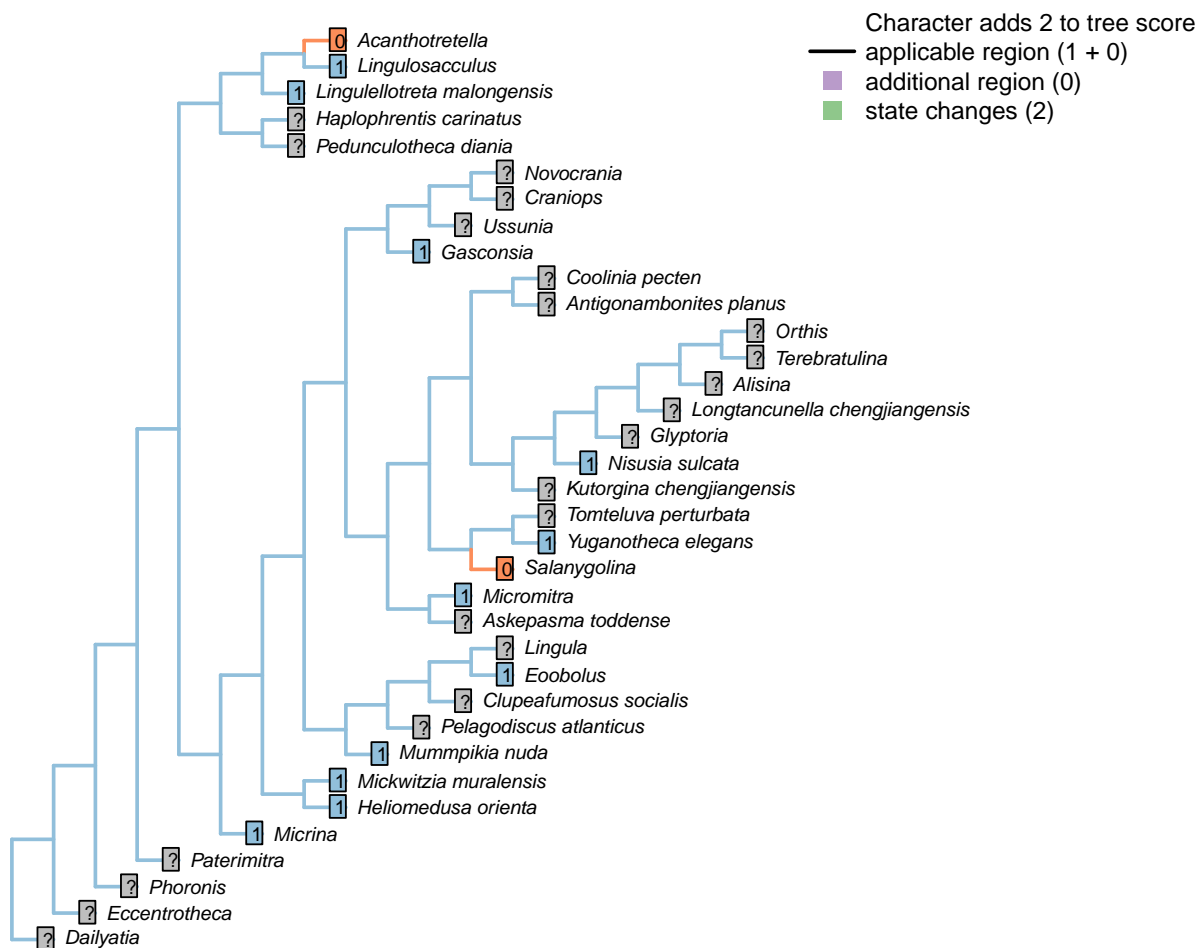


Character 91 – 'Prominent pharynx'

Character 92 – 'Anus'



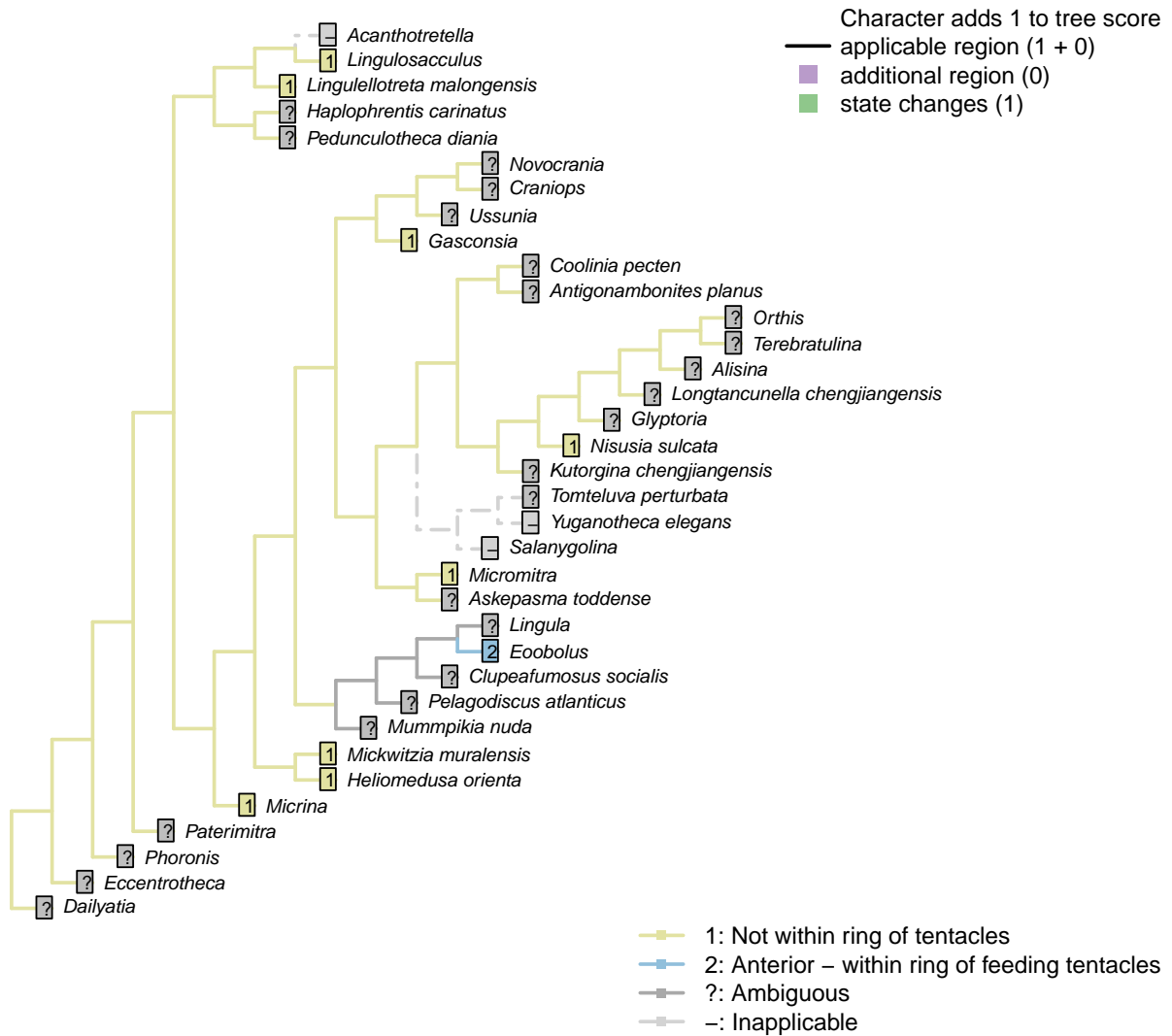
Character 93 – 'Anus: migration'



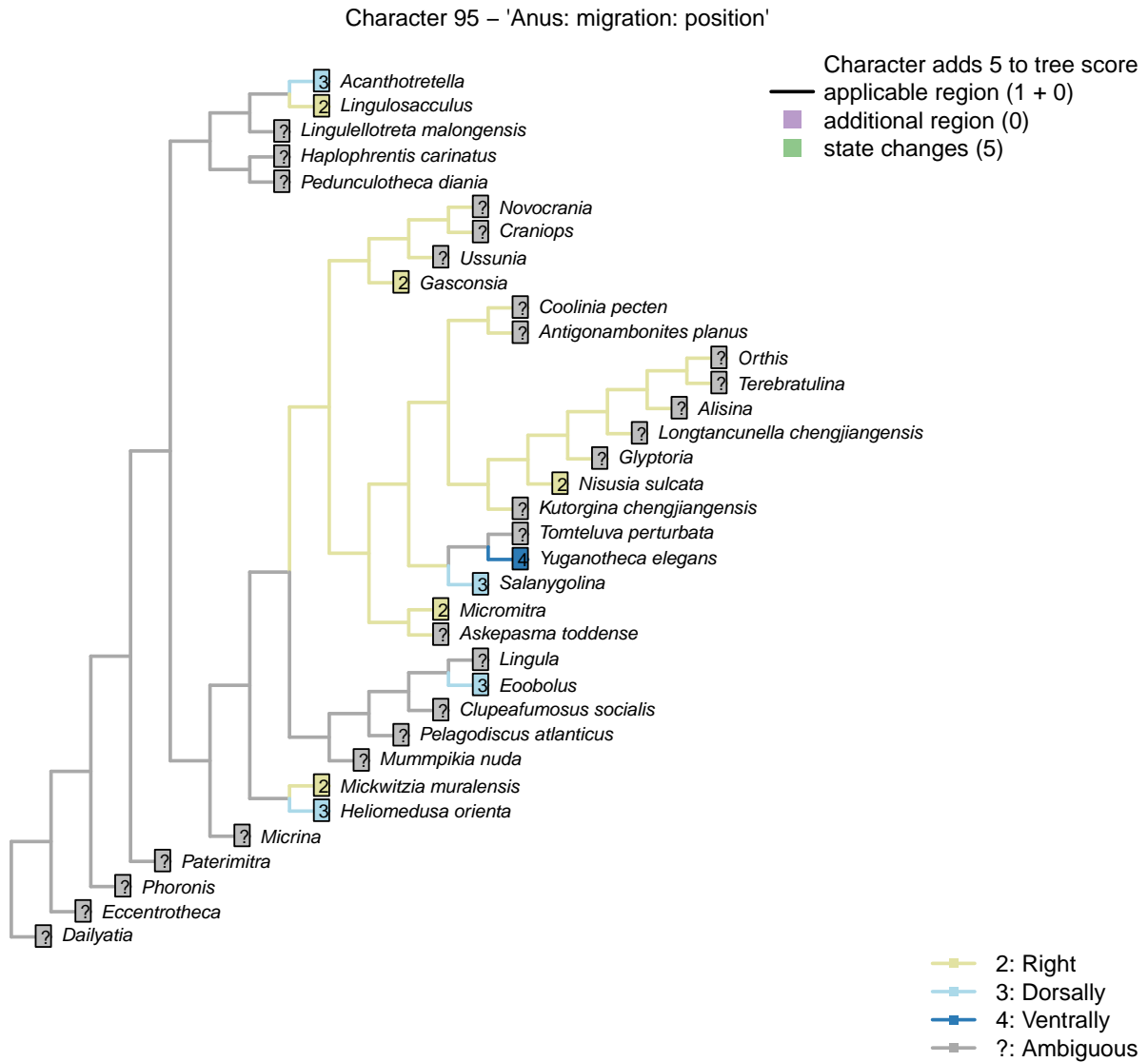
- 0: Not migrated: straight gut with posterior anus
 — 1: Migrated: anus has migrated posteriad to create U-shaped gut

Character 93 – 'Anus: migration'

Character 94 – 'Anus: migration: within ring of tentacles'



Character 94 – 'Anus: migration: within ring of tentacles'



Character 95 – 'Anus: migration: position'

These reconstructions were created using the *Inapp R* package [Brazeau et al., 2017a].

Full character definitions can be found by browsing the morphological dataset on MorphoBank (project 2800).

Chapter 4

Fitch parsimony

Parsimony search was conducted in TNT v1.5 [Goloboff and Catalano, 2016] using sectorial and ratchet heuristics under equal and implied weights. We acknowledge the Willi Hennig Society for their sponsorship of the TNT software.

4.1 Implied weights

The consensus of all implied weights runs is not very well resolved:

This lack of resolution is largely a product of a few wildcard taxa, which obscure relationships that are nevertheless present in all most parsimonious trees:

4.1.1 Paterinids included

4.1.2 Paterinids excluded

4.2 Equal weights

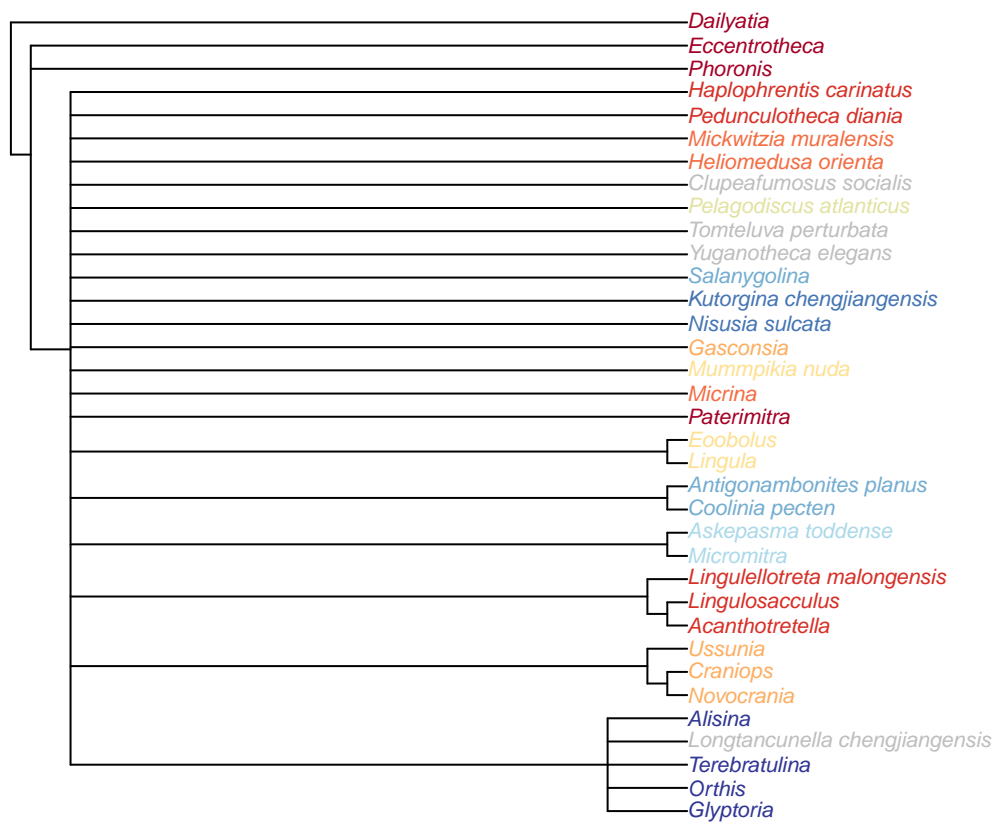


Figure 4.1: TNT implied weights consensus

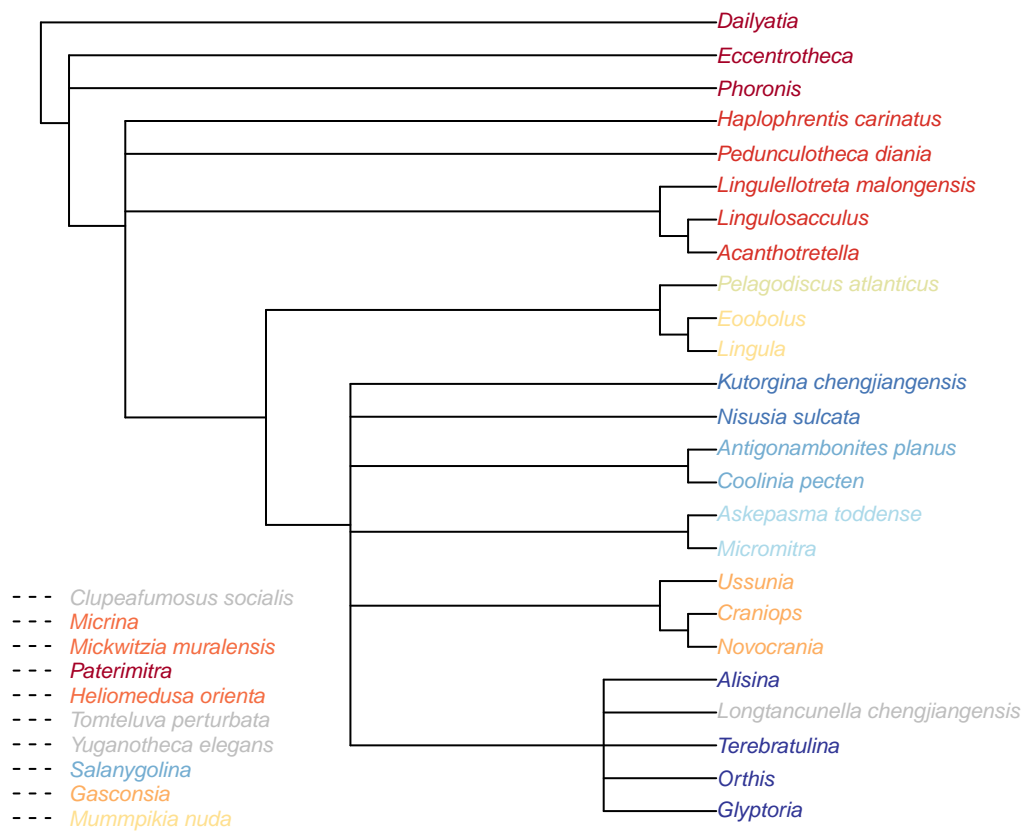


Figure 4.2: TNT implied weights consensus

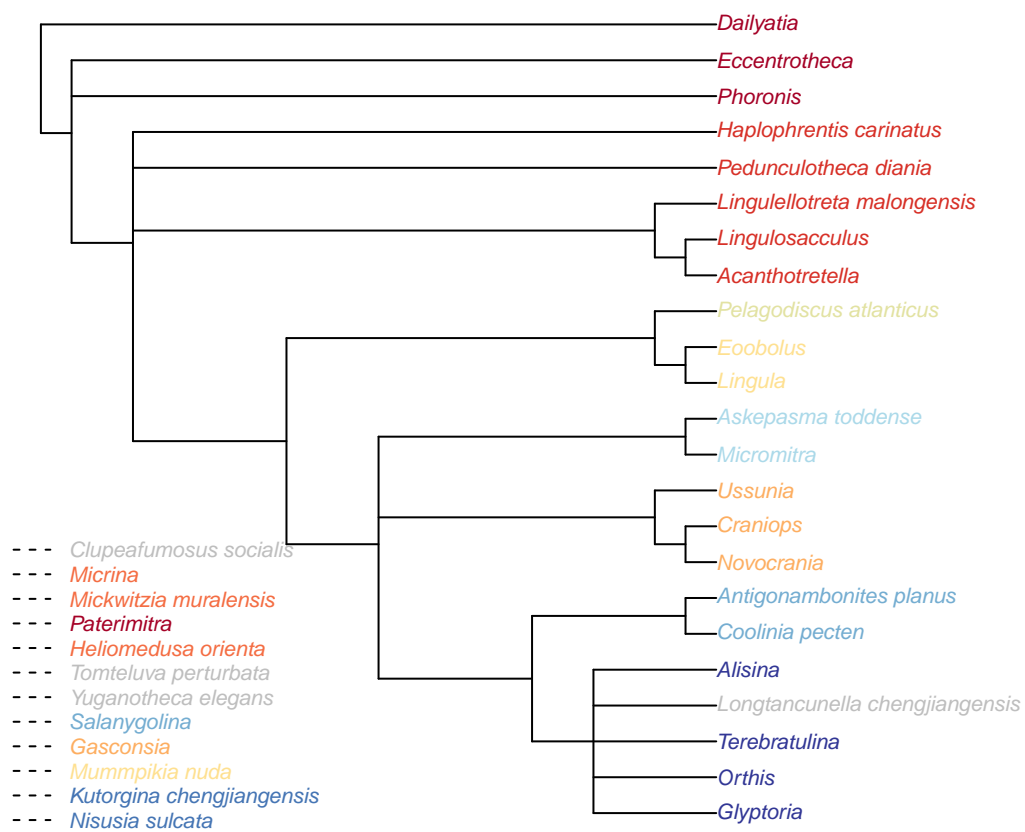


Figure 4.3: TNT implied weights consensus

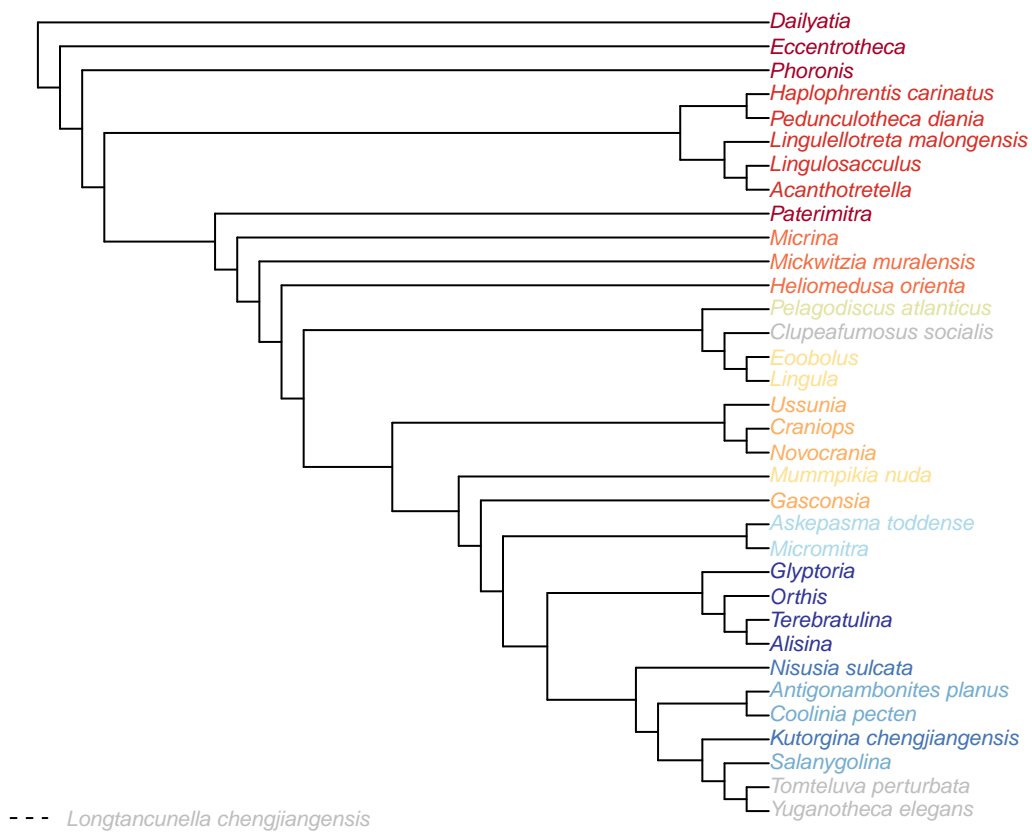


Figure 4.4: TNT Equal weights consensus

Chapter 5

Bayesian analysis

Bayesian search was conducted in MrBayes v3.2.6 [Ronquist et al., 2012] using the Mk model [Lewis, 2001] with a gamma parameter:

```
lset coding=variable rates=gamma;
```

Branch length was drawn from a dirichlet prior distribution, which is less informative than an exponential model [Rannala et al., 2012], but requires a prior mean tree length within about two orders of magnitude of the true value [Zhang et al., 2012]. To satisfy this latter criterion, we specified the prior mean tree length to be equal to the length of the most parsimonious tree under equal weights, using a Dirichlet prior with $T = 1$, $T = 1 / (\text{equal weights tree length} / \text{number of characters})$, $c = 1$:

```
prset brlenspr = unconstrained: gammadir(1, 0.33, 1, 1);
```

Neomorphic and transformational characters [sensu Sereno, 2007] were allocated to two separate partitions whose proportion of invariant characters and gamma shape parameters were allowed to vary independently:

```
charset Neomorphic = 2 3 5 10 13 14 18 19 24 25 29 30 32 34 36 37 38 39 40 43 50 51 53 54 55  
60 63 64 67 70 72 73 76 77 78 79 84 88 89 92 94 95;
```

```
charset Transformational = 1 4 6 7 8 9 11 12 15 16 17 20 21 22 23 26 27 28 31 33 35 41 42 44 45  
46 47 48 49 52 56 57 58 59 61 62 65 66 68 69 71 74 75 80 81 82 83 85 86 87 90 91 93;
```

```
partition chartype = 2: Neomorphic, Transformational;
```

```
set partition = chartype;
```

```
unlink shape=(all) pinvar=(all);
```

Neomorphic characters were not assumed to have a symmetrical transition rate – that is, the probability of the absent \rightarrow present transition was allowed to differ from that of the present \rightarrow absent transition, being drawn from a uniform prior:

```
prset applyto=(1) symdirihyperpr=fixed(1.0);
```

Four MrBayes runs were executed, each sampling eight chains for 1 000 000 generations, with samples taken every 500 generations:

```
mcmc ngen=1000000 samplefreq=500 nruns=2 nchains=8;
```

The first 10% of samples were discarded as burn-in (`burninfrac=0.1`), and a posterior tree topology was derived from the combined posterior sample of both runs.

Convergence was indicated by PSRF = 1.00 and an estimated sample size of > 500 for each parameter:

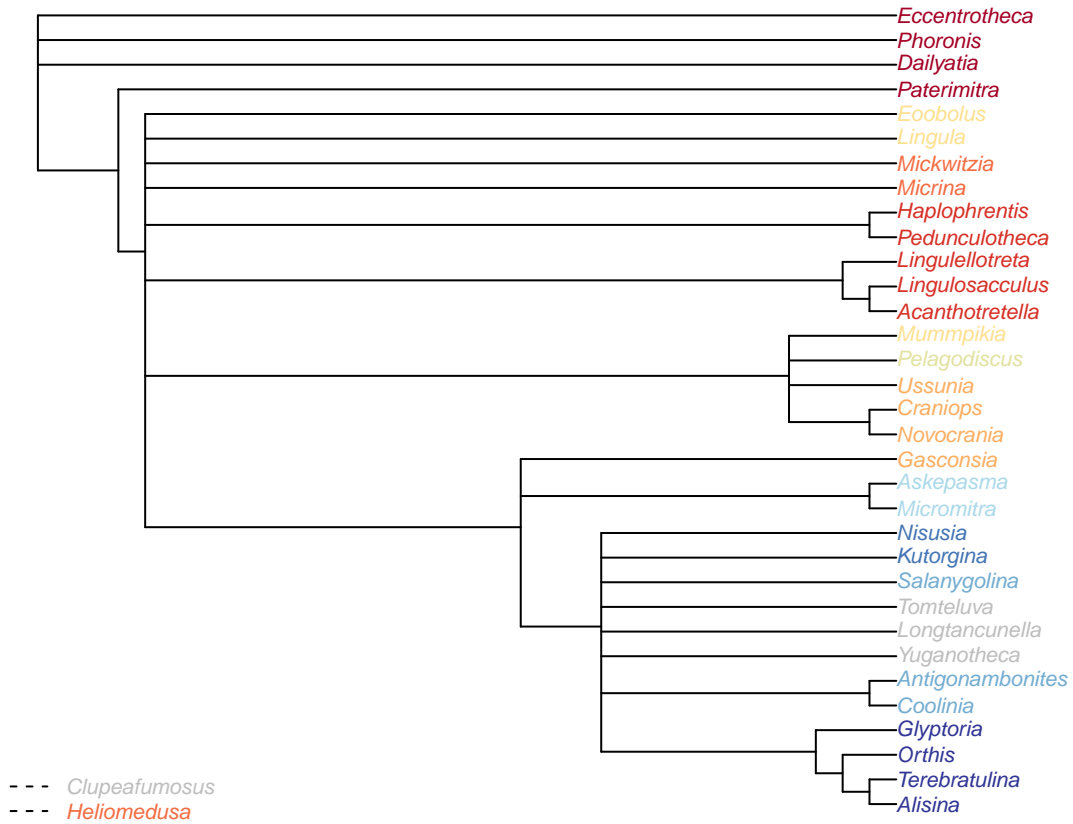


Figure 5.1: Bayesian analysis, posterior probability > 50%

Table 5.1: (#tab:MrBayes parameter summary)MrBayes parameter estimates (.pstat file)

Parameter	Mean	Variance	Lower	Upper	Median	minESS	avgESS	PSRF
TL{all}	6.708892	1.624940	4.8329690	9.249889	6.781895	9.742945	877.9326	1.022541
alpha{1}	2.403829	1.536554	0.0001827	4.702963	2.194241	23.533840	1038.9600	1.005475
alpha{2}	2.950148	2.036612	0.0022876	5.567708	2.770201	22.238850	1073.5860	1.004902

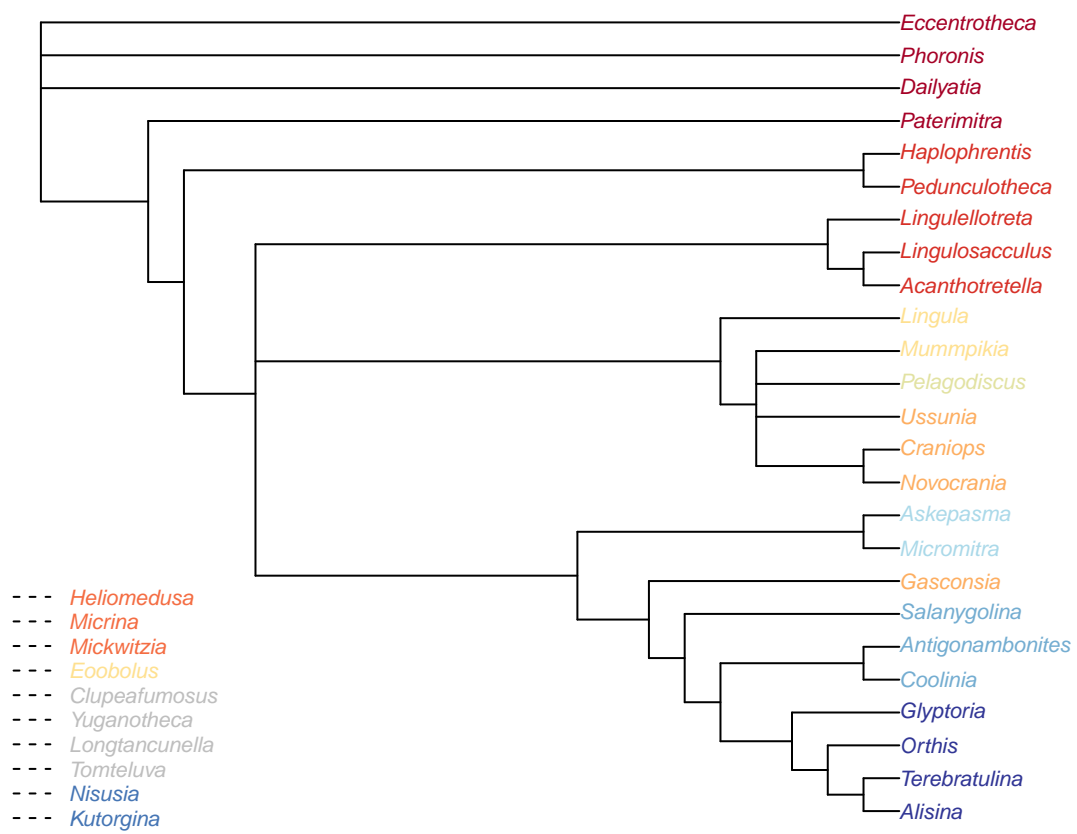


Figure 5.2: Bayesian analysis, posterior probability > 50%

Bibliography

- Martin D. Brazeau, Thomas Guillaume, and Martin Ross Smith. Morphological phylogenetic analysis with inapplicable data. *bioRxiv*, 2017a. doi: 10.1101/209775. URL <https://www.biorxiv.org/content/early/2017/10/26/209775>.
- Martin D. Brazeau, Martin R. Smith, and Thomas Guillaume. MorphyLib: a library for phylogenetic analysis of categorical trait data with inapplicability, 2017b.
- Pablo A. Goloboff. Self-weighted optimization: tree searches and character state reconstructions under implied transformation costs. *Cladistics*, 13(3):225–245, 1997. doi: 10.1111/j.1096-0031.1997.tb00317.x.
- Pablo A Goloboff and Santiago A Catalano. TNT version 1.5, including a full implementation of phylogenetic morphometrics. *Cladistics*, 32(3):221–238, 2016. doi: 10.1111/cla.12160.
- Paul O Lewis. A likelihood approach to estimating phylogeny from discrete morphological character data. *Systematic Biology*, 50(6):913–925, 2001. doi: 10.1080/106351501753462876.
- Wayne P. Maddison. Missing data versus missing characters in phylogenetic analysis. *Systematic Biology*, 42(4):576–581, 1993. doi: 10.1093/sysbio/42.4.576.
- Kevin C. Nixon. The Parsimony Ratchet, a new method for rapid parsimony analysis. *Cladistics*, 15(4): 407–414, 1999. ISSN 0748-3007. doi: 10.1111/j.1096-0031.1999.tb00277.x.
- Bruce Rannala, Tianqi Zhu, and Ziheng Yang. Tail Paradox, Partial Identifiability, and Influential Priors in Bayesian Branch Length Inference. *Molecular Biology and Evolution*, 29(1):325–335, 2012. doi: 10.1093/molbev/msr210.
- F. Ronquist, M. Teslenko, P. van der Mark, D. L. Ayres, A. Darling, S. Hohna, B. Larget, L. Liu, M. A. Suchard, and J. P. Huelsenbeck. MrBayes 3.2: efficient Bayesian phylogenetic inference and model choice across a large model space. *Systematic Biology*, 61(3):539–42, 2012.
- Paul C. Sereno. Logical basis for morphological characters in phylogenetics. *Cladistics*, 23(6):565–587, 2007. doi: 10.1111/j.1096-0031.2007.00161.x.
- Martin Ross Smith. Quantifying and visualising divergence between pairs of phylogenetic trees: implications for phylogenetic reconstruction. *bioRxiv*, 2017. doi: 10.1101/227942.
- Martin Ross Smith. TreeSearch 0.0.8, 2018.
- Hai-Jing Sun, Martin Ross Smith, Mao-Yan Zhu, Han Zeng, and Fang-Chen Zhao. Hyoliths are linguliform brachiopods. page In review, 2018.
- Lars Vogt. The logical basis for coding ontologically dependent characters. *Cladistics*, 2017. doi: 10.1111/cla.12209.
- Chi Zhang, Bruce Rannala, and Ziheng Yang. Robustness of compound Dirichlet priors for Bayesian inference of branch lengths. 61(5):779–84, 2012. doi: 10.1093/sysbio/sys030.